Universidade do Estado do Rio de Janeiro
Instituto de Biologia Roberto Alcântara Gomes
Pós-Graduação em Biociências

Gilson Costa dos Santos Junior

Estudo da cromatina nos sítios de fixação à matriz nuclear no domínio do gene *TP53* e das modificações epigenéticas no modelo de progressão tumoral mamária 21T

Rio de Janeiro
2014

Gilson Costa dos Santos Junior

Estudo da cromatina nos sítios de fixação à matriz nuclear no domínio do gene *TP53* e das modificações epigenéticas e no modelo de progressão tumoral mamária 21T

Tese apresentada como requisito parcial para obtenção do título de Doutor ao Programa de Pós-Graduação em Biociências da Universidade do Estado do Rio de Janeiro.

Orientadora: Prof.ª Dra. Cláudia Vitória de Moura Gallo

Coorientadora: Prof.ª Dra. Andréa Carla de Souza Góes

Rio de Janeiro

2014

CATALOGAÇÃO NA FONTE
UERJ/REDE SIRIUS/BIBLIOTECA CB-A

S237 Santos Junior, Gilson Costa dos.
Estudo da cromatina nos sítios de fixação à matriz nuclear no domínio do gene *TP53* e das modificações epigenéticas e no modelo de progressão tumoral mamária 21T/ Gilson Costa dos Santos Junior.– 2014.
137f.

Orientadora: Cláudia Vitória de Moura Gallo.
Coorientadora: Andréa Carla de Souza Góes.

Tese (Doutorado) - Universidade do Estado do Rio de Janeiro, Instituto de Biologia Roberto Alcântara Gomes. Pós-graduação em Biociências.

1. Cromatina - Teses. 2. Mamas - Câncer – Teses. 3. Antioncogenes – Teses. 4. Matriz nuclear - Teses. 5. Epigenética - Teses. 6. Genes p53. I. Gallo, Claudia Vitória de Moura. II. Goés, Andréa Carla de Souza. II. Universidade do Estado do Rio de Janeiro. Instituto de Biologia Roberto Alcântara Gomes. III. Título.

CDU 575.224.4

_____ _____

Assinatura Data

Gilson Costa dos Santos Junior

Estudo da cromatina nos sítios de fixação à matriz nuclear no domínio do gene *TP53* e das modificações epigenéticas no modelo de progressão tumoral mamária 21T

Tese apresentada como requisito parcial para obtenção do título de Doutor ao Programa de Pós-Graduação em Biociências da Universidade do Estado do Rio de Janeiro.

Aprovada em 13 de Fevereiro de 2014.

Coorientadora: Prof.ª Dra. Andréa Carla de Souza Góes
Instituto de Biologia Roberto Alcântara Gomes – UERJ

Banca Examinadora: _____
Prof.ª Dra. Cláudia Vitória de Moura Gallo (Orientadora)
Instituto de Biologia Roberto Alcântara Gomes – UERJ

_____
Prof.ª Dra. Deborah Schechtman
Universidade de São Paulo

_____
Prof.ª Dra. Verônica Maria Morandi da Silva
Instituto de Biologia Roberto Alcântara Gomes - UERJ

_____
Prof.ª Dra. Lidia Maria da Fonte de Amorim
Universidade Federal Fluminense

Rio de Janeiro
2014

DEDICATÓRIA

Dedico este trabalho à minha amada esposa e à minha família, por todo amor e carinho

AGRADECIMENTOS

A Deus pelo fôlego de vida, à minha amada esposa Thaís e a toda a minha família, por terem me fornecido todo o suporte necessário, durante estes 4 anos de doutoramento, culminando na realização desta tese.

À querida Prof.ª e Orientadora Claudia Gallo, do Departamento de Genética da UERJ e chefe do Laboratório de Biologia Molecular de Tumores (LBMT), por ter contribuído demasiadamente para o meu amadurecimento como jovem cientista, dando-me sempre o suporte necessário para a realização dos experimentos e me permitido realizar um maravilhoso doutorado-sanduíche na França.

À querida Prof.ª Andréa Góes, do Departamento de Ensino de Ciências e Biologia da UERJ, por ter me iniciado na ciência, ensinando-me os primeiros passos dentro da vida acadêmica.

Ao Prof. Ulisses Gazos Lopes e ao Aislan (aluno de mestrado na época) do Instituto de Biofísica da UFRJ, local onde realizei os primeiros experimentos de ChIP, por me ter concedido o anticorpo anti-histona total H3.

Ao Yegor Vassetzky, diretor de pesquisa do CNRS e chefe do laboratório de Cromatina, Desenvolvimento e Câncer; à Manel, Yara, Ana e Diana; ao Pietr, Andrei, Charlie Henry, Vasily e todos os demais da unidade de pesquisa UMR-8126, do Instituto Gustave Roussy onde realizei o meu doutorado sanduíche em Paris, França, e 90% dos ensaios de ChIP. Agradeço também à Chloe, do Laboratório do Desenvolvimento de Ferramentas Proteômicas para Estudo dos Mecanismos Epigenéticos, chefiado pelo prof. Vasily Ogryzko, por ter me fornecido inúmeras alíquotas dos anticorpos anti-H3k4me3 e anti-H3k9me3.

Ao Prof. Marcelo Rosado Fantappié do Instituto de Bioquímica Médica da UFRJ pelas discussões e idéias pertinentes para os meus experimentos em seu laboratório. Agradeço também ao Vitor, por ter me concedido uma alíquota do anticorpo anti-H3Ac, e a todos os demais integrantes do laboratório por terem me ensinado a técnica de Gel-Shift, incluindo o manuseio de radioisótopos e todos os demais equipamentos necessários.

A todos do Laboratório de Micologia Celular e Proteômica (LMCprot) da UERJ, por terem me permitido utilizar o espectrofotômetro, o leitor de ELISA para

dosagem de proteínas, e o ultra-freezer -80˚C para armazenamento dos extratos de proteínas.

A todos do Laboratório de Ciências Radiológicas (LCR) da UERJ, por terem me cedido o sistema de corrida e transferência para Western Blot e pelo empréstimo de alguns reagentes, quando necessário.

Ao técnico Paulo, do laboratório da prof.ª Marsen do Departamento de Bioquímica da UERJ, por me ajudar a utilizar o sonicador, e a todos do laboratório da Prof.ª Jacyara, do mesmo departamento, por me deixarem utilizar o fotodocumentador para as fotos dos géis de agarose.

A todos do Laboratório de Biologia Molecular de Tumores (LBMT), onde realizei todo o meu doutorado, por sempre me ajudarem e fornecerem todo o apoio necessário. Agradeço à Luiza, por sempre trazer discussões e nova idéias pertinentes aos experimentos; à Ana Silva, que realizou toda a parte de imunofluorescência, sempre ajudando, quando necessário.

A natureza tem perfeições que mostram que é a imagem de Deus, e defeitos que mostram que é apenas a imagem

Blaise Pascal

RESUMO

SANTOS JUNIOR, Gilson Costa dos. **Estudo da cromatina nos sítios de fixação à matriz nuclear no domínio do gene *TP53* e das modificações epigenéticas e no modelo de progressão tumoral mamária 21T**. 2014. 137 f. Tese (Doutorado em Biociências) – Instituto de Biologia Roberto Alcântara Gomes, Universidade do Estado do Rio de Janeiro, Rio de Janeiro, 2014.

Dentre os diversos tipos de câncer agressivos, o câncer de mama é o mais comum em mulheres. Mutações hereditárias e adquiridas, assim como alterações epigenéticas atuam em sinergia na carcinogênese mamária e na progressão tumoral. A proteína P53 é uma supressora de tumor e possui uma atuação fundamental na integridade genômica. Apesar do vasto conhecimento sobre o controle da P53 a nível de proteína, ainda pouco se sabe sobre o controle transcricional do gene *TP53*. A série 21T, uma série de 4 linhagens celulares originadas da mama da mesma paciente, representando diferentes estágios de progressão tumoral mamária, é um eficiente modelo para investigação das alterações epigenéticas e suas influências na expressão gênica ao longo da progressão do câncer de mama. Nós analisamos a organização do domínio do gene *TP53* através da técnica de arranjo de DNA, em diversas linhagens celulares de câncer de mama e linhagens controle, e realizamos uma tentativa de caracterizar estes elementos de DNA nas linhagens controle não-tumorais HB2 e MCF10A e nas tumorais MCF-7, MDA-MB-231, T47D, através dos marcadores epigenéticos de eucromatina, H4Ac, e heterocromatina, H3K9me3. Ainda analisamos a ligação de proteínas à região associada à matriz nuclear (MAR), denominada MAR 2, e a possível ligação da proteína ligante à matriz nuclear (MARBP), PARP-1, através de ensaios de gel shift (EMSA). Detectamos que na linhagem controle epitelial mamária, HB2, o gene *TP53* está posicionado num domínio de DNA relativamente pequeno, aproximadamente 50 kb, delimitado por dois sítios de fixação à matriz nuclear. Interessantemente, esta estrutura de domínio se apresentou radicalmente diferente nas linhagens de câncer de mama estudadas, MCF7, T47D, MDA-MB-231 e BT474, nos quais o tamanho do domínio estudado estava aumentado e a transcrição do *TP53* diminuída. Os enriquecimentos com os marcadores epigenéticos de cromatina H4Ac e H3K9me3 estão diferentemente distribuídos nas MARs nas linhagens celulares. Surpreendentemente, a MAR 2 apresentou uma ligação altamente específica, o que poderia representar a atuação de fatores transcricionais envolvidos na organização da cromatina. Através de programas de bioinformática, detectamos putativos sítios para interessantes fatores de transcrição, tais como o c/EBP-beta e c-myb, que poderiam atuar em *cis* regulando a expressão do gene *TP53* e outros flanqueadores. Nós propusemos um modelo para a organização da cromatina na região de domínio do gene *TP53* com os genes flanqueadores. Através da série 21T, detectamos uma hipometilação global genômica, nas células cancerosas 21NT e 21MT1. Uma importante diminuição da expressão global do marcador H4Ac nas células metastáticas 21MT1, foi detectada em relação às outras linhagens. Os níveis de RNAm das principais enzimas relacionadas as modificações epigenéticas são consistentes com as observadas hipometilação genômica e hipoacetilação. Através de microscopia confocal, verificamos que o marcador H4Ac está localizado, na maior parte na periferia e o marcador H3K9me3, pericêntrico nos núcleos tumorais. Por fim, verificamos que o promotor P1 do gene TP53 apresenta um estado de cromatina aberta, e a expressão do gene *TP53* é similar em todas as células da série 21T.

Palavras- chave: Câncer de mama. Cromatina. Loop. MAR. Epigenética. *TP53*.

ABSTRACT

SANTOS JUNIOR, Gilson Costa dos. **MARs chromatin study on *TP53* gene domain and epigenetic modifications in a breast cancer progression model**. 2014. 137 f. 2014. 137 f. Tese (Doutorado em Biociências) – Instituto de Biologia Roberto Alcântara Gomes, Universidade do Estado do Rio de Janeiro, Rio de Janeiro, 2014.

Breast cancer is the most common aggressive cancer type in women. Inherited and acquired mutations as well as epigenetic alterations act together in breast carcinogenesis and tumor progression. P53 is a tumor suppressor protein critical for genome integrity. Although its control at the protein level is well known, the transcriptional regulation of the *TP53* gene is still unclear. The 21T series, a series of 4 breast cell lines originating from the same patient and representative of the breast tumor progression stages, is a suitable model to investigate epigenetic alterations and their influences upon gene expression during breast tumor progression. We have analyzed the organization of the TP53 gene domain using DNA arrays in several breast cancer and control cell lines and we made an attempt to characterize these DNA elements in breast non-cancerous cell lines HB2 and MCF-10, and cancerous MCF-7, MDA-MB-231 and T47D, through the determination of epigenetic markers of euchromatin, H4Ac, and heterochromatin, H3K9me3. We further analyzed the matrix attachment region (MAR), named MAR 2, protein binding, and possible MAR 2 binding of the important MAR binding protein (MARBP), PARP-1, by Electrophoretic mobility Shift Assay (EMSA). We have found that in the control breast epithelial cell line, HB2, the TP53 gene is positioned within a relatively small DNA domain, encompassing 50 kb, delimited by two nuclear matrix attachment sites. Interestingly, this domain structure was found to be radically different in the studied breast cancer cell lines, MCF7, T47D, MDA-MB-231 and BT474, in which the domain size was increased and TP53 transcription was decreased. H4Ac and H3K9me3, chromatin epigenetic markers enrichment are differentially distributed through MARs in cell lines. Surprinsingly, MAR 2 presented a defined band-shift, which could represent trans-acting factor(s), involved in chromatin organization. By bioinformatics software, we found interesting transcription factors putative binding sites, such as for c/EBP-beta and c-myb, which could be cis-acting elements regulating *TP53* and neighboring genes expression. We propose a model for the chromatin organization of the *TP53* gene domain with neighboring genes. Through 21T cell line series, we detected a global genomic hypomethylation profile in the cancerous 21NT and 21MT1. An important global decrease of the active chromatin mark H4Ac in the metastatic 21MT1 relative to other cell lines was detected. mRNA levels of key enzymes linked to epigenetic modifications are consistent with the observed genomic hypomethylation and hypoacetylation. By confocal immunofluorescent assay we observed that H4Ac is mostly located at periphery, and the repressive mark H3K9Me3 located pericentric, in tumorigenic cells nuclei. *TP53* P1 promoter in 21T series was found to be in an open state and *TP53* transcription level was found to be similar in all 21T cell lines.

Keywords: Breast cancer. Chromatin. Loop. MAR. Epigenetics. *TP53*.

LISTA DE ILUSTRAÇÕES

LISTAS DE ABREVIATURAS E SIGLAS

DNA	Ácido desoxirribonucléico
pb	Pares de base
kb	Kilobase
RNA	Àcido ribonucléico
RNAm	Àcido ribonucléico mensageiro
PCR	Reação em cadeia da polimerase
S/MARs	*Scaffold/Matrix attachment regions*
MN	Matriz nuclear
NaCl	Cloreto de Sódio
SARs	*Scaffold attachment regions*
LIS	Lítio 3,5-diiodosalicilato
HAT	Histona acetil-transferase
HDAC	Histona desacetilase
KAT	Lisina acetil-transferase
SAM	S-adenosil-metionina
HMT	Histona metil-transferase
DNMT	DNA metil-transferase
ICG	Ilha CpG
TSS	Início do sitio de transcrição
BUR	Região de despareamento de base
MARs	*Matrix attachment regions*
TRIS	Tris(hidroximetil)aminometano
HCl	Ácido clorídrico
KCl	Cloreto de potássio
PMSF	Fluoreto de fenilmetilsulfonilo
EDTA	Ácido etilenodiamino tetra-acético
$CaCl_2$	Cloreto de cálcio
$MgCl_2$	Cloreto de magnesio
$CuCl_2$	Cloreto de cobre
TE	Tris-EDTA

H_2O	Molécula da água
qPCR	PCR quantitativo
RT-qPCR	Reação de transcriptase reversa seguida de PCR quantitativo
cDNA	DNA complementar
pH	Potencial de hidrogênio
ChIP	Imunoprecipitação da cromatina
EMSA	*Eletrophoretic Mobility Shift Assay*
PBS	Tampão fosfato salino
SDS	Docecil sulfato de sódio
PAGE	Eletroforese em gel de poliacrilamida
PIC	Coquetel inibidor de proteases
DTT	ditiotreitol
Poly dI-dC	Ácido polideóxiinosínico e deóxicitidílico
BSA	Albumina soro bovino
ROI	Região de interesse
S.E.M.	Erro padrão das médias
ANOVA	Análise de múltipla variância

LISTA DE SÍMBOLOS

µm	micrometro
nm	nanometro
M	molar
%	porcentagem
mL	mililitro
g; xg	força G
min	minutos
˚C	grau Celsius
µCi	microcurie

SUMÁRIO

INTRODUÇÃO

Dentre os diversos tipos de câncer agressivos, o câncer de mama é o mais comum em mulheres. Mutações hereditárias e adquiridas, assim como alterações epigenéticas atuam em sinergia na carcinogênese mamária e na progressão tumoral. A proteína P53 é uma supressora de tumor e possui uma atuação fundamental na integridade genômica. Apesar do vasto conhecimento sobre o controle da P53 a nível de proteína, ainda pouco se sabe sobre o controle transcricional do gene *TP53*. A série 21T, uma série de 4 linhagens celulares originadas da mama da mesma paciente, representando diferentes estágios de progressão tumoral mamária, é um eficiente modelo para investigação das alterações epigenéticas e suas influências na expressão gênica ao longo da progressão do câncer de mama. Nós analisamos a organização do domínio do gene *TP53* através da técnica de arranjo de DNA, em diversas linhagens celulares de câncer de mama e linhagens controle, e realizamos uma tentativa de caracterizar estes elementos de DNA nas linhagens controle não-tumorais HB2 e MCF10A e nas tumorais MCF-7, MDA-MB-231, T47D, através dos marcadores epigenéticos de eucromatina, H4Ac, e heterocromatina, H3K9me3. Ainda analisamos a ligação de proteínas à região associada à matriz nuclear (MAR), denominada MAR 2, e a possível ligação da proteína ligante à matriz nuclear (MARBP), PARP-1, através de ensaios de gel shift (EMSA).

1 **A CROMATINA**

Um dos aspectos mais intrigantes do núcleo de uma célula eucariótica é a sua capacidade de empacotamento do DNA formando uma estrutura altamente organizada, complexa e que pode se encaixar perfeitamente dentro de um espaço muito limitado, de aproximadamente 10 µm. Esta estrutura é denominada cromatina e é constituída principalmente por DNA e proteínas (1).

Os nucleossomos formam a unidade básica organizacional da cromatina, e são constituídos pelas histonas H2A, H2B, H3, H4 e H1, 145 pb do DNA que vai circundar o *core* nucleossômico (dímeros das histonas H2A, H2B, H3 e H4), e a região do DNA ligadora (DNA *linker*), de aproximadamente 10-80 pb e associada a histona H1 (2).

O complexo DNA-nucleossomo forma uma fibra de 10 nm de diâmetro se assemelhando a um colar de pérolas (*beads on a string*) (3,4), conforme mostra a Figura 1. A fibra de 10 nm possui a capacidade *in vitro* de formar uma fibra helicoidal ainda mais complexa de 30 nm de diâmetro, contendo de 6 a 11 nucleossomos por cada volta, que possui a capacidade de formar uma fibra ainda mais complexa de 200-300 nm na interfase, chamada cromonema (5–7).

Na fase de metáfase da mitose, o complexo se encontra no seu estado máximo de empacotamento chegando a 1400 nm de diâmetro e foi neste alto nível de ordem da cromatina que este complexo, visualizado por microscopia ótica densamente corado, recebeu o nome de cromossomo (derivado da palavra grega utilizada para “corpo colorido”). Entretanto, o termo cromossomo também se refere a molécula de ácido nucléico que armazena a informação genética nos mais diversos organismos (2,8,9).

Durante décadas, a cromatina foi subdividida em dois tipos clássicos: eucromatina (forma mais relaxada de cromatina e mais permissiva à maquinaria de transcrição) e heterocromatina (forma mais compacta e menos acessível à maquinaria de transcrição), através da marcação clara e escura observadas na microscopia eletrônica, respectivamente (10). Porém, nos últimos anos, foram classificados 5 diferentes tipos de cromatina baseados no enriquecimento de proteínas não-histônicas em células de *Drosophila* Kc167 (11) e 51 diferentes tipos

de cromatina baseados no enriquecimento de modificações epigenéticas específicas nas histonas em células T humanas CD4+ (12).

As regiões de heterocromatina estão geralmente localizadas nos domínios de associação ao nucléolo (NADs- *Nucleolus-Associated Domains*) (13) e nos domínios de associação à lamina (LADs- *Lamina-Associated Domains*) (14), sendo esta localizada principalmente na periferia interna do núcleo onde existe uma quantidade baixa de genes. Entretanto, as regiões de eucromatina estão localizadas na maior parte, no centro do núcleo e são regiões que possuem uma quantidade maior de genes (15,16).

1.1 **Sítios de fixação à matriz nuclear**

Além de apresentar diferentes níveis de empacotamento, a fibra de cromatina pode ser organizada em domínios de *loops* com tamanhos entre 4 e 200 kb que são delimitados por seqüências de DNA, com tamanho entre 100 e 1000 pb, denominadas S/MARs (*Scaffold* or *Matrix Attachment Regions*), que se ligam a proteínas da matriz nuclear (17–20), conforme mostra a Figura 1.

A matriz nuclear (MN) também pode ser chamada de *nuclear scaffold* ou esqueleto nuclear, dependendo da técnica utilizada para a sua extração. Para a extração da matriz nuclear e estudo das MARs, realiza-se a extração por alta concentração salina (2,0 M NaCl) (21). Entretanto, para a extração do *nuclear scaffold* ou esqueleto nuclear e estudo das SARs (*Scaffold Attachment Regions*), realiza-se a extração utilizando Lítio 3,5-diiodosalicilato (LIS) (22) ou eletroforese com encapsulamento das células em agarose sob concentrações salinas fisiológicas, possibilitando a extração do núcleo e MN intactos (23–25).

A MN é formada pela lamina nuclear e uma extensa rede de fibras protéicas interconectadas à lamina nuclear e distribuídas por todo o núcleo (26). Longe desta aparente complexidade estática, a MN é uma estrutura extremamente dinâmica que funciona como uma grande plataforma organizacional que estabelece domínios estruturais e funcionais no núcleo (27). Uma boa descrição da MN talvez seja: “Uma esponja dinâmica com compartimentos abertos para a livre difusão no nucleoplasma” (28,29).

Figura 1 - Compactação da cromatina em eucariotos

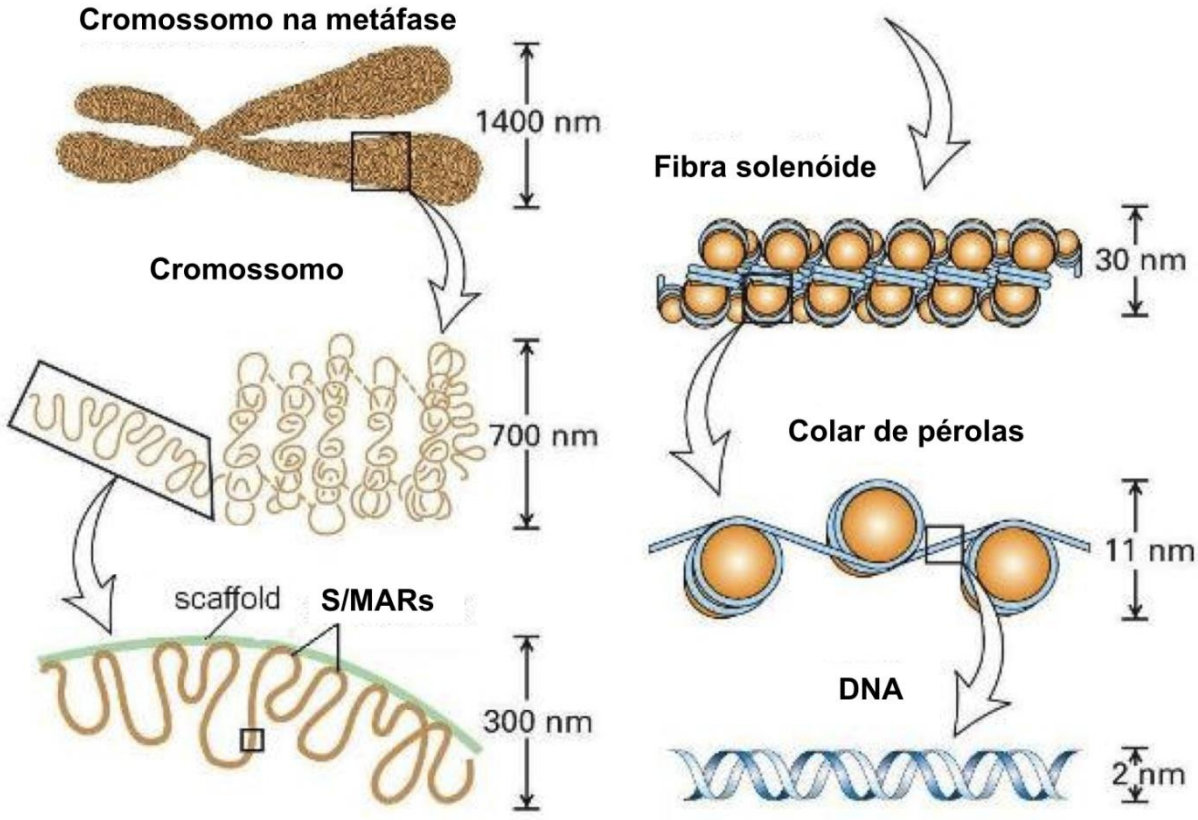

Legenda: Este modelo mostra os diferentes níveis de organização da cromatina. Primeiro o DNA circunda os octâmeros de histonas, depois a histona H1 estimula a formação da fibra de cromatina de 30 nm. Os níveis mais complexos são até hoje objeto de estudo e não são tão uniformes como os mostrados aqui. As S/MARs são responsáveis pela conexão entre a cromatina e a matriz nuclear

Fonte: Adaptado de http://www.genomasur.com/BCH/BCH_libro/capitulo_03.htm) (30).

As MARs estão co-localizadas com a origem de replicação (31,32), sítios de topoisomerases II (33,34) e apesar de não terem uma seqüência consenso, as MARs são regiões ricas em AT, estão em regiões onde o DNA possui uma curvatura e torção incomum e em regiões que estão mais propensas ao despareamento das bases (BURs-*Base Unparing Regions)* (35). Também apresentam uma desestabilização no duplex induzida por estresse (SIDD; *stress induced duplex destabilization*) e exacerbada flexibilidade (36).

Todas estas características anteriores são utilizadas por programas como o MAR-Wiz (http://www.futuresoft.org/) e SMARTest (http://www.genomatix.de/cgi-bin/smartest_pd/smartest.pl) para a predição *in-silico* de MARs putativas. No entanto, o uso destas ferramentas de bioinformática deve ser cauteloso (37).

Os sítios no DNA de fixação à matriz nuclear estão freqüentemente co-localizadas com acentuassomos ou com a periferia dos genes. Quando associadas aos acentuassomos, MARs podem estimular a expressão dos genes, aumentando a acessibilidade à cromatina, porém, quando estão localizadas entre o promotor e o acentuassomo, elas podem interferir na interação promotor-acentuassomo (38–46).

Além da importância na regulação da expressão gênica, algumas MARs são extremamente dinâmicas e podem fazer com que os *loops* de DNA se movam de forma seqüencial, como se deslizassem na MN durante a replicação (47,48). Os *loops* de DNA podem passar a ficar ancorados à MN como condição *sine qua non* para a expressão de alguns genes, através do remodelamento da cromatina, e resultando em uma nova conformação, permissiva à transcrição (49,50).

Diversos modelos foram propostos ao longo dos anos para elucidar a dinâmica de remodelamento da cromatina e o rearranjo dos *loops* de DNA, conforme mostra a Figura 2. Os primeiros estudos trouxeram a idéia do conceito de *loops* de cromatina intermitentes (Fig. 2A) (51,52). Estudos mais recentes atualizaram este modelo com a inclusão de *loops* de diferentes tamanhos, somando-se a observação de S/MARs que são facultativas (53) e de que não só pelo fato de uma seqüência ser uma potencial S/MAR, ela será recrutada pela MN (54) (Fig. 2B).

Mais tardiamente, uma série de estudos mostraram que as origens de replicação tem um potencial para se associarem à matriz nuclear, porém esta associação não é constitutiva, sendo recrutada tardiamente na fase G1 e perdida durante a fase S (Fig. 2C) (55–57). Contudo, é possível imaginar que o agrupamento das origens de replicação permitiria uma grande economia de energia, uma vez que a alta concentração dos diversos fatores recrutados pela maquinaria de replicação num mesmo espaço possibilitaria um processamento mais eficiente (58).

Além da dinâmica dos *loops*, as MARs quando existem dentro de um gene, podem levar ao silenciamento deste. O mesmo não acontece nas SARs, pois quando ocorrem montante à algum gene estimulam a sua expressão (59). As S/MARs estão associadas à regiões pobres em genes e regulam a expressão do conjunto de genes específicos para um determinado tipo celular, incluindo mudanças no fenótipo (60).

Ao contrário dos *loops* de DNA, as S/MARs são em geral regiões resistentes à digestão por DNase I devido à forte associação com a MN (61,62), ainda, podem ser herdadas por *imprinting* paterno e são específicas para cada tecido (63). As

S/MARs também podem ser utilizadas em vetores episssomais para a restauração de um gene inativado para o estado selvagem (64).

Figura 2 - Possíveis interações entre a replicação do DNA e a MN

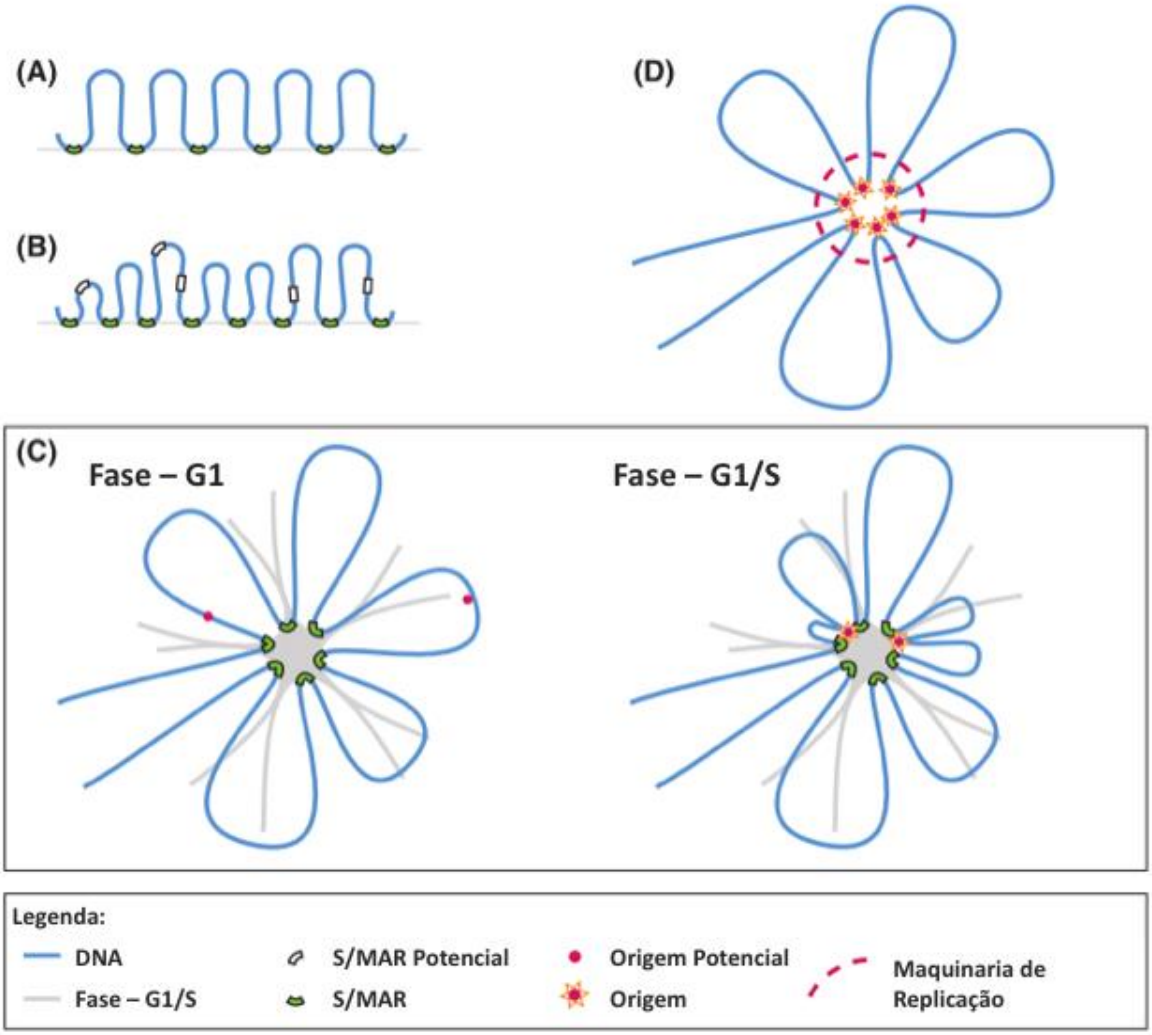

Legenda: (A) O DNA é periodicamente fixado à matriz nuclear nas S/MARs formando *loops* intercalados. (B) Modelo refinado ilustrando a variação no tamanho dos *loops* incluindo as S/MARs utilizadas e potenciais. (C) Modelo mostrando a fixação à matriz nuclear através de S/MARs não associadas à origem de replicação e o recrutamento de regiões de origem de replicação concomitantes às S/MARs na fase G1/S do ciclo celular com impacto no tamanho do *loop*. (D) Representação dos *loops* de cromatina mostrando as regiões de origem de replicação associadas à maquinaria de replicação, sem a representação da MN. A estrutura de *loops* de DNA unidos à MN é chamada de halo.
Fonte: Adaptado de Coverley & Wilson, 2013 (65).

Diversas proteínas podem se ligar as S/MARs, sendo que algumas delas fazem parte da MN, como as laminas, matrinas, topoisomerases II e outras relacionadas a um tipo celular, a uma sinalização celular específica, no

desenvolvimento do câncer e inativação do cromossomo X, como a hnRNP-U/SAF-A, SATB1, SMAR1 e PARP-1 (66,67).

1.2 **Modificações epigenéticas**

A cromatina em seus diferentes níveis de organização, desde a simples molécula de DNA aos complexos *loops* de DNA e sítios de fixação à matriz nuclear, pode sofrer uma série de modificações sem que haja alterações na seqüência de DNA, e estas modificações são denominadas epigenéticas.

A epigenética foi primeiramente descrita em 1942, como o ramo da biologia que estuda a interação causal entre os genes e seus produtos, responsáveis pela formação do fenótipo. Entretanto, em 2008, devido às novas descobertas, ela foi redefinida como o estudo dos fenótipos estáveis herdáveis resultantes de mudanças cromossômicas, mas sem quaisquer alterações na seqüência de DNA (68,69).

Dentre as modificações epigenéticas mais importantes, podemos destacar a acetilação e a metilação que ocorrem nas lisinas dos domínios N-terminais das histonas, e a metilação no DNA. Estas diferentes modificações podem influenciar drasticamente no balanceamento entre a eucromatina e heterocromatina, e também podem estar associadas às regiões promotoras e acentuassomos, conforme mostra a Figura 3.

A acetilação nas histonas é um processo reversível, está fortemente associada à transcrição, replicação, reparo do DNA (70–73) e o processo de acetilação nas lisinas das histonas é ordenado. Dentre muitos, podemos destacar o processo de acetilação que ocorre na histona H4 em mamíferos, pois este começa na lisina 16, depois segue uma ordem progressiva acetilando a lisina 8 ou 12, e por fim a lisina 5. Além do mais, a histona H4 é acetilada no citoplasma e depois é incorporada junto à cromatina no núcleo (74–77).

A acetilação e desacetilação das histonas é catalisada pelas histonas acetil-transferases (HATs) e histonas desacetilases (HDACs), respectivamente. Dentre as diversas HATs, a HAT1 (KAT1) é a mais importante para a acetilação da histona H4

Figura 3. Modelo de estrutura do epigenoma em células humanas normais

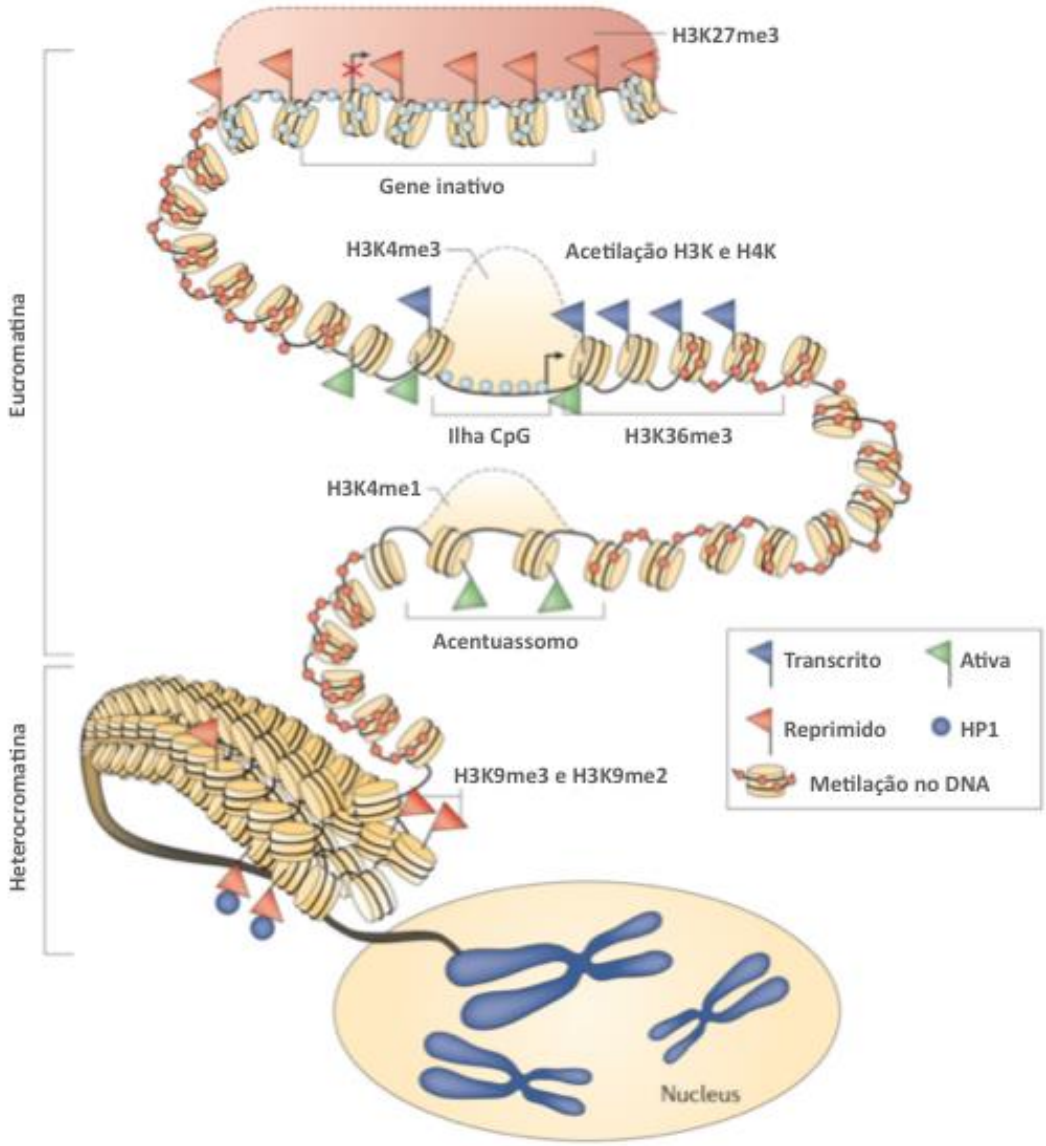

Legenda: Este diagrama mostra o estado balanceado da cromatina, o posicionamento dos nucleossomos e a metilação no DNA, que mantêm o estado normal de empacotamento do DNA. Um gene silenciado (indicado por um X vermelho sobre o início do sítio de transcrição designado por uma seta) no topo da figura, tem a ilha CpG na região promotora ocupada por um complexo, denominado *Polycomb Group* (PcG), indicado na área sombreada vermelha, associado a trimetilação na lisina 27 da histona H3 (H3K27me3), marcador de heterocromatina facultativa. Não existe metilação na lha CpG na região promotora do gene (mostrado pelas bolas azul-claros) e os nucleossomos estão posicionados no início dos sítios de transcrição. Sítios montantes ao promotor são intensamente metilados (mostrado pelas bolas vermelhas). O promotor do gene ilustrado abaixo do gene silenciado possui um estado transcricional totalmente ativo e possui o marcador de cromatina ativa H3K4me3. O mesmo acontece com a acetilação das lisinas das histonas H3, H4 e o marcador H3K36me3 no corpo do gene para facilitar alongamento transcricional. A região de início do sitio de transcrição (indicado por uma seta) não é ocupado por nucleossomos. Mais abaixo, um acentuassomo distal é mostrado para o mesmo gene ativo, com uma configuração nucleossômica característica de ativação transcricional e um marcador típico de acentuassomo, o H3K4me1, está presente. Finalmente, na parte inferior da figura, o empacotamento da maior parte do DNA celular

numa configuração de cromatina inativa, com os nucleossomos compactados, presença dos marcadores de heterocromatina constitutiva H3k9me2, H3K9me3, presença da proteína da heterocromatina 1 (HP1 ou CBX5) e extensa metilação no DNA.

Fonte: Adaptado de Baylin & Jones, 2011 (78).

e a acetilação ocorre através da transferência do grupo acetil do cofator acetil-Coenzima A para as lisinas 5 e 12 da histona H4 (79–81).

Diferente da acetilação, a metilação nas histonas pode estar relacionada tanto à ativação quanto à repressão da transcrição, conforme mostra a Figura 3. A metilação ocorre através da transferência do radical metil da S-adenosil-L-metionina (SAM), tanto nas histonas como no DNA e é mediada por histonas metil-transferases (HMTs) e DNA-metil-transferases (DNMTs).

De modo semelhante à metilação, a desmetilação nas histonas é mediada por histonas demetilases (HDMs), entretanto no DNA, é um processo mais complexo e ainda em estudo, mas já se sabe que é mediado por dois fatores, TET1 (tet metil-citosina digoxigenase 1) e TDG (timina DNA-glicosidade) (82).

Nas histonas de mamíferos, a metilação ocorre em todos os resíduos básicos das histonas (argininas, lisinas e histidinas), sendo que somente os resíduos de lisina das histonas podem ser monometilados (me1) ou dimetilados (me2) ou trimetilados (me3) (83).

A trimetilação é uma das modificações mais estudadas e podemos destacar as 3 mais importantes, que são, a trimetilação na lisina 4 da histona H3 (H3K4me3), a trimetilação na lisina 27 da histona H3 (H3K27me3) e a trimetilação na lisina 9 da histona H3 (H3K9me3). Estes diferentes marcadores epigenéticos executam papéis cruciais no processo de manutenção da pluripotência, diferenciação de células tronco embrionárias em células maduras (84) e equilíbrio da eucromatina/heterocromatina (85).

A modificação H3K4me3, associada à ativação gênica, e a modificação H3K27me3, associada à repressão gênica, catalisadas pelo grupo *trithorax* (TrxG) e pelo grupo *polycomb* (PcG), respectivamente, são marcadores epigenéticos essenciais para o desenvolvimento celular (84,86,87).

Regiões promotoras, ricas em ilhas CpGs, de genes fortemente relacionados ao desenvolvimento em células tronco embrionárias em humanos e camundongos, apresentam um grande enriquecimento de ambos os marcadores H3K4me3 e H3K27me3, fazendo com que o domínio destes genes sejam denominados domínios bivalentes (84,86,87).

Os genes localizados nestes domínios estão de maneira geral silenciados em células pluripotentes, porém ao longo da diferenciação celular, este domínio passa a ser monovalente, contendo somente um dos marcadores. Esta mudança pode resultar na ativação (enriquecimento do promotor com H3K4me3) ou na manutenção do silenciamento do gene (enriquecimento do promotor com H3K27me3) de forma específica para cada linhagem celular e também permite uma maior plasticidade nas células tronco (84,86,87).

A modificação H3K9me3 está associada à formação da heterocromatina constitutiva, principalmente pericentromérica, o que a torna um excelente marcador de cromatina inativa ou silenciada (85). A presença da trimetilação na lisina 9 da histona H3 permite uma forte interação com a proteína da heterocromatina 1 (HP1), que vai participar na manutenção da heterocromatina (88), conforme a ilustração na Figura 3.

Para a formação do marcador H3K9me3, primeiramente a histona H3 sofre a modificação H3K9me1 no citoplasma, através da ação das HMTs, Prdm3 e Prdm16. Esta histona pré-metilada é depois incorporada na cromatina através de regiões satélites no genoma, previamente ligadas aos fatores de transcrição Pax3 e Pax9, e sofre a conversão para H3K9me3 através da ação da HMT, SUV39H1 (KMT1A). Somente após o estabelecimento deste marcador na heterocromatina ocorre a ligação da proteína HP1 (89).

Diferentemente das histonas, a metilação e desmetilação do DNA não é tão dinâmica. A metilação no DNA ocorre principalmente no carbono 5 de uma citosina (formando a 5-metil-Citosina; 5mC), levando à formação de uma ligação carbono-carbono (C-C) que necessitará de uma grande quantidade de energia para sua quebra. Portanto, isto faz com que a desmetilação no DNA, ao contrário das histonas, seja um processo de maior complexidade (82).

A maior parte dos estudos têm focado na ocorrência de 5mC em sítios de DNA ricos em CpGs (dinucleotídeos citosina e guanina), chamadas ilhas CpGs (ICGs). Estes sítios estão em mais da metade dos genes, localizados principalmente em regiões promotoras, ausente de nucleossomos, perto do início do sítio transcricional (TSS) em vertebrados e possuem aproximadamente 1 kb (90).

A metilação em ICGs em regiões promotoras está associada ao silenciamento gênico, principalmente quando estes estão localizados em regiões de heterocromatina, enriquecidas com o marcador H3K9me3 (Figura 3), onde existe um

estado repressivo de longo prazo, como o cromossomo X inativo e regiões de *imprinting* (90).

Também podemos destacar a presença da 5mC em ICGs nos promotores de genes que estão silenciados somente em células somáticas, e de genes inativos em tecidos específicos (90).

A ocorrência da 5mC em sítios pobres em CpGs, como dentro de alguns genes, ocorre em uma forma tecido-específica e não está associada à repressão da transcrição (91,92). Entretanto, a presença da 5mC é crucial para o silenciamento dos elementos de transposição (93).

A formação da 5mC no DNA é catalisada por 3 DNMTs: DNMT1, DNMT3a e DNMT3b. A DNMT1 é responsável por metilar as novas fitas de DNA sintetizadas, copiando o padrão de metilação da fita molde, possui uma preferência por DNAs hemi-metilados como substrato e por isso ela tem a função de manter o padrão de metilação no DNA, gerado após a implantação do embrião, ao longo da divisão celular (94,95)

A DNMT3a e DNMT3b, são responsáveis pela metilação denominada *de novo*, restaurando o padrão inicial de metilação do início do desenvolvimento embrionário e diferentemente da DNMT1, não possuem preferência por DNAs hemi-metilados como substrato (95,96).

Além das duas enzimas DNMT3a/b, existe uma variante denominada DNMT3-*like* (DNMT3L), que forma os sub-complexos heterodiméricos DNMT3a:DNMT3L ou DNMT3b:DNMT3L, aumentando a afinidade pela SAM e uma maior atividade catalítica (97–99).

A ação *de novo* da DNMT3a:DNMT3L e DNMT3b:DNMT3L, em ICGs perto dos TSS e ausentes de nucleossomos, pode ser reprimida pela presença da modificação H3K4me3 (associada a regiões de cromatina ativa) nos nucleossomos flanqueadores (100). Isto pode corroborar a ausência de metilação nestas regiões e manutenção da expressão gênica, conforme mostra a Figura 3.

A presença da hipermetilação e inibição da transcrição gênica na heterocromatina em regiões satélites é realizada através da ação da DNMT3b:DNMT3L e interação desta com a HP1 e SUV39H1, responsável pela modificação H3K9me3 (101,102). Um outro estudo corroborou a interação da DNMT3b:DNMT3L com a SUV39H1 e HP1, e mostrou que a DNMT3a:DNMT3L e a DNMT1 também interagem com as mesmas (101).

A presença da metilação no DNA, estimula a interação do DNA metilado com proteínas denominadas MBDs (*Methyl Binding Domains*). Estas proteínas recrutam HDACs que vão desacetilar as histonas, tornando-as permissíveis à ação de HMTs (103,104). Como exemplo, Hashimshony et al. em 2003, descreveram a presença da metilação no DNA em regiões com baixo enriquecimento de H4Ac e um alto enriquecimento de H3K9me3 (105).

Não obstante as muitas interações entre as modificações epigenéticas no DNA e nas histonas, ainda existe a atuação sinérgica dos sítios de fixação à matriz nuclear, essenciais nas alterações da cromatina. Estas alterações têm sido cada vez mais estudadas e associadas principalmente ao desenvolvimento do câncer.

1.3 **Estado da cromatina e modificações epigenéticas no câncer**

Dentre as inúmeras mudanças drásticas que ocorrem no núcleo de uma célula cancerosa, a deformação na distribuição da heterocromatina periférica, incluindo a formação de agregados no centro/pericentro nuclear e perda global da compactação, tem sido destacada através de microscopia, e associada à carcinomas de alta malignidade e prognóstico ruim (106,107).

Como já mencionado anteriormente, a heterocromatina pode ser classificada em constitutiva e facultativa, sendo que cada tipo de heterocromatina é definida pelas modificações H3K9me3 e H3K27me3, respectivamente. Estas modificações podem apresentar diferentes perfis de expressão global, nos diferentes tipos de câncer e também nos prognósticos.

A alta expressão global da modificação H3K9me3, tem sido associada ao adenocarcinoma gástrico e baixa sobrevivência. Entretanto, a baixa expressão global da modificação H3K27me3, tem sido associada ao câncer de mama, câncer pancreático e câncer de ovário, também com baixa sobrevivência (83).

Os diferentes perfis de expressão das histonas é mediado principalmente pelas HMTs. Sabe-se que a desregulação das HMTs têm sido associada a diversos tipos de doenças, e de aproxidamente 50 lisina e arginina metil-transferases codificadas pelo genoma humano, pelo menos 22 têm sido associadas com o câncer e outras doenças (108).

A HMT SUV39H1 é responsável pela manutenção da heterocromatina e atua na estabilidade genômica, porém quando ocorrem danos no DNA em células cancerosas, sua atividade pode ser comprometida, resultando na perda de suas funções (109). Esta HMT interage fisicamente com as HDACs 1, 2 e 3, em células de osteosarcoma, sugerindo que a repressão da transcrição pode ser conseqüência da interação com as HDACs (110).

Ao nível de RNAm, a expressão da SUV39H1 está associada à da DNMT1 no câncer colorretal (111) e a comprovação de que a proteína SUV39H1 interage fisicamente com as DNMTs 1, 3a e 3b, foi realizada em células cancerosas da linhagem HeLa (101). Estes estudos mostraram que existe uma cooperação entre a metilação no DNA e na histona H3 para a formação da cromatina repressiva.

A expressão do marcador H3K9me3 está mais elevada na maior parte dos cânceres em comparação as células normais e em fibroblastos normais que foram induzidos à senescência através do oncogene mutante *H-Rasv12*. Entretanto, o tratamento dos mesmos fibroblastos com o inibidor de HDAC, ácico valpróico, resulta em grandes perdas dos domínios de heterocromatina e menor expressão do marcador H3K9me3 (112).

Além da HMT SUV39H1, outra importante enzima catalisadora de modificações nas histonas e relacionada ao câncer é a HAT1. A alta expressão de HAT1 está associada a linfomas malignos (113), porém a baixa expressão já foi verificada em algumas linhagens de câncer, principalmente em carcinomas mamários, concomitante aos baixos níves de H4Ac (114). Além do mais, a acetilação na histona H4 está relacionada ao sistema de resposta a danos no DNA e a perda desta acetilação no câncer, pode levar ao mal funcionamento deste sistema (115).

As modificações epigenéticas nas histonas estão associadas ao desenvolvimento do câncer assim como a metilação no DNA. Tanto a hipometilação global genômica, quanto a hipermetilação na região promotora de alguns genes, vão atuar sinergicamente no desenvolvimento do câncer e também na manutenção do estado tumoral.

A hipometilação global genômica, está fortemente associada à reestruturação da cromatina e desorganização do núcleo em células cancerosas, levando a instabilidades cromossômicas. Já a hipermetilação em regiões promotoras,

principalmente de gene supressores de tumor, pode levar à repressão da transcrição em células cancerosas (116).

A hipermetilação local no câncer, ocorre principalmente em ICGs, e pode resultar numa maior incidência de desaminação da 5mC em timina e da transição de CpG para TpG. Esta mutação é detectada em regiões promotoras de alguns genes supressores de tumor (117–119).

Em 2011, Daniel et al., listaram 10 genes supressores de tumor (*p15, p16, RASSF1, MLH1, MGMT, FHIT, DAP-K, APC, Caderina* e *RAR*) que sofrem hipermetilação na região promotora nos carcinomas, de cavidade oral, hepáticos, salivares, de cabeça e pescoço, colorretais, renais, de pulmão, nasofaringeais, de bexiga e pancreáticos (120).

Os efeitos da hipometilação global genômica observada em diversos tipos de câncer ainda não foram totalmente compreendidos. Alguns autores sugeriram que a hipometilação pode induzir a re-expressão de genes antes silenciados, como os oncogenes. Genes reativados pela hipometilação global incluem: genes imprintados, genes localizados no cromossomo X inativo, retrovírus endógenos, elementos de transposição e genes relacionados à resistência às drogas (121–123).

As enzimas catalisadoras da metilação no DNA, DNMT1 e DNMTs 3a/3b, possuem funções de manutenção e metilação *de novo* em células normais, respectivamente, entretanto na carcinogênese, ambas podem assumir as duas funções (124). Estas DNMTs apresentam elevados níveis de expressão, tanto à nível de RNAm quanto à nível de proteína, na grande maioria dos tecidos e linhagens celulares tumorais (120).

As alterações na cromatina associadas ao câncer, também ocorrem nas S/MARs, *loops* de DNA e na expressão das proteínas associadas a estas regiões. Como exemplo, a alta expressão das proteínas associadas à matriz nuclear PARP, Ku, HMGBs (I/Y), NMP e SAF-A/B é observada na transformação maligna e marca a transformação do fenótipo cancerígeno avançado para metástase (66).

Ao longo da progressão tumoral acompanhada da diminuição da diferenciação celular, os *loops* de cromatina também podem sofrer um intenso alongamento junto a diminuição dos sítios de fixação à matriz (125), conforme mostra a Figura 4.

Figura 4 - O organização dos loops de DNA nas células de câncer de próstata LNCa e PPC3

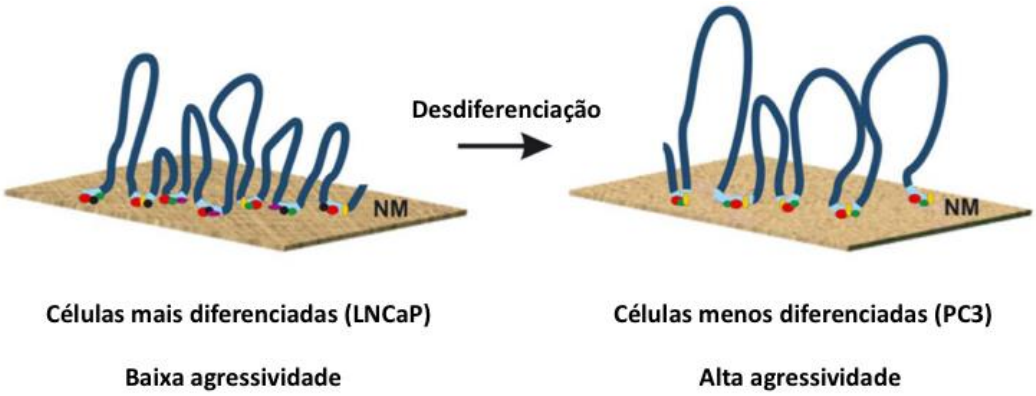

Legenda: Modelo esquemático da inter-relação entre os *loops* de DNA e a matriz nuclear (NM) na desdiferenciação de células de câncer de próstata. Nas células mais diferenciadas (LNCaP) a NM está mais bem organizada com muitas proteínas (em colorido) se ligando às MARs. Nas células PC3, onde desaparecem algumas regularidades estruturais da NM, um pequeno número de proteínas está ancorado à NM, resultando em *loops* mais largos.

Fonte: Adaptado de Barboro et al. 2012 (125).

Conforme mostrado anteriormente, todos os tipos de câncer estão associados à drásticas alterações na cromatina e na matriz nuclear. Entretanto, vale a pena ressaltar a importância destas associações especificamente com o câncer de mama, pois é um dos mais estudados e o segundo tipo mais freqüente no mundo (126).

1.3.1 Estado da cromatina e modificações epigenéticas no câncer de mama

A hipometilação global genômica pode estar associada ao concomitante maior enriquecimento no genoma dos marcadores de heterocromatina H3K9me3 e H3K27me3 no carcinoma ductal infiltrante, grau III, formando um complexo epigenoma característico de carcinomas mamários (127).

Esteller e Stefansson em 2013, listaram 10 genes que sofrem hipermetilação na ICG no promotor, *BRCA1, CDH1, RARB2, CDKN2A, PTEN, RASSF1, RUNX3, ESR1, PITX2* e *GSTP1*, no câncer de mama (128). Outros grupos identificaram

perfis distintos de metilação no DNA associados com diferentes tipos de câncer, diferente tecidos e subtipos de carcinomas mamários (129,130).

A presença do fenótipo de hipermetilação no DNA em ICGs no câncer de mama, denominado B-CIMP (*Breast CpG Island Methylator Phenotype*), está fortemente associada ao baixo risco de metástase e sobrevivência, enquanto a ausência do B-CIMP, está associada ao elevado risco de metástase e morte (131).

Os carcinomas mamários do subtipo luminal B, que apresentam os receptores de estrogênio, progesterona e HER-2 (*Human Epidermal Growth Factor Receptor* 2) positivos (RE +, RP + e HER-2 +) apresentam o fenótipo de hipermetilação no DNA, enquanto os carcinomas do subtipo basal, também denominado triplo negativo (RE -, RP -, HER-2 -), apresentam uma hipometilação no DNA (132). Os subtipos moleculares no câncer de mama serão mais bem discutidos adiante.

Concomitante à hipometilação global no DNA, algumas modificações epigenéticas nas histonas, como a hipoacetilação global na histona H4 tem sido observada na maior parte dos tumores de mamários. Esta hipoacetilação também tem sido fortemente associada a progressão tumoral mamária, desde o tecido normal, passando pelo carcinoma ductal in-situ, até o carcinoma invasivo (133). Em contrapartida, os altos níveis de acetilação e metilação globais nas histonas H4 e H3, estão associados com um diagnóstico favorável e ocorrem quase exclusivamente nos carcinomas do subtipo basal (134).

Estudos associando a expressão do marcador de heterocromatina H3K9me3 e da HMT SUV39H1 em carcinomas mamários ainda são muito escassos. Entretanto, sabe-se que tumores mamários invasivos apresentam um baixo enriquecimento de H3K9me3 na heterocromatina pericentromérica no cromossomo 5, acarretando no aumento de instabilidades cromossômicas, quando comparados ao tecido normal mamário adjacente (135).

A perda da heterocromatina no cromossomo X, manifestada principalmente pela perda do corpúsculo de barr, é frequentemente detectada no câncer de mama e está associada à baixa sobrevida (136,137). A perda da heterocromatina é também observada na periferia nuclear de células provenientes de tecido normal mamário, quando comparadas às células tumorais (106).

Ao longo da progressão tumoral mamária, as proteínas da MN se ligam diferentemente ao DNA e são expressas de forma altamente heterogênea de acordo com cada estágio de progressão tumoral (138). Diversas proteínas associadas à

cromatina que reconhecem especificamente as regiões em que ocorrem o despareamento de bases, denominadas BURs, apresentam elevados níveis de expressão no câncer de mama maligno (139).

Dentre as proteínas que se ligam às MARs, podemos destacar a p114 que apresenta elevados níveis de expressão e ancoragem às MARs exclusivamente em carcinomas mamários malignos (140), e a SATB1, também muito expressa em carcinomas mamários malignos, onde atua no remodelamento dos *loops* de cromatina e reprogramação da expressão gênica associada ao estado tumoral mamário agressivo (141). Além do mais, a expressão elevada de ambas as proteínas podem ser indicadores apropriados para um prognóstico ruim.

Apesar dos inúmeros estudos realizados associando as MARs com os diferentes tipos de câncer, conforme mostrado anteriormente, estudos com o mapeamento das MARs e sua associação com o câncer de mama ainda são insuficientes. Em 2011, em estudo realizado pelo nosso grupo, foi mostrado que existem MARs exclusivas de células normais mamárias que podem favorecer o ancoramento de fatores transcricionais, levando ao aumento da expressão de genes flanqueadores localizados nos loops de cromatina (Artigo I;142)

Contudo, estudos associando as diferentes interações entre as modificações epigenéticas e os sítios de fixação à matriz nuclear no desenvolvimento do câncer de mama, ainda são raros, ratificando a importância de mais estudos para a elucidação do processo de progressão tumoral e metástase.

2 **O CÂNCER DE MAMA E O GENE SUPRESSOR DE TUMOR *TP53***

O câncer de mama é o tipo de câncer que mais acomete as mulheres no mundo todo. No Brasil, foram estimados para o ano de 2012 mais de 52 mil novos casos (126). Conforme mencionado anteriormente, o câncer de mama pode ser classificado em diversos subtipos moleculares de acordo com a expressão dos receptores de estrogênio, progesterona e do oncogene *HER-2*. Estas classificações também devem ser levadas em consideração na utilização de linhagens celulares provenientes de tecido mamário, e elas são*:* Luminal A (RE+/RP+/HER-2-), luminal B (RE+/RP+/HER-2+), subtipo HER-2 (RE-/RP-/HER-2+) e basal ou triplo negativo (RE-/RP-/HER-2-) (143).

Existem diversos fatores de risco associados ao desenvolvimento do câncer de mama, como por exemplo, aqueles relacionados à vida reprodutiva da mulher e a alta densidade do tecido mamário (144). Entretanto, dentre todos os fatores associados ao desenvolvimento de câncer de mama, devemos ressaltar a importância das alterações no gene supressor de tumor *TP53*.

A presença de mutação no gene *TP53*, é a característica mais comum nos diversos tipos de câncer (145) e no câncer de mama, esta mutação ocorre em aproximadamente 30-40% dos casos (146–148). A presença destas mutações pode inibir algumas das funções crucias exercidas pelo produto do gene *TP53*, favorecendo o desenvolvimento do câncer, tais como, regulação da apoptose, parada do ciclo celular, senescência, sensor de danos no DNA, resposta imune e estabilidade genômica (149,150).

Apesar de tudo o que já se sabe sobre o papel das diferentes mutações no gene *TP53* e, suas conseqüências na proteína P53 no organismo, é ainda importante ressaltar que o gene *TP53* possui 19.200 pb, contêm 11 exons e apresenta dois promotores, P1 e P2, que permitem a síntese de 9 isoformas de RNAm e 12 isoformas de proteínas (151,152).

Contudo, ainda pouco se sabe sobre a regulação da transcrição do gene *TP53* e sua relação com a organização da cromatina e as modificações epigenéticas em seu domínio gênico.

3 **OBJETIVOS**

Para compreender melhor a organização da cromatina, através das MARs e das principais modificações epigenéticas no genoma e nas histonas, e suas implicações na transcrição do gene *TP53* nos diferentes níveis de progressão do câncer de mama, foram designados os seguintes objetivos específicos:

(a) Mapear os possíveis sítios de fixação à matriz nuclear (MARs), na região de domínio do gene TP53, em linhagens provenientes de tecidos mamários normais e tumorais.
(b) Verificar a expressão do gene *TP53* e dos genes flanqueadores nas mesmas linhagens;
(c) Analisar o estado da cromatina nas MARs, através dos marcadores H4Ac (cromatina aberta) e H3K9me3 (cromatina fechada), incluindo a região promotora P1 do gene *TP53*, e a especificidade e intensidade da ligação de complexos protéicos nas MARs, nas mesmas linhagens.
(d) Verificar o estado da metilação global genômica, expressão global e distribuição nuclear, dos principais marcadores epigenéticos de histonas, H4Ac, H3K9me3 e H3K27me3, no desenvolvimento tumoral, através do modelo celular de progressão tumoral mamária, contendo 4 linhagens provenientes do mesmo paciente, denominado série 21T (H16N2, 21PT, 21NT e 21MT1);
(e) Verificar a expressão dos genes responsáveis pela modificações epigenéticas, citadas acima, no DNA e nas histonas na série 21T;
(f) Verificar a expressão do importante gene supressor de tumor *TP53* e o enriquecimento com os marcadores H4Ac e H3K9me3 em sua região promotora P1 na série 21T.

4 **METODOLOGIA**

Nesta seção, optamos somente por descrever as linhagens celulares utilizadas em nosso trabalho. Entretanto, as metodologias empregadas nos demais experimentos realizados estão descritas detalhadamente nos Artigos I, II e III.

Para o estudo das MARs foram utilizadas as linhagens mamárias normais MCF-10A e HB2, e as linhagens tumorais mamárias BT474, T47D, MCF7 e MDA-MB-231, doadas gentilmente pelo Dr. David Cappellen. Para o estudo das modificações epigenéticas na progressão tumoral mamária, foram utilizadas as linhagens da série de progressão tumoral 21T. A tabela 1, mostra as principais características de todas as linhagens utilizadas, incluindo as mutações descritas no importante gene supressor de tumor *TP53*.

A série 21T é um conjunto de 5 linhagens (H16N2, 21PT, 21NT, 21MT1 e 21MT2) derivadas e estabelecidas a partir do mesmo paciente em diferentes estágios de progressão tumoral mamária. A H16N2 é proveniente de tecido normal mamário adjacente ao tumor, a 21PT é proveniente de um carcinoma infiltrante, a 21NT é proveniente de carcinoma intraductal ou Ductal In-Situ (CDIS) e as linhagens 21MT1 e 21MT2 são provenientes de uma efusão pleural, estabelecida um ano após a mastectomia que originou as linhagens 21PT e 21NT, sendo as únicas linhagens que possuem potencial metastático (153,154).

As células da série 21T mimetizam os estágios específicos da progressão tumoral mamária quando são injetadas e crescem na camada adiposa mamária de camundongos nus: 21PT- Hiperplasia Ductal Atípica (HDA), 21NT- CDIS e 21MT1- Carcinoma Metastático Invasivo (CMI). Além disto, as linhagens expressam as citoqueratinas 8, 18 e 19, assim como a proteína HMFG-2, identificando-as como pertencentes ao tecido epitelial de origem mamária (154,155).

A linhagem H16N2 foi gentilmente cedida pela Dr^{a} Vimla Band (Departamento de Genética, Biologia Celular e Anatomia, Instituto Médico da Universidade de Nebraska) e as demais linhagens 21PT, 21NT, 21MT1 e 21MT2, foram cedidas pelo Dr. Pierre Hainaut (Agência Internacional de Pesquisa e Prevenção ao Câncer-IARC, Lyon, França).

Vale a pena ressaltar que todas as linhagens da série 21T foram submetidas à teste de genotipagem no laboratório do Prof. Dr. Franklin Rumjanek no Instituto de Bioquímica Médica da UFRJ.

Tabela 1 - Características das linhagens celulares utilizadas neste trabalho (145,152–154 e ATCC®)

Linhagem celular	**RE[1]**	**RP[2]**	**Subtipo de carcinoma mamário**	**Origem**	**Estado do *TP53***
MCF-10A	-		-	Tecido normal mamário de paciente com doença fibrocística e imortalizada espontaneamente	Selvagem
HB2	-		-	Linhagem obtida através de subclonagem e imortalização, com vírus SV-40, da linhagem MTSV-1.7, proveniente de células do ducto normal mamário, a partir do leite (157,158)	Selvagem
BT474	(+)	(+)	Carcinoma Ductal Infiltrante	Ducto glandular mamário	c.853G>A
T47D	(+)	(+)	Carcinoma Ductal Infiltrante	Sítio metastático/Efusão pleural	c.580C>T
MCF7	(+)	(+)	Adenocarcinoma	Sítio metastático/Efusão pleural	Selvagem
MDA-MB-231	(-)	(-)	Adenocarcinoma	Sítio metastático/Efusão pleural	c.839G>A
HeLa	-		Adenocarcinoma	Cervix	Selvagem
H16N2	-		-	Linhagem obtida através de transfecção com HPV-16 E6/E7 em uma linhagem proveniente de tecido normal (159)	Selvagem
21PT	(-)	(-)	HDA[3]	Carcinoma intraductal	c.96_97ins1
21NT	(-)	(-)	CDIS[3]	Carcinoma infiltrante	c.96_97ins1
21MT1	(-)	(-)	CMI[3]	Sítio metastático/Efusão pleural	c.96_97ins1
21MT2	(-)	(-)	CMI[3]	Sítio metastático/Efusão pleural	c.96_97ins1

Legenda: 1-Receptor de estrogênio;2-Receptor de progesterona;3-Subtipos de carcinomas mamários mimetizados pela série 21T quando crescem em camundongos *nudes*.

5 **RESULTADOS**

Os resultados obtidos estão compreendidos em 3 artigos, compondo cada um uma seção secundária, conforme será mostrado posteriormente. O primeiro artigo publicado em 2011 na revista *Journal of Cellular Biochemistry*, intitulado "*Loop domain organization of the p53 locus in normal and breast cancer cells correlates with the transcriptional status of the TP53 and the neighboring genes*", descreve os sítios de fixação à matriz nuclear na região de domínio do gene *TP53* e sua possível influência, tanto na regulação da expressão do gene *TP53* como nos seus genes flanqueadores, em linhagens celulares de câncer de mama.

O segundo artigo, ainda não publicado (ainda em processo de escrita), e intitulado "*MARs and TP53 gene domain in breast cells",* descreve o estado da cromatina nos sítios de fixação à matriz nuclear, descritos no primeiro artigo. Além disto, este artigo também mostra a ligação de complexos de proteínas, de forma altamente específica, no sitio de fixação à matriz nuclear, detectado somente nas linhagens normais MCF-10A e HB2, no Artigo I.

O terceiro artigo, encontra-se em análise na revista Molecular Cancer, sob o número: 1497872969115980, e é intitulado "*Epigenetic modifications and chromatin distribution in breast cancer progression*", descreve importantes modificações epigenéticas no modelo de progressão tumoral denominado de série 21T. Além disto, descreve a manutenção do estado da cromatina na região promotora do gene *TP53* nesta série de linhagens*,* e sugere que esta manutenção pode ser um importante fator na manutenção da expressão gênica ao longo da progressão tumoral mamária.

Todos os resultados não inseridos nos artigos, estão na seção "Apêndice".

5.1 **Artigo I:** ***Loop domain organization of the p53 locus in normal and breast cancer cells correlates with the transcriptional status of the TP53 and the neighboring genes***

A proteína P53, apresenta uma papel crítico na supressão de tumor e integridade do genoma. Apesar do vasto conhecimento sobre o controle da proteína P53, pouco se sabe sobre a regulação transcricional do importante gene supressor de tumor *TP53*.

Neste artigo, foi analisada a organização do domínio do gene *TP53,* utilizando a técnica de arranjos de DNA em diversas linhagens de câncer de mama e linhagens controles. Foi detectado que na linhagem controle HB2, o gene *TP53* está posicionado num domínio de DNA relativamente pequeno, de 50kb, delimitado por dois sítios de fixação à matriz nuclear, MAR2 e MAR3.

Minha participação neste artigo, foi a confirmação do sitio de fixação à matriz nuclear, MAR2, por PCR em tempo real (qPCR) na linhagem HB2 e na linhagem não cancerosa MCF10A. Ainda, realizei as análises *in silico*, na busca de putativas MARs, que corroboraram os resultados obtidos pelo arranjo de DNA.

Foi interessante a descoberta de que esta estrutura de domínio de DNA é radicalmente diferente nas linhagens de carcinoma mamário, MCF-7, T47D, MDA-MB-231 e BT-474, nos quais o tamanho do domínio é aumentado e a expressão do gene *TP53* é diminuído. Por fim, foi proposto um modelo correlacionando a organização do domínio do gene *TP53* e a transcrição deste gene com os genes flanqueadores.

ARTICLE
Journal of Cellular Biochemistry 112:2072–2081 (2011)

Journal of Cellular Biochemistry

Loop Domain Organization of the p53 Locus in Normal and Breast Cancer Cells Correlates With the Transcriptional Status of the *TP53* and the Neighboring Genes

Andrea C.S. Goes,[1,2] David Cappellen,[1] Gilson C. Santos Jr.,[3] Iryna Pirozhkova,[1] Marc Lipinski,[1] Yegor Vassetzky,[1*] and Claudia V. de Moura-Gallo[1,3]

[1]*Unité Mixte de Recherche 8126, Signalisation, Noyaux et Innovations en Cancérologie, Centre NaTional de la Recherche Scientifique, Institut de Cancérologie Gustave-Roussy, Université Paris-Sud 11, F-94805 Villejuif Cedex, France*

[2]*Departamento de Ensino de Ciências e Biologia, Universidade do Estado do Rio de Janeiro, Instituto de Biologia Roberto Alcantara Gomes, Rio de Janeiro 20550-013, Brazil*

[3]*Departamento de Genética, Universidade do Estado do Rio de Janeiro, Instituto de Biologia Roberto Alcantara Gomes, Rio de Janeiro 20550-013, Brazil*

ABSTRACT

P53 is a tumor suppressor protein critical for genome integrity. Although its control at the protein level is well known, the transcriptional regulation of the *TP53* gene is still unclear. We have analyzed the organization of the *TP53* gene domain using DNA arrays in several breast cancer and control cell lines. We have found that in the control breast epithelial cell line, HB2, the *TP53* gene is positioned within a relatively small DNA domain, encompassing 50 kb, delimited by two nuclear matrix attachment sites. Interestingly, this domain structure was found to be radically different in the studied breast cancer cell lines, MCF7, T47D, MDA-MB-231, and BT474, in which the domain size was increased and *TP53* transcription was decreased. We propose a model in which the organization of the *TP53* gene domain correlates with the transcriptional status of *TP53* and neighboring genes. J. Cell. Biochem. 112: 2072–2081, 2011.

KEY WORDS: p53; CHROMATIN LOOP DOMAIN; MAR; TRANSCRIPTION; BREAST CANCER

Several levels of DNA compaction exist in the eukaryotic nucleus. The DNA is packed into nucleosomes, and the resulting chromatin is further compacted into 30 nm fibers and chromatin loop domains which are anchored to a proteinaceous nucleoskeleton, also called nuclear matrix or scaffold [Paulson and Laemmli, 1977; Hancock and Boulikas, 1982]. Chromatin loop domain size varies from 20 to 200 kb with many genes and clusters of functionally related genes being organized into distinct loops which are attached to the nuclear matrix via the nuclear scaffold or matrix attachment regions (MARs) [reviewed in Vassetzky et al., 2000a; Razin et al., 2007]. These in vivo MARs are identified by analysis of DNA composition of high salt-extracted nuclear matrix and may include topoisomerase II binding sites [Razin et al., 1991; Eivazova et al., 2009] as well as other sequence motifs. Changes observed in the organization of chromatin loop domains may be involved in the establishment of stable programs of transcription during development and may contribute to the determination of stable cell lineages. Rearrangement of DNA loops occurs during development when the loop size increases in somatic cells [Buongiorno-Nardelli et al., 1982; Vassetzky et al., 2000a]. Conversely, the average loop size decreases in transformed cells [Linskens et al., 1987] and in several human cancer cell lines in which it was found to be smaller than in their non-transformed counterparts [Oberhammer et al., 1993]. This may reflect a reversal

Supporting information may be found in the online version of this article.

Grant sponsor: Institut National du Cancer (INCa); Grant sponsor: Fondation de France; Grant sponsor: CAPES-COFECUB.

David Cappellen's present address is Equipe 2406, Histologie et Pathologie Moléculaire des Tumeurs, Université Bordeaux-Segalen, 33076 Bordeaux, France.

*Correspondence to: Dr. Yegor Vassetzky, Unité mixte de Recherche 8126, Signalisation, Noyaux et Innovations en Cancérologie, Centre NaTional de la Recherche Scientifique, Institut de Cancérologie Gustave-Roussy, Université Paris-Sud 11, F-94805 Villejuif Cedex, France. E-mail: vassetzky@igr.fr

Received 2 September 2010; Accepted 23 March 2011 • DOI 10.1002/jcb.23129 • © 2011 Wiley-Liss, Inc.
Published online 4 April 2011 in Wiley Online Library (wileyonlinelibrary.com).

in the differentiated state of the normal cells. Hence, a study of the chromatin loop domain organization may provide important data on the large-scale mechanisms involved in oncogenic transformation. The *TP53* gene is a well-known tumor suppressor gene, critical for the maintenance of genome integrity [Vogelstein et al., 2000; Levine and Oren, 2009]. At the genomic level, the *TP53* gene is located at the 17p13.1 locus and contains 11 exons, spanning 19 kb. Three promoters have been described and recent data support the idea that a complex pattern of RNA transcription produces different p53 isoforms [Bourdon, 2007; Hollstein and Hainaut, 2010]. However, the mechanisms of promoter choice and the functions of the different isoforms remain to be clarified. Hence, despite all the accumulated knowledge on *TP53* mutations and functions, little is known about its large-scale chromatin organization and transcriptional control.

Breast cancer is one of the most important types of cancer affecting women worldwide. Several studies have demonstrated that p53 alterations are associated with breast cancer development. Besides, *TP53* deleterious mutations as well as losses of heterozygosity (LOH) at the *TP53* locus have been shown to be associated with poor prognosis in breast cancer patients [Simão et al., 2002; Olivier et al., 2006; Olivier et al., 2009]. Therefore, mechanisms which contribute to impair p53 transcription are anticipated to be involved in breast epithelial cell transformation.

In the present work, we have selected the breast cancer cell lines MCF7, T47D, MDA-MB-231, and BT474 and the control non-transformed mammary epithelial cell line HB2 in order to analyze MARs distribution in a region of 167 kb at 17p13.1, where *TP53* and at least seven other genes are located. Surprisingly, we have found that in the control mammary epithelial cell line the *p53* chromatin loop domain is smaller than in breast cancer cell lines and that the size of this domain correlated with the transcriptional status of *p53* and neighboring genes.

MATERIALS AND METHODS

CELL CULTURES

All the cell lines were obtained from David Cappellen and Nancy Hynes (Friedrich Miescher Institute for BioMedical Research, Novartis Research Foundation, Basel, Switzerland). The human mammary carcinoma cell lines MDA-MB-231, T47D, and the HeLa cervix carcinoma cell line were cultured in DMEM medium supplemented with 10% horse serum, 0.5% penicillin/streptomycin, and 1% glutamine. The human mammary carcinoma cell lines MCF7 and BT474 were cultured in RPMI medium supplemented with 10% horse serum, 0.5% penicillin/streptomycin, and 1% glutamine. The control normal epithelial cell lines MCF10A and HB2 were cultured in DMEM medium supplemented with 10% horse serum, 0.5 μg/ml hydrocortisone, 10 μg/ml insulin, 0.5% penicillin/streptomycin, and 1% glutamine.

PURIFICATION OF NUCLEI AND NUCLEAR MATRIX

Nuclei were purified from cell cultures grown as described earlier [Gasser and Vassetzky, 1998]. Nuclear matrices were prepared by treatment of the isolated nuclei with DNase I followed by extraction with 2 M NaCl as previously described [Gasser and Vassetzky, 1998]. Briefly, cells were harvested and washed twice with phosphate buffered saline (PBS) solution. The pellet was washed twice in 2 ml of buffer 1 (5 mM Tris-HCl pH 7.4, 125 μM spermidine, 50 μM spermine, 20 mM KCl, 100 μM PMSF in ethanol, 1 mM EDTA pH 8.0, 0.25 M sucrose) by centrifugation at 800*g* for 5 min at 4°C. The pellet was resuspended in 2 ml buffer 1 supplemented with 0.4% NP40 and the cells were incubated at 4°C for 30 min, followed by centrifugation at 1,000*g* for 5 min at 4°C. The pellet was washed twice in 1 ml buffer 1 by centrifugation at 1,000*g* for 5 min at 4°C. The final pellet was resuspended in 1 ml buffer 2 (10 mM Tris-HCl pH 7.4, 250 μM spermidine, 100 μM spermine, 40 mM KCl, 100 μM PMSF in ethanol, 1 mM $CaCl_2$, 10 mM $MgCl_2$) and the recovered nuclei were digested with 100 μg/ml DNase I for 2 h at 4°C. The nuclear matrix was stabilized with 1 ml of 1 mM $CuCl_2$ for 10 min at 4°C. The nuclear matrix was extracted with the addition of 1 ml buffer 3 (4 M NaCl, 20 mM Tris-HCl pH 8.0, 20 mM EDTA pH 8.0) and incubation for 20 min at 4°C. The suspension was centrifuged at 2,500*g* for 5 min at 4°C. The pellet was washed twice in buffer 4 (2 M NaCl, 20 mM Tris-HCl pH 8.0, 10 mM EDTA pH 8.0) by centrifugation at 2,500*g* for 5 min at 4°C. The final pellet was resuspended in 360 μl TE and 5 μl 0.5 M EDTA pH 8.0 and digested with 20 μl proteinase K (0.4 mg/ml) for 1 h at 60°C and at 37°C overnight. The matrix DNA was extracted with phenol/chloroform followed by ethanol/sodium acetate precipitation. The DNA was recovered in 200 μl TE and treated with 5 μl RNase (10 mg/ml) for 30 min at 37°C. Again, the DNA was extracted with phenol/chloroform followed by ethanol/sodium acetate precipitation and the final matrix-associated DNA was recovered in 50 μl TE.

The obtained nuclear matrix-associated DNA was labeled with digoxygenin (DIG) using DIG-High Prime Kit (Roche Applied Science, Indianapolis, IN) and used as a probe for hybridization with the DNA array covering the 167 kb of the 17p13.1 region, including *TP53* and neighboring genes, as shown in Figure 1. Nuclear matrices obtained from three independent experiments were used for hybridizations.

DNA ARRAY

The in vivo MAR mapping, using DNA arrays, was carried out as described elsewhere [Ioudinkova et al., 2005; Petrov et al., 2006]. The DNA array consisted of 35–45-mer oligonucleotides spaced approximately 1 kb apart (Supplementary Table 1), covering 167 kb encompassing the *TP53* gene within the 17p13.1 chromosomal region. They were designed after sequence analysis using the WebGene software (http://www.itb.cnr.it/webgene/), in order to avoid repetitive sequences. All oligonucleotides had a similar melting temperature (Tm). The oligonucleotides were dot-blotted onto Hybond N+ filters (Amersham/GE Healthcare Europe GmbH, Orsay, France) and hybridized with the corresponding probes at 40.5°C overnight. The membrane was incubated with the anti-DIG antibodies (Roche) and revealed using the ECL+ kit (Amersham/GE Healthcare Europe GmbH). The films were scanned and quantified using the Image Gauge 4.0 software (Fuji Photo Film Co., Tokyo, Japan). The experiments were carried out in triplicate. Only the hybridization signals consistently found in at least three independent experiments were considered as in vivo MARs.

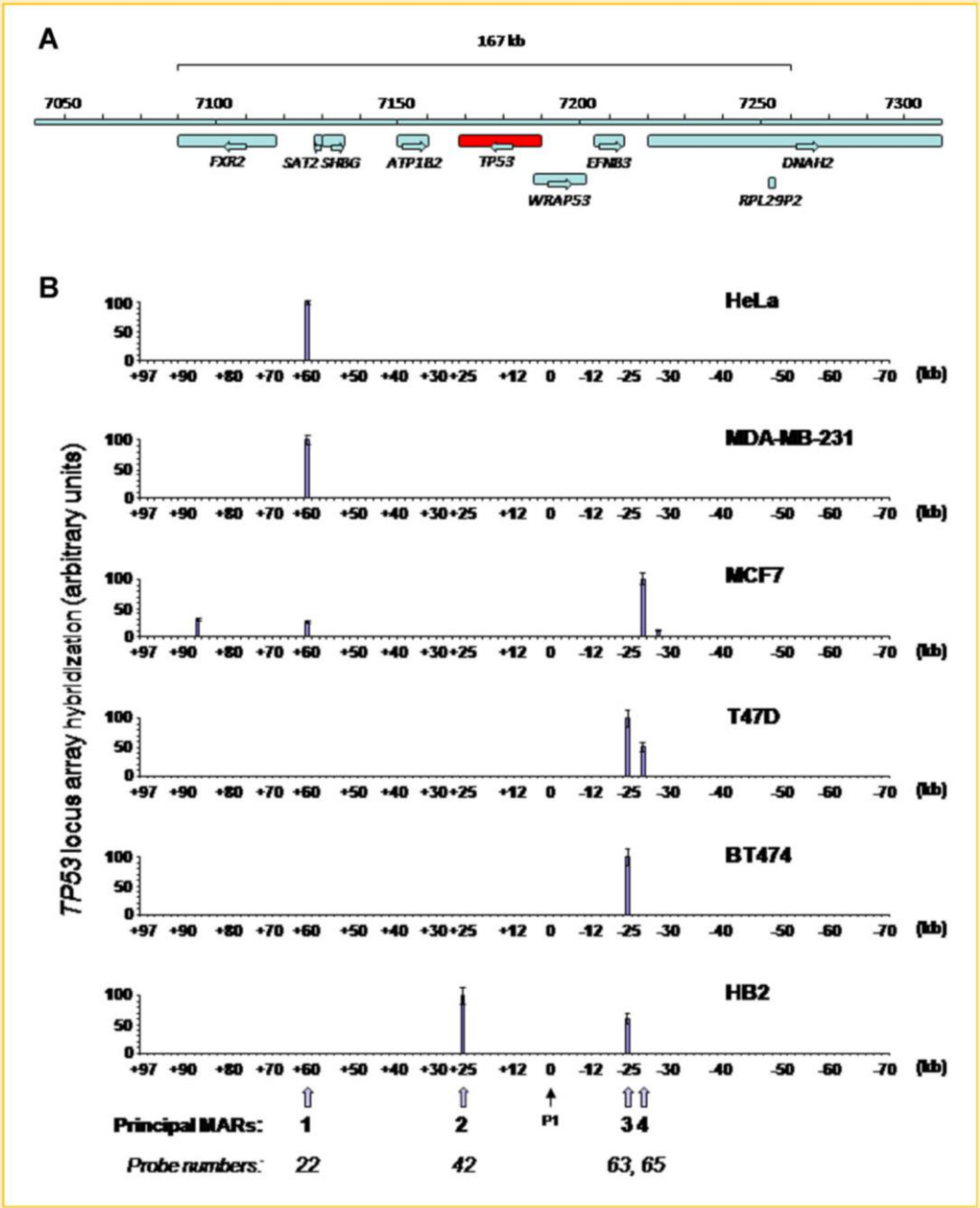

Fig. 1. Mapping of nuclear matrix attachment sites at the *TP53* gene locus and neighboring genes by DNA array hybridization. (A) Organization of the genomic locus, nucleotide counts (in kilobase pairs, kb), position of genes, and transcription orientation (arrows) are indicated. DNA remaining attached to the nuclear matrix was extracted from cells nuclei and hybridized to a DNA array covering the 167 kb genomic domain at the 17p13.1 chromosomal region. At least eight genes were contained in this region: *FXR2*, *SAT2*, *SHBG*, *ATP1B2*, *TP53*, *WRAP53*, *EFNB3*, and *DNAH2*. (B) Bar graphs represent, for each tested cell line (HB2, MCF7, T47D, MDA-MB-231, BT474, HeLa), relative hybridization signals for each of the 95 probes spanning the 167 kb genomic region, encompassing the *TP53* gene. Probe positions (in kb) are indicated below each graph and hybridization values are expressed, for each cell line, as a percentage of the strongest signal on the array. The results displayed are the mean (± s.e.m.) from three independent experiments, each hybridized onto DNA arrays in triplicates. The positions of the principal in vivo nuclear matrix-attachment sites (called MARs), found in that region, are indicated by large arrows and numbered from 1 (left) to 4 (right), with base counts in kb indicating their positions relatively to position 0 (small arrow), which corresponds to the major transcription start site (*P1*) of *TP53*. The numbers of the corresponding oligonucleotide probes are indicated below the positions of each MAR. (C) Representative examples of DNA array hybridization profiles of nuclear matrix attached DNA. Grids indicate positions of each probe. For each of the tested cell lines, hybridization signals are circled in red. As a control for array quality and hybridization efficiency, hybridization of total genomic DNA to a similar array shows that all probes give comparable signals. Only the hybridization signals consistently found in at least three independent experiments were considered as in vivo MARs.

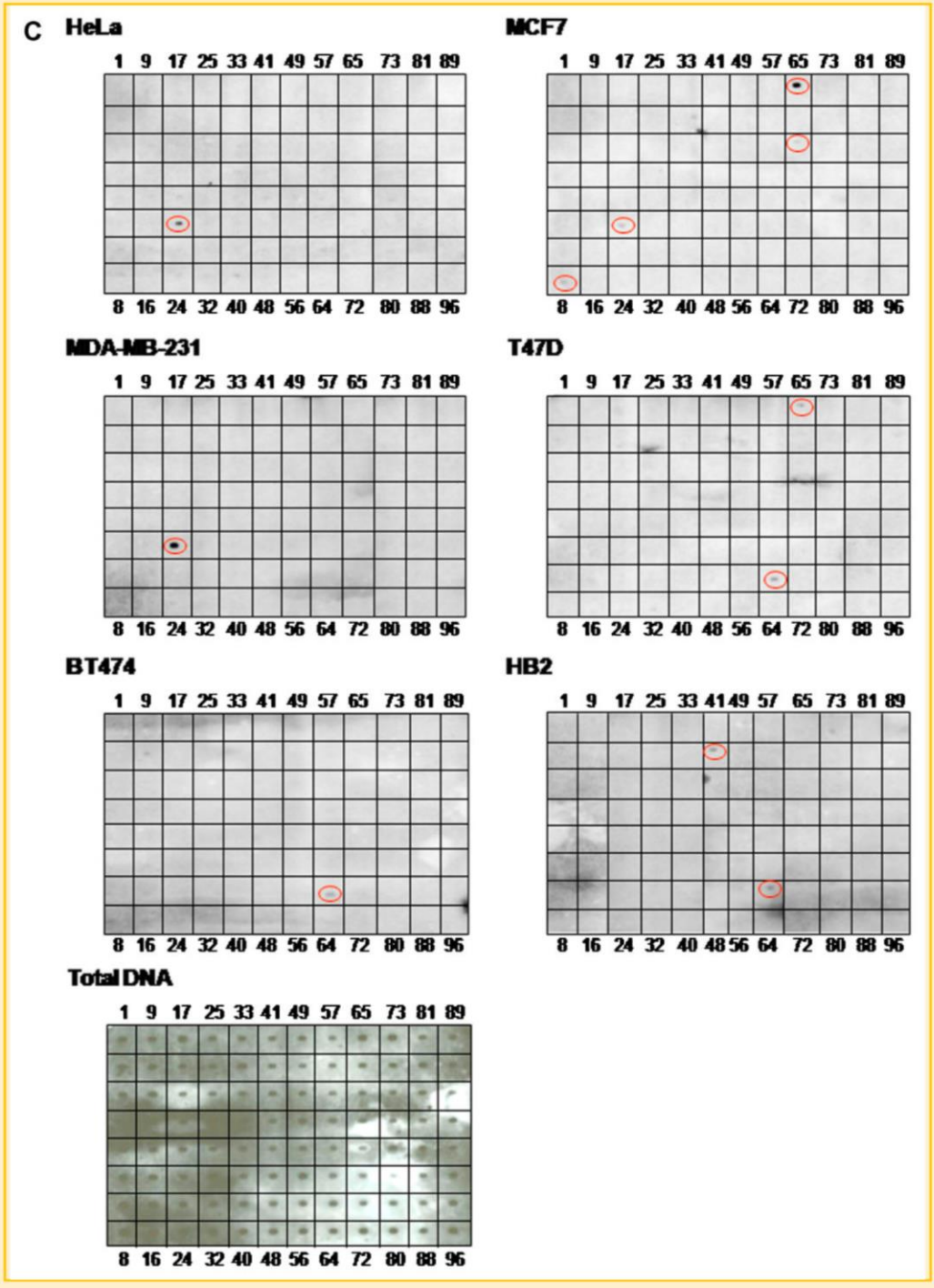

Fig. 1. (*Continued*)

QUANTITATIVE PCR AND RT-PCR

Quantitative PCR (qPCR) was carried out in order to validate the matrix-attached sites for the breast cancer cell lines MDA-MB-231 and BT474, the cervix cancer cell line HeLa, and the control normal epithelial breast cell lines HB2 and MCF10A. The extracted matrix-bound DNAs were used as templates to amplify the sequences of the array-hybridized oligonucleotidic probes as well as the immediately upstream and downstream regions. For each primer pair, 50 ng of total genomic DNA was amplified as a positive control. PCR reactions were performed using the SYBR Green I dye on the ABI PRISM 7000 Detection System (Applied Biosystems, Foster City, CA) in a total volume of 25 µl containing 12.5 µl of SYBR Green PCR

master mix (Euromedex, Souffelweyersheim, France), 10.5 µl of sterile H_2O, 1.0 µl of 12.5 µM forward and reverse primers mix and 1.0 µl of matrix-attached DNA or total genomic DNA (for primers sequences, see Supplementary Table 2). All PCR reactions were performed in duplicate in 96-well optical reaction plates (Applied Biosystems). Cycling conditions consisted of a single step at 50°C for 2 min, subsequent 10 min polymerase activation at 95°C, followed by 40 cycles of 95°C for 15 s and 60°C for 1 min. To quantify gene transcription, quantitative RT-PCR (qRT-PCR) was performed. In brief, total RNA was isolated from cell lines (1×10^6–2×10^6 cells) using RNeasy mini spin column kit (Qiagen, Courtaboeuf, France) and reverse-transcribed with ImProm-II reverse transcription system (Promega Corporation, Madison, WI). The PCR reaction was carried out in the same conditions described above for genomic and matrix-bound DNA, using two-fold diluted first-strand cDNA as template (for primers sequences, see Supplementary Table 3). Gene expression was normalized for RNA concentration with the endogenous *EF1α* (EEF1A1, eukaryotic translation elongation factor 1 alpha 1) gene. The relative mRNA expression level was calculated using the comparative expression level formula as previously described [Simon, 2003].

IN SILICO ANALYSIS

To detect potential in vivo MARs within the studied DNA sequence, an Internet tool (MAR-WIZ; http://genomecluster.secs.oakland.edu/

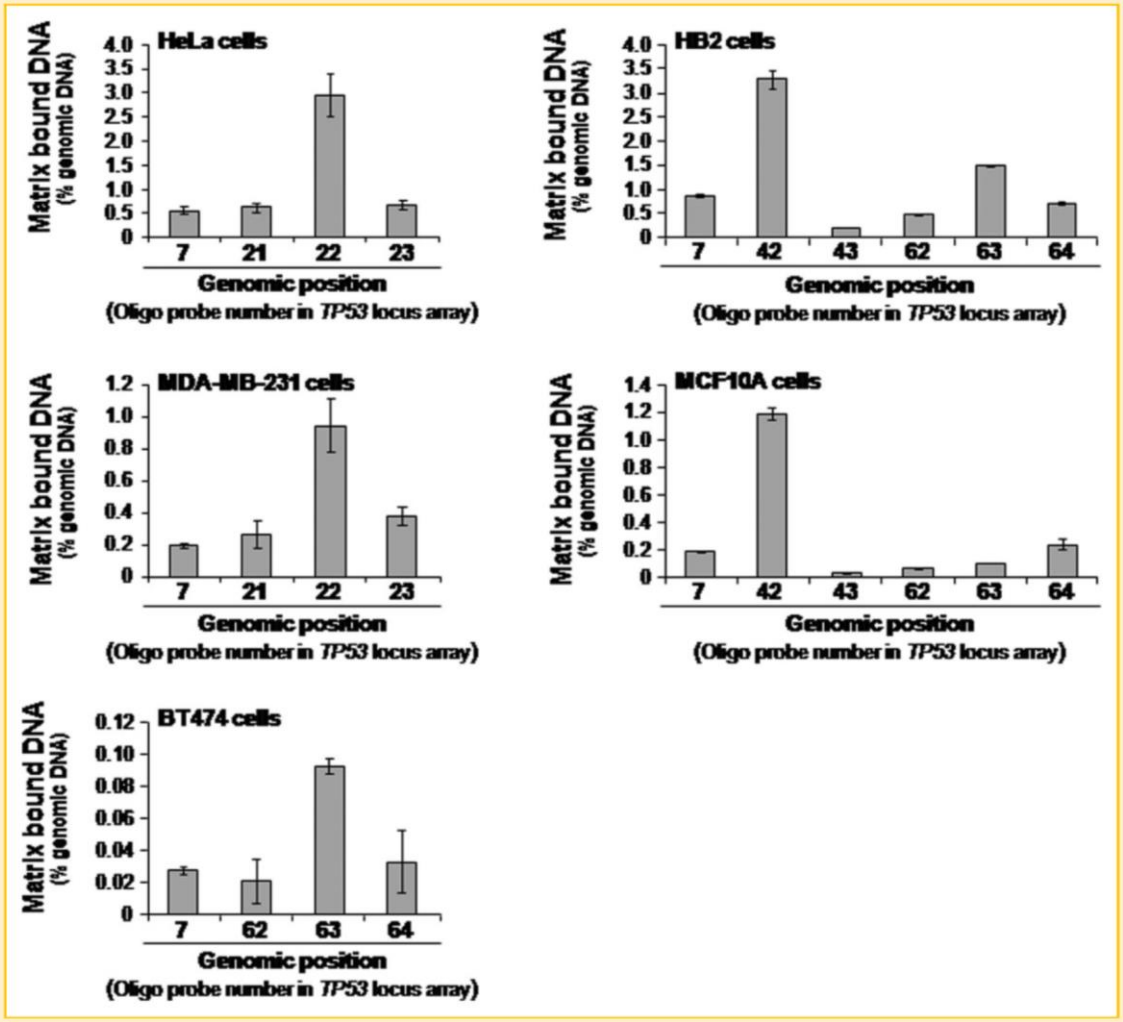

Fig. 2. Validation of nuclear matrix binding DNA segments for *TP53* locus by quantitative PCR. Matrix-bound DNA and total genomic DNA from HeLa (cervix carcinoma cell line), MDA-MB-231 and BT474 (breast carcinoma cell lines) and HB2 and MCF10A (control mammary epithelial cell lines) were independently amplified by real-time quantitative polymerase chain reaction (qPCR). Primer pairs used were flanking the oligonucleotidic probes constituting the *TP53* locus array and are numbered accordingly. The sequences of the array-hybridized probes and the upstream and downstream flanking regions were amplified for each cell line. The region in which the probe 7 is located was amplified as a negative control for all cell lines. For each genomic position, the amount of nuclear matrix bound DNA was determined relatively to that of total genomic DNA. Mean ratios ± SEM from three independent measurements are shown.

marwiz/) developed by Singh et al., 1997, was used. MAR-WIZ assesses a list of a variety of sequence patterns with known properties of MAR sites and a mathematical potential value, the MAR-Potential, is assigned to a sequence region. The MAR motifs are characteristic for origins of replication, TG-rich sequences, curved DNA, kinked DNA, topoisomerase II sites, and AT-rich sequences. The analysis was run with the default settings. To confirm the potential MARs, another Internet tool (SMARtest; http://www.genomatix.de/cgi-bin/smartest_pd/smartest.pl) developed by Frisch et al. [2002] was used. The SMARtest is based on a density analysis of S/MAR-associated patterns represented by a weight matrix library. The analysis was run with the default settings. Because of the software limitations we could only analyze the first 135,781 base pairs of the 167 kb *TP53* domain sequence.

RESULTS

LARGE-SCALE CHROMATIN ORGANIZATION AT THE *TP53* GENE LOCUS

Although the *TP53* gene has been intensively studied over the past 30 years, surprisingly little is known about its large-scale organization and transcription control in human cells.

Isolation of nuclear matrix has allowed the identification and mapping of the DNA regions that structurally define the bases of the chromatin loop domains, the matrix attachment sites [Mirkovitch et al., 1984; Gasser and Laemmli, 1986]. Extensive treatment of the isolated nuclei with DNase I, under the conditions similar to those used for in vivo footprinting, leads to the digestion of non-protein-associated DNA. Subsequent extraction of the nuclei in a high-salt buffer removes histones and other highly soluble proteins with associated DNA. The remaining nucleoskeleton contains the nuclear MARs. The extracted MARs showed to range between 100 bp and 1 kb (Supplementary Figure 1). This DNA fraction, called here MAR, was purified, labeled, and used as a probe to examine the in vivo chromatin loop organization of the human *TP53* gene domain and surroundings. Formation of loops in DNA is an important feature which is responsible for gene domains organization. These loops are delimited by MARs. Therefore, to determine the organization of in vivo MARs within the 167 kb region containing the *TP53* and neighbouring genes, we have employed a DNA array approach (DNA array technique). Figure 1A shows the map of the studied genomic region with genes position and transcription orientation. Figure 1B presents the in vivo MARs mapping of the different cells lines and in 1C the DNA array hybridization results. As described elsewhere [Ioudinkova et al., 2005; Petrov et al., 2006], the sequence of the genomic domain was previously analysed for the presence of DNA repeats and the oligonucleotidic probes were designed to avoid repetitive sequences. We have next shown that total human DNA hybridizes almost equally to all chosen probes in the studied genomic region (Fig. 1C), excluding the presence of repetitive sequences in the array.

The hybridization pattern observed with the nuclear matrix DNA was quite different among the breast cell lines. As presented in Figure 1B, we identified four principal in vivo MARs in the 167 kb analyzed genomic region. They were arbitrarily numbered from 1 to 4 for comprehensive description and the localization in kilobase pairs (kb) was designated as positive or negative relative to the main *TP53* transcription start site, at P1. Interestingly, MAR 2, at position +25 kb, was found only in HB2, the control mammary epithelial cell line. This control cell line also presented MAR 3, at position −25 kb. Breast cancer cells exhibited different MAR patterns. MDA-MB-231 cells showed only MAR 1, at position +60 kb. BT474 cells showed only MAR 3, at position −25 kb. T47D cells also showed MAR 3, together with MAR 4, at position −26 kb. Finally, MCF7 cells presented a more complex pattern of MARs distribution, with MARs

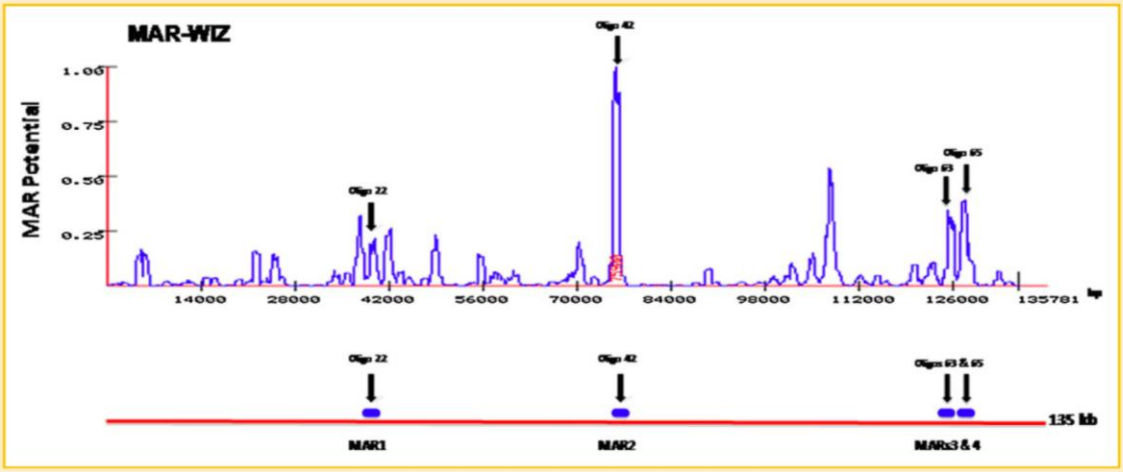

Fig. 3. In silico analysis for putative MARs sites at the *TP53* gene domain by MAR–WIZ. The y-axis represents MAR-potential at MAR–WIZ test. The blue blocks represent putative S/MARs regions consistent between the in silico test and the in vivo detection of MARs. The arrows indicate the position of the oligonucleotidic probes. The first 135,781 base pairs of the 167 kb *TP53* domain sequence were analyzed.

1 and 4, at positions +60 kb and −26 kb, respectively, and two other MARs, located at positions +87 kb and −27 kb.

In order to analyze if the observed MARs were specific for the tested normal control cells and cancerous breast epithelial cells, we have also performed MARs extraction and DNA array analysis for HeLa cervix carcinomas cells. Similar to MDA-MB-231 cells, HeLa cells were found to exhibit a single MAR (MAR 1) in the tested 167 kb region, at position +60 kb. Altogether, these data strongly suggest that a chromatin loop of approximately 50 kb, delimitated by MARs 2 (at + 25 kb) and 3 (at −25 kb) and enclosing the *TP53*, *WRAP53*, and *EFNB3* genes, is formed in control cells. A different MARs pattern and loop formation was observed in the studied breast cancer cell lines that all share the loss of MAR 2 at position +25 kb, and can present, in addition, the appearance of different novel MARs, such as MARs 1 and 4 at positions +60 kb and −26 kb, respectively (Fig. 1B).

In order to validate the observed in vivo MARs, we performed a quantitative PCR (qPCR) assay to determine the presence, in the matrix-bound fraction, of the major array-hybridized DNA sequences, as well as the sequences located immediately upstream and downstream. We amplified the matrix-bound DNA obtained from the carcinoma cells MDA-MB-231 and HeLa (the regions of the probes 7, 21, 22, and 23), BT474 (the regions of the probes 7, 62, 63, and 64), and the control breast epithelial cells HB2 and MCF10A (the regions of the probes 7, 42, 43, 62, 63, and 64) (see Figure 1 for probes localization). The results are shown in Figure 2. As expected, the sequence corresponding to probe 22 was highly represented in matrix-bound DNA from HeLa and MDA-MB-231 cells, while the sequence enclosing probe 63 was the major amplicon in matrix-bound DNA from BT474 cells. The qPCR analysis also confirmed the two in vivo MARs observed in HB2 cells. A very prominent peak corresponding to probe 42 was observed, while the sequence encompassing probe 63, although less represented, was also clearly present. Interestingly, a similar profile was observed with MCF10A cells, with an amplicon corresponding to probe 42 strongly represented and a second sequence, corresponding to probe 64, positioned 1.0 kb downstream of the probe 63, is also well represented (Fig. 2). Therefore, the results obtained with qPCR analysis of the nuclear matrix-bound DNA showed to be very similar among the control breast epithelial cells. These observations are consistent with the occurrence of a chromatin loop of approximately 50 kb in normal cells, with a specific in vivo MAR, situated at probe 42 (MAR2) (see Fig. 1B).

As a complementary investigation of MARs in the 167 kb region, we performed in silico tests. As shown in Figure 3, the obtained in vivo MAR profile is similar to that predicted by the in silico analysis (MAR–WIZ test). The highest peak presented by MAR–WIZ test corresponds to the position of MAR 2, namely probe 42, and the hypothetical loop would be formed by MARs 2 and 3, the latter being located at probe 63 region. A peak located between MARs 2 and 3 was also anticipated by in silico analysis (Fig. 3), but we did not detect it in our experiments. The in silico SMARtest detected an overall content of 1.5% of S/MARs in this region, and 3 of 4 predicted MARs were coincident with the in vivo observed MARs (probes 42, 63, and 65) as well as with the higher peaks indicated by MAR–WIZ test.

EXPRESSION PROFILE OF THE *TP53* AND THE NEIGHBORING GENES IN THE CONTROL AND BREAST CANCER CELL LINES

To assess the transcriptional level of *TP53* and neighboring genes in non-transformed and cancerous epithelial cell lines and analyze whether it was associated with MARs organization, we performed quantitative reverse transcription-polymerase chain reaction (q-RT-PCR). Expression levels of the genes of interest were normalized for RNA concentration using the endogenous *EF1α* transcripts as a reference. We analyzed transcript levels of all genes located within the 167 kb DNA region (see Fig. 1A) in the HB2 breast epithelial cells and breast (MCF7, T47D, MDA-MB-231, BT474) as well as cervix (HeLa) carcinoma cell lines. Figure 4 shows the transcript levels of

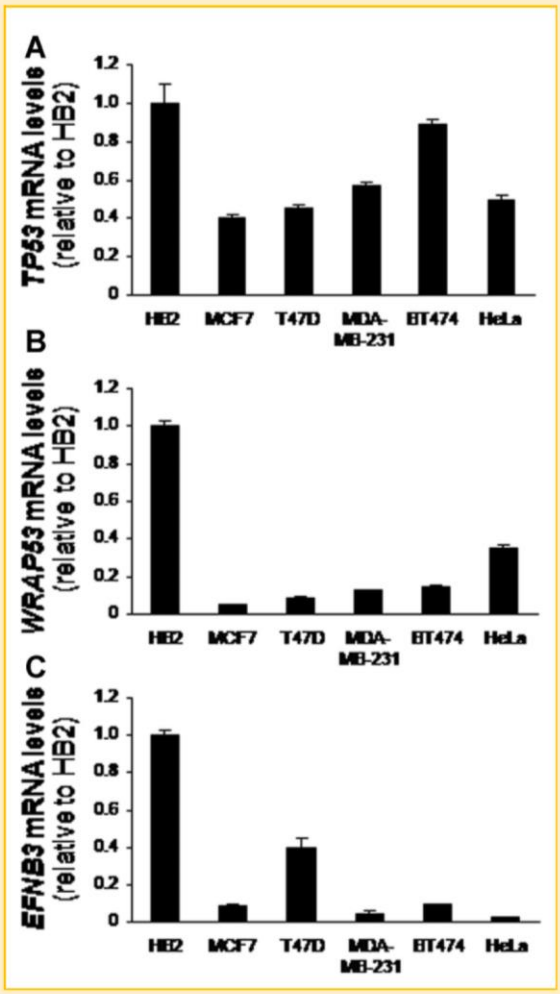

Fig. 4. Analysis of *TP53* and neighboring genes transcript levels in non-transformed mammary epithelial cells and carcinoma cell lines. Gene expression levels were determined using quantitative reverse transcription-polymerase chain reaction (q-RT-PCR) for the genes located between matrix attachment regions (MARs) 2 and 3. *TP53* (A), *WRAP53* (B), and *EFNB3* (C) messenger RNA (mRNA) levels were normalized by those of *EF1α*. Data are presented for each cell line as ratios relative to the levels in the HB2 mammary epithelial cell line.

the *TP53*, *WRAP53*, and *EFNB3* genes, located between MARs 2 and 3, within the chromatin loop, in the HB2 breast epithelial cells, and breast and cervix carcinoma cells. *TP53*, *WRAP53*, and *EFNB3* transcript levels are displayed as normalized ratios relatively to those in HB2 cells that were arbitrarily set up as 1. Relative transcript levels of neighboring genes located outside the loop are presented in supplementary data. Overall, the absolute expression levels were quite different among the genes, *SHBG* and *TP53* being the most

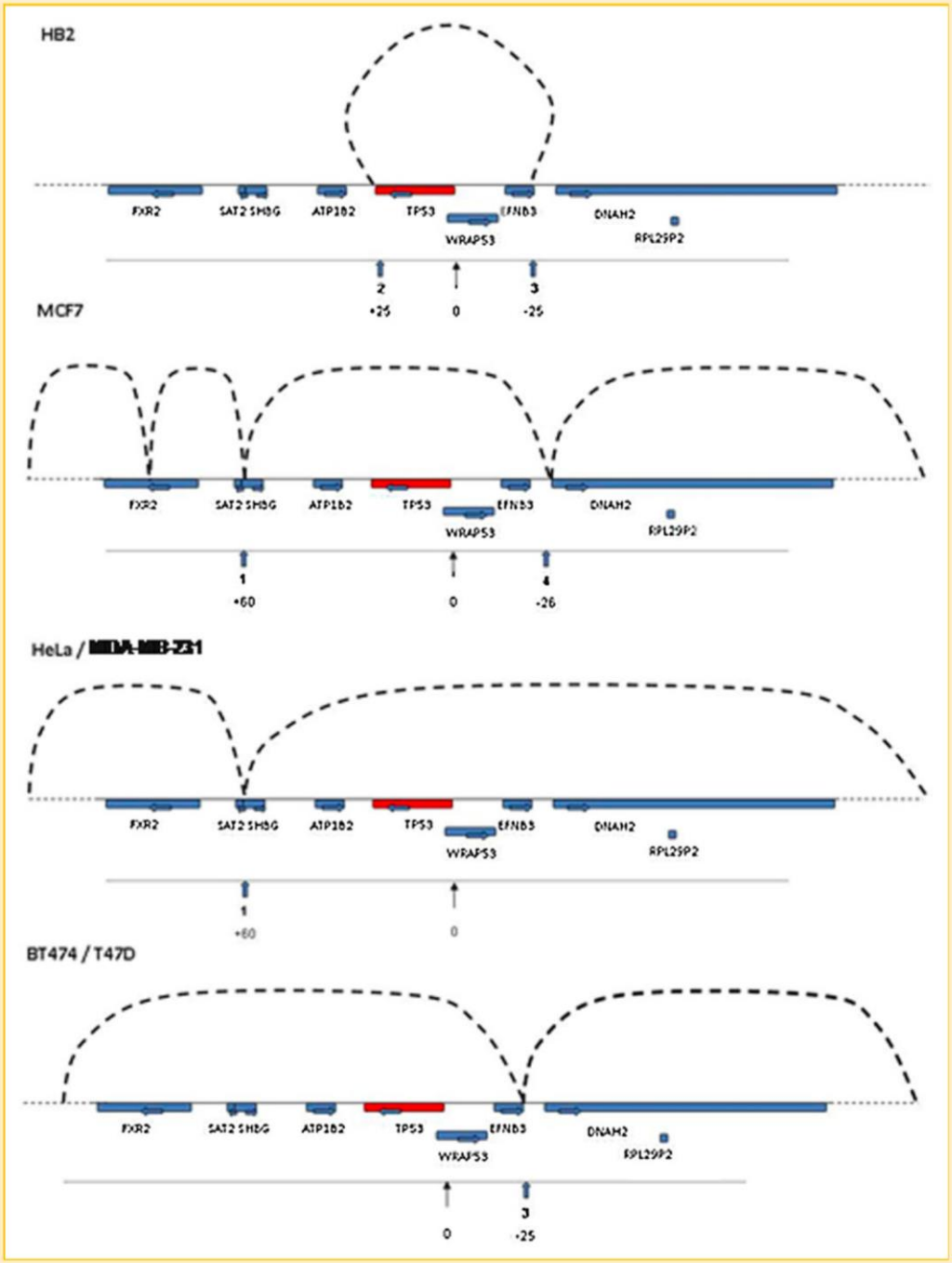

Fig. 5. Models of dynamic changes of MARs and loop conformation at the *TP53* gene domain in control breast epithelial cells and carcinoma cell lines. Distribution of matrix attachment regions (MARs) and modeled spatial configurations of the *TP53* gene domain are summarized. Base count in kb shows positions of MARs, indicated with numbers 1–4, relatively to position 0, which corresponds to the major transcription start site (P1) of *TP53*. In the control breast epithelial cells HB2, MARs 2 and 3 delimitate a 50 kb loop encompassing the *TP53*, *WRAP53*, and *EFNB3* genes. In breast cancer cells MCF7, MARs 1 and 4 delimitate a larger 86 kb loop. In breast cancer cells MDA-MB-231, T47D, and BT474 and in cervix carcinoma HeLa cells, MARs numbers 1 and 3 delimitate large open loops.

highly transcribed, and *EFNB3* and *ATP1B2* the most weakly transcribed genes (see Supplementary Figure 2). However, when comparing the relative expression of each gene, we found that, as compared to the carcinoma cell lines, the HB2 breast epithelial cells consistently showed the highest transcript levels. The *SAT2* gene, which presented higher expression levels in BT474 breast cancer cells, was the only exception (see Supplementary Figure 2).

DISCUSSION

Analysis of MARs continues to reveal a multitude of roles in development and the pathogenesis of diseases and their implication in cancer has been proposed. For example, sites of chromosomal breakpoints preferentially localize to MARs [Schoenlein et al., 1999] and aberrant binding of DNA to the nuclear matrix may destabilize the expression of a host of genes that maintain cells in a non-cancerous state [Linnemann and Krawetz, 2009a]. In the present study, we investigated for the first time the role of MARs in the regulation of transcription of the *TP53* gene domain in breast cells. Our experiments showed an interesting in vivo distribution of MARs among the studied breast cell lines. In HB2 breast epithelial cells, we demonstrated the existence of a relatively small loop, of 50 kb, delimitated by two MARs, including a specific MAR (MAR 2) located 25 kb downstream of the major *TP53* transcription start at *P1*. The non-transformed breast epithelial cell line MCF10A also exhibited a similar in vivo MAR profile, including the specific MAR 2 characteristic of HB2 cells. This MAR 2 anchorage site is missing in all studied breast carcinoma cells, resulting in the formation of larger chromatin loops in these cell lines. In Figure 5, we propose a model of chromatin organization of the studied 167 kb genomic region containing p53 and neighboring genes. Our results are quite surprising, since the average loop size is believed to be smaller in cancer cells as compared to that in normal controls [Linskens et al., 1987; Oberhammer et al., 1993]. Considering the importance of the *TP53* tumor suppressor, it is possible that the studied region is contextually dependent on the state of the cell. This could explain the fact that, in the case of normal cells, this genomic region is organized in a functional and relatively small 50 kb loop. It was previously shown that the association of MARs with the nucleoskeleton may change during development [Vassetzky et al., 2000b] and such changes are also expected during the carcinogenic process. The 50 kb loop flanked by MARs 2 and 3 described in HB2 cells comprises entirely *TP53*, *WRAP53*, and *EFBN3* genes, suggesting a functional arrangement for all three genes. Interestingly, each breast cancer cell line presented a different MARs pattern. This is not totally surprising since breast cancers display a characteristic large variability of phenotypes, which is also observed in the derived cell lines [Neve et al., 2006].

The small number of attachment sites observed in the studied 167 kb region comprising the *TP53* gene locus is in agreement with the previous study of Linnemann and Krawetz [2009b]. They have shown, by screening human chromosomes 14–18, a correlation between high gene density and low number of MARs. Interestingly, the 17p13.1 region presents the highest gene density of the chromosome 17.

Next we have analyzed the mRNA levels of *TP53* as well as of the neighboring genes in order to investigate whether *TP53* transcription could be affected by flanking MARs and loop formation; we found that transcript levels inversely correlate with the size of the chromatin loop and that *TP53* and neighboring genes were more highly expressed in HB2 breast epithelial cells than in carcinoma cells. Interestingly, the transcription start site of the major *TP53* promoter, P1, here arbitrarily considered as nucleotide position zero, is located in the exact middle of the loop, being flanked by MAR 2, at +25 kb, and MAR 3, at −25 kb. This arrangement could indicate that the promoter is conveniently located and exposed to be easily accessible for the RNA polymerase II machinery. Indeed, loop formation has recently been shown to favor transcription in yeast [Tan-Wong et al., 2009; Lainé et al., 2009].

MARs may be found to be related to different chromatin active specific sites such as enhancers, insulators, and replication origins [Petrov et al., 2008; Yochum et al., 2010]. The MAR 2 that we have identified in the 167 kb studied region may have some transcription enhancing activity as it is detected in HB2 cells that express higher levels of genes located in that region. In our model, MAR 2 may act by opening the local chromatin and facilitating the expression of the anti-sense strand genes from this domain (Fig. 5). This effect is reflected through the higher expression levels observed for the *TP53*, *SAT2*, and *FXR2* genes (Supplementary Figure 2). Therefore, it is plausible to expect that p53 transcripts should be produced and available, mainly in response to stress conditions, in part as a consequence of an appropriate chromatin conformation due to specific MARs.

ACKNOWLEDGMENTS

This study has been supported by grants from the Institut National du Cancer (INCa) and Fondation de France to YSV and CAPES-COFECUB to YSV and CG. AG was a recipient of the CAPES fellowship. GCSJ was a recipient of CNPq fellowship.

REFERENCES

Bourdon JC. 2007. p53 and its isoforms in cancer. Br J Cancer 97:277–282.

Buongiorno-Nardelli M, Micheli G, Carri MT, Marilley M. 1982. A relationship beween replicon size and supercoiled loop domains in the eukaryotic genome. Nature 298:100–102.

Eivazova ER, Gavrilov A, Pirozhkova I, Petrov A, Iarovaia OV, Razin SV, Lipinski M, Vassetzky YS. 2009. Interaction in vivo between the two matrix attachment regions flanking a single chromatin loop. J Mol Biol 386(4):929–937.

Frisch M, Frech K, Klingenhoff A, Cartharius K, Liebich I, Werner T. 2002. In silico prediction of scaffold/matrix attachment regions in large genomic sequences. Genome Res 12:349–354.

Gasser SM, Vassetzky YS. 1998. In: Gould H, editors. Chromatin. A practical approach. Oxford, UK: Oxford University Press. pp 111–124.

Gasser SM, Laemmli UK. 1986. Cohabitation of scaffold binding regions with upstream/enhancer elements of three developmentally regulated genes of D. melanogaster. Cell 46(4):521–530.

Hancock R, Boulikas T. 1982. Functional organization in the nucleus. Int Rev Cytol 79:165–214. Review.

Hollstein M, Hainaut P. 2010. Massively regulated genes: the example of TP53. J Pathol 220(2):164–173.

Ioudinkova E, Petrov A, Razin SV, Vassetzky YS. 2005. Mapping long-range chromatin organization within the chicken alpha-globin gene domain using oligonucleotide DNA arrays. Genomics 85(1):143–151.

Lainé JP, Singh BN, Krishnamurthy S, Hampsey M. 2009. A physiological role for gene loops in yeast. Genes Dev 23:2604–2609.

Levine AJ, Oren M. 2009. The first 30 years of p53: growing ever more complex. Nat Rev Cancer 9(10):749–758.

Linnemann A, Krawetz S. 2009a. Maintenance of a functional higher order chromatin structure: the role of the nuclear matrix in normal and disease states. Gene Ther Mol Biol 13:231–243.

Linnemann A, Krawetz S. 2009b. Silencing by nuclear matrix attachment distinguishes cell-type specificity: association with increased proliferation capacity. Nucleic Acids Res 37(9):2779–2788.

Linskens MH, Eijsermans A, Dijkwel PA. 1987. Comparative analysis of DNA loop length in nontransformed and transformed hamster cells. Mutat Res 178(2):245–256.

Mirkovitch J, Mirault ME, Laemmli UK. 1984. Organization of the higher-order chromatin loop: specific DNA attachment sites on nuclear scaffold. Cell 39(1):223–232.

Neve RM, Chin K, Fridlyand J, Yeh J, Baehner FL, Fevr T, Clark L, Bayani N, Coppe J-P, Tong F, Speed T, Spellman PT, DeVries S, Lapuk A, Wang NJ, Kuo W-L, Stilwell JL, Pinkel D, Albertson DG, Waldman FM, McCormick F, Dickson RB, Johnson MD, Lippman M, Ethier S, Gazdar A, Gray JW. 2006. A collection of breast cancer cell lines for the study of functionally distinct cancer subtypes. Cancer Cell 10:515–527.

Oberhammer F, Wilson JW, Dive C, Morris ID, Hickman JA, Wakeling AE, Walker PR, Sikorska M. 1993. Apoptotic death in epithelial cells: cleavage of DNA to 300 and/or 50kb fragments prior to or in the absence of internucleosomal fragmentation. EMBO J 12(9):3679–3684.

Olivier M, Petitjean A, Marcel V, Pétré A, Mounawar M, Plymoth A, de Fromentel CC, Hainaut P. 2009. Recent advances in p53 research: an interdisciplinary perspective. Cancer Gene Ther 16:1–12.

Olivier M, Langerod A, Carrieri P, Bergh J, Klaar S, Eyfjord J, Theillet C, Rodriguez C, Lidereau R, Bieche I, Varley J, Bignon Y, Uhrhammer N, Winqvist R, Jukkola-Vuorinen A, Niederacher D, Kato S, Ishioka C, Hainaut P, Borresen-Dale AL. 2006. The clinical value of somatic TP53 gene mutations in 1,794 patients with breast cancer. Clin Cancer Res 12:1157–1167.

Paulson JR, Laemmli UK. 1977. The structure of histone-depleted metaphase chromosomes. Cell 12(3):817–828.

Petrov A, Pirozhkova I, Carnac G, Laoudj D, Lipinski M, Vassetzky YS. 2006. Chromatin loop domain organization within the 4q35 locus in facioscapulohumeral dystrophy patients versus normal human myoblasts. Proc Natl Acad Sci USA 103:6982–6987.

Petrov A, Allinne J, Pirozhkova I, Laoudj D, Lipinski M, Vassetzky YS. 2008. A nuclear matrix attachment site in the 4q35 locus has an enhancer-blocking activity in vivo: implications for the facio-scapulo-humeral dystrophy. Genome Res 18:39–45.

Razin SV, Vassetzky YS, Hancock R. 1991. Nuclear matrix attachment regions and topoisomerase II binding and reaction sites in the vicinity of a chicken DNA replication origin. Biochem Biophys Res Commun 177(1): 265–270.

Razin SV, Iarovaia OV, Sjakste N, Sjakste T, Bagdoniene L, Rynditch AV, Eivazova ER, Lipinski M, Vassetzky YS. 2007. Chromatin domains and regulation of transcription. J Mol Biol 369:597–607.

Schoenlein PV, Barrett JT, Welter D. 1999. The degradation profile of extrachromosomal circular DNA during cisplatin-induced apoptosis is consistent with preferential cleavage at matrix attachment regions. Chromosoma 108(2):121–131.

Simão TA, Ribeiro FS, Amorim LM, Albano RM, Andrada-Serpa MJ, Cardoso LE, Mendonça GAS, De Moura Gallo CV. 2002. TP53 mutations in breast cancer tumors of patients from Rio de Janeiro, Brazil: association with risk factors and tumor characteristics. Int J Cancer 101:69–73.

Simon P. 2003. Q-Gene: processing quantitative real-time RT-PCR data. Bioinformatics 19:1439–1440.

Tan-Wong SM, Wijayatilake HD, Proudfoot NJ. 2009. Gene loops function to maintain transcriptional memory through interaction with the nuclear pore complex. Genes Dev 23:2610–2624.

Singh GB, Kramer JA, Krawetz SA. 1997. Mathematical model to predict regions of chromatin attachment to the nuclear matrix. Nucleic Acids Res 25:1419–1425.

Vassetzky YS, Hair A, Razin SV. 2000a. Rearrangement of chromatin domains in cancer and development. J Cell Biochem Suppl 35:54–60. Review.

Vassetzky YS, Hair A, Méchali M. 2000b. Rearrangement of chromatin domains during development in Xenopus. Genes Dev 14(12):1541–1552.

Vogelstein B, Lane D, Levine AJ. 2000. Surfing the p53 network. Nature 408:307–310.

Yochum GS, Sherrick CM, Macpartlin M, Goodman RH. 2010. A β-catenin/TCF-coordinated chromatin loop at *MYC* integrates 5′and 3′ Wnt responsive enhancers. Proc Natl Acad Sci USA 107:145–150.

Supplementary Figure 1

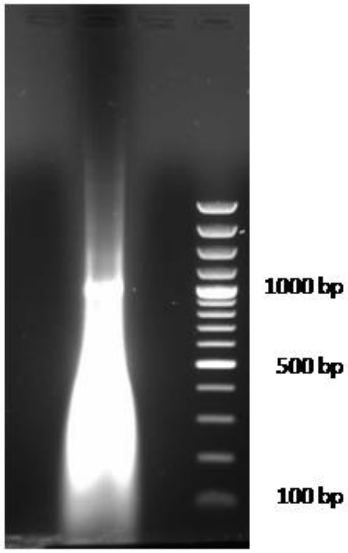

Supplementary Fig. 1: Agarose gel electrophoresis of the extracted matrix-bound DNA from HB2 cells.

Supplementary Figure 2

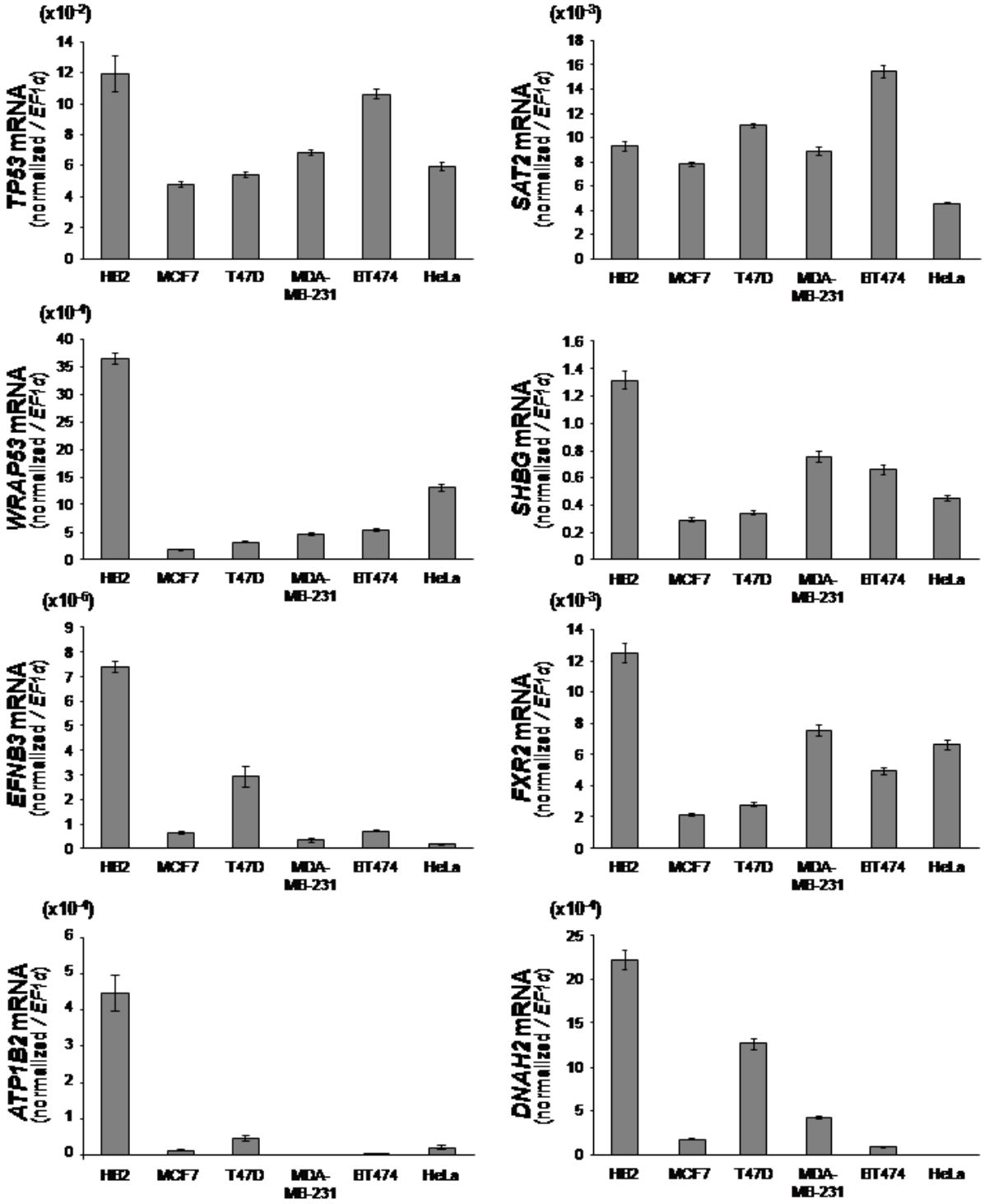

Supplementary Fig. 2: Analysis of *TP53* and neighboring genes transcript levels in non-transformed mammary epithelial cells and carcinoma cell lines. Transcript levels were determined by quantitative reverse transcription-polymerase chain reaction analysis (qRT-PCR). Absolute messenger RNA (mRNA) levels normalized by *EF1α* (elongation factor 1-alpha, Mean ratios ± SEM from 3 independent measurements) are shown. Similar results were obtained when using *18S* ribosomal RNA as a reference (data not shown). HB2: non-transformed mammary epithelial cell line; MCF7, T47D, MDA-MB-231 and BT474: breast carcinoma cell lines; HeLa: cervix carcinoma cell line.

Supplementary Table 1: Oligonucleotide sequences for the DNA array.

Oligo name	Sequence	Size (bp)	Probe
TP53-589	TACCTGAGCTAATAGATGAAGAATTGTATCTCGAA	35	1
TP53-2096	TTTTACAGGACAAAATGTTACAATCCCTAGAAATTTATTC	40	2
TP53-3666	CTTTGCATAACTTAAATAAGGAAAACTGTGTGATATTAAT	40	3
TP53-4981	AAAATAAACTAAGTTGAGTGTTCAAAATCACTACATTAGG	40	4
TP53-7118	TAGAATAGTATAATACCAACGAAAGGGAATCTGACAATTA	40	5
TP53-8811	CTAAAAGAAATTTGAAAATAATTGCACTATACCATGATAG	40	6
TP53-10390	CAATAAAGTCCTCTTGACAAATAAATATAAGCACATTTAAG	41	7
TP53-11679	GAGAATAAACCTAAAGAAAAGTAGAGAATCAAAGAGATAT	40	8
TP53-13016	CTGGATTTTAGATGTTGTTACCATAAATGGAAGGCAAATC	40	9
TP53-14347	ATTGAATCTAGAATGACACTGATAATTTATAAAGGATAATAA	42	10
TP53-16325	AATTTAATGTATAATGACAGAAGATTGGTAGTTGATGGAG	40	11
TP53-18729	TTCATTTGGGAGAGTACAACTTAAAGAATAAAATACATTA	40	12
TP53-19811	CATCATATCTTGATCTTGGACTCAACTTAAGAATCACTTT	40	13
TP53-21038	TAGAAAATAGATTCAGAGCAGATAAGGAAGGTGGTATTATA	41	14
TP53-23043	TTTAAGAATCTGTAACTCTCTACTGTAGTAGATTTAACAG	40	15
TP53-24712	CATAGGAGATAAAGGTTTAGAAAATAAGGTGATGAATTTA	40	16
TP53-27749	AAAATTGAAAAAGAAAAAGAGACATCAAGAAGTGGTAATA	40	17
TP53-29757	TTTTCTTTATTCTCCCTTTAAAAAGCCATTAGCCTAAATA	40	18
TP53-31024	TATTAAGTTTCCTAGTTTATACTCTTTTATCTTCTGCATTA	41	19
TP53-34597	TCCCTTCCATGTACTGTAGATGAAATAGTATATCCCATAG	40	20
TP53-35689	TGCTTTTTAAATTGACATATGCAGTGATAACCTGCTTTAG	40	21
TP53-37118	TTCTTAATATTCACTGAATCATACACACAGACAATACCTT	40	22
TP53-39155	CTGATTTCTACATCCCCGTATCTTATCTCTGTCAC	35	23
TP53-42977	CAAGACTCCTAATTTCTTACAAGAATCTTTTCACCAGTAA	40	24
TP53-44337	AACTTTCATTCAATTAACATGTATTGGCTGCTGATACATT	40	25
TP53-45989	TTCTTATTAATCTCACACAGTTCCTGACATATTAGTTCTC	40	26
TP53-47097	CTTCTCTTATTTTCTTTTTCTTTCTTTCCTTCCCTTCCTT	40	27
TP53- 48198	TTTCAGAAGTCTTCTCTTTCCTTGTTCTTGTCTTT	35	28
TP53-50458	CTTGAGTTTGAAGAAAGTATAAATAGTCTAAGATAAAGGC	40	29
TP53-52461	CAATCTCTTGCTGTATTCATCTTGTCTTTGCTCATTAAAG	40	30
TP53-53834	TCATTATCTCCACCTCTTTTAATCTTTCTTCAAATCTTGC	40	31
TP53-57602	AGATAATGATTCTTAACATGTGGTATGTAGAGCAAGTGTA	40	32
TP53-60468	TTAGGTCTTTCATTTCAGGAACTGTGTTCAAAGTT	35	33
TP53-61713	TATTACGAACAGCCAGATAATGGAGTCCTCAACTA	35	34
TP53-62792	CTTCCTATTCAACCCTTAATCATGTATCTCTTCTTTCTTG	40	35
TP53-64871	TTTTAGCAAGTTATCAACTAATCACTAACTCCTTCCTTTT	40	36
TP53-66284	CAATATGAACTATAAGATCCTAATTTTGTGGAAAGTAAAC	40	37
TP53-67373	CATTGTTCCTATCTATTGTTTGTCTCTTGACTTTGTAGTA	40	38
TP53-68470	CAAATATATCTAATGTGTTCCAATTAAATTGAAATGCTAAT	41	39
TP53-70623	CTACTTATCTGCCTTACTAAATTCTGTTAATTCCATAATAT	41	40
TP53-72489	CTCTTGACCTTAATTGAAATTATCTTAATGTTTAACTTATTAG	43	41
TP53-73864	AATAGAACATATTGATTTAAGGTTGTGAATTACAAGTTTA	40	42
TP53-76030	GGCAGCAAAGTTTTATTGTAAAATAAGAGATCGATATAAA	40	43
TP53-77897	AACTCTGGCTGTATTCAGTATTACACAATTATTAG	35	44

TP53-80958	TATATATTATGGTATAAGTTGGTGTTCTGAAGTTAGTTAG	40	45
TP53-83443	AGGAGTCAGAGATCACACATTAAGTGGGTAAACTATAAAA	40	46
TP53-85072	CTTCTTTAATCTCATCTCTTAACAACCACTCCCTC	35	47
TP53-86461	CTTTATGCCAAATTTGTCATCAGATTTGCTAAGAAACATG	40	48
TP53-87529	TGTCTTTATCTCTCAAATCTTCAGTAGCAACTAAAATCTC	40	49
TP53-94577	CTCTAAAATATACAGCTATGAGTTCTCAATGTTTCGAGAT	40	50
TP53-97460	CTGAAGTTATTTAGAGAGAGGTTTCCCCTTTCTTTAATTA	40	51
TP53-99755	TTTTAAAACAGAAGAGTGAATGGTTTATGGGTGGG	35	52
TP53-101554	TAAATAAGTTTTTGATGAAGCTGAATAAATTGTCATGGTA	40	53
TP53-102863	TTAAATAGATAAAATTTGTATAGGTCAGAAAATTGGGGAA	40	54
TP53-104208	GACTCAGAGATTTTTATGGGAATTAGCAGATAGAGATAAG	40	55
TP53-106018	GAGGGATGTATATGATATAATACCATTACTGTTAAGTCTA	40	56
TP53-107918	AGGTATTATTATTTGTTTCTTCCTCTCTAAGTGTTTATAA	40	57
TP53-109662	CTAGAAAATTGTTGATAAAGCTGATTCCGTTTTCCTGTAG	40	58
TP53-111088	GATATAAAAAGGTTTTTATGATACTAGAGTCTTCGTGTCT	40	59
TP53-114385	GTAAGGTGTTTGAATGTATTATGTGCTCATTAAAGGAGAG	40	60
TP53-116496	TGGAAACCAAATGAGGAAAAGACTCAATTAGAACTAATTA	40	61
TP53-118406	TAATTTGTCTTGTTCTTTCCTTTCCATATCCCAGTATAAT	40	62
TP53-120483	AAATACACACACATATTCCTAGAGTAACAACTGCAACAAA	40	63
TP53-122123	AATGGTTGACATCATATCTGGAATTTTAATTAGAATGAAA	40	64
TP53-123272	ACTTTAATATCATTTCATTAAGTCAGCAAGTTCAGAGAAG	40	65
TP53-124382	AAGAAAATGTCATAAATTTCGCTCCTCATGGAAATGTAAT	40	66
TP53-126644	CTTGATAGATCTTTTCCTGATTATCTTATGTTCTCATACC	40	67
TP53-128269	ATAGTAGCTTGTGAAATAGAATCCCCTTCTAAAATTAAAG	40	68
TP53-130103	GACTCCTATATCTTTACTTGTAAGTTGCATCAGAG	35	69
TP53-131601	GAAGATATTGTCCTAATTGGATACTAATTTCTAAGACATG	40	70
TP53-133456	CCTGTCTATATGTATTATAGGAAAGATTTTAGATCACTATTA	42	71
TP53-134536	TATTACTCTTAGAGGCAAGAAATCTTATTTTTCTGTTTCT	40	72
TP53-135737	TTTAGATAGATAACTATTTCAACAGTGTGGAGAATACATTA	41	73
TP53-136842	GAACTTGAGAGGGTGTAATAAAATCTTAGTAAAGAGAAAG	40	74
TP53-138133	CATCTTGGCTAAGCTACTCAATTGTAGGAAAAATTAATTC	40	75
TP53-140149	ATATGTAGCAGTCAGAACTTTAAGGAATTTTATATTTAAT	40	76
TP53-141444	CTTCAACTTAGACTTGGAAATTTCTAAAAGCACAT	35	77
TP53-142497	AGAGAGACATCAAGTTAACCAATAAATATACATCAAGTAC	40	78
TP53-143801	AATTTGATATGATGTGACAGGCTGATTATGTTAGT	35	79
TP53-144944	CAGAGGATCTGTGGTTGAAAAGGTAGTGAAGATTG	35	80
TP53-146320	AAATTCTATTATGTATGAATCTGCTCCTAGAACTTAGATG	40	81
TP53-147436	GAACTTGCTGGAGATTGAGGACATCTTTCATAAAA	35	82
TP53-149706	AAAGACAGCACAAAGAAACAACAGAAAAACATTGTTTTAA	40	83
TP53-150951	TTACAACTTATCTTAAAACACAACAAAACAAAACAATGAT	40	84
TP53-152550	ATTGTATTCAAATAACAGGATTTCCTTAAACACTAATGAT	40	85
TP53-154008	GTACTATACATATTGTTCTATATATTCCAAGTGCTTTCAAA	41	86
TP53-155356	ATTGTTTTCCAGAGAGATGTTATAGGATACTTTACATTTT	40	87
TP53-157099	ATAATACGTTTATGCTACTAGAAATGTTTCTGTATCTATT	40	88
TP53-158581	TCAATATTCTTTCCAAATAACATTTCAGCAGTATTTAGAA	40	89
TP53-160702	TAGGTGTCTGAATTTCTGAACTTTGCTTTAGCATATTAAA	40	90

TP53-162054	TATCAAGAAACCGCGATCACAAAGATACAAATCTCTTAAG	40	91
TP53-163369	CACTTAAGATGAAGGCTTCATATGCAATTTAAAATTGCCT	40	92
TP53-164872	CTTCAAGATGCTATTTTATTCCTTCTTTTTCTCTTATCTG	40	93
TP53-165988	TCTAGAATCTAGACTAGTGGTCTAGAAATGTTCACATTTC	40	94
TP53-167253	ATTGCATCTTATTTGTCAGTTTCCCTTAATTCCTAAACTT	40	95

Supplementary Table 2: Sequences of quantitative RT-PCR primers for validation of matrix-attached sites.

Localization	**Primers sequence**
Oligo 7	**F**: CTGTAGGAGTCAGGAGCAATA **R**: TGCCTGAATTTCACATAAGCC
Oligo 21	**F**: GACAGCTGGATCTTGTGACTG **R**: GCTGAGGGTCTTAAGGCTTAC
Oligo 22	**F**: GAGTGGGTGATTTCTACTGCT **R**: AACTCCTCCCCCAGTCTTTTC
Oligo 23	**F**: CAAATGCTCAGAGGGGAGTCA **R**: TGTTTGTCCAGCCAGGAATCC
Oligo 42	**F**: TCCTCAGAGTACGAATTTTAG **R**: GAGATCTGAAATCAAATCTCC
Oligo 43	**F**: GACGGTTGGTTCCTGAGTTAT **R**: AAGCACATCTGCATTTTCACC
Oligo 62	**F**: GCTCTGTGCTGATTTTAGGAC **R**: GGATGGAATGAACAAGACAGC
Oligo 63	**F**: GTCTGGAGCTATTTGAAAATG **R**: TGTCTTCCTGTGCCTGTAGTC
Oligo 64	**F**: GGAATTTCTGATGCGGAATGG **R**: TCCCAGGTCTCAAAACTCTCC

Supplementary Table 3: Sequences of quantitative RT-PCR primers.

Gene	**Localization**	**Amplified exons**	**Primers sequence**
TP53	17p13.1	5	**F**: GGCCATCTACAAGCAGTCAC **R**: CCAGACCATCGCTATCTGAG
WRAP53	17p13.1	4-5	**F**: CTTGACCAATAGTGCTGATAAC **R**: GCTGAGGACATCAGAGAATAC
EFNB3	17p13.1	2-4	**F**: CCGCTCGCACCACGATTACT **R**: CTCGGGGACTTTGTCCCACT
SAT2	17p13.1	2-4	**F**: GCCCTGAGAGCAGATGGCTT **R**: GTGCGTCCCTTCCATGTACT
SHBG	17p13.1	3-4	**F**: TTATGCTGGGACTTCGAGACG **R**: CCAAGCGCAATCCTCATGATG
ATP1B2	17p13.1	4-5	**F**: GGCAGCCCTGTGTCTTCATC **R**: ACCAGGGGCTGTGTGTAGTT
DNAH2	17p13.1	8-11	**F**: AGCCCAAGGACATCTCTAGCA **R**: GTGATACTGACAGTCACATAC
FXR2	17p13.1	7-8	**F**: GAGACAAGCAAGCAGTTGGCA **R**: CGGTCACCCCAGGTACTTTTC
EF1α	6q14.1	3-5	**F**: CTGGAGCCAAGTGCTAACATG **R**: CCGGGTTTGAGAACACCAGT

5.2 **Artigo II:** ***MARs and the TP53 gene domain in breast cells***

No artigo anterior, foram determinados os sítios de fixação à matriz nuclear (MARs) no domínio do gene *TP53* em 4 linhagens de carcinomas mamários e duas linhagens não-cancerosas controle. Além do mais, foi verificada a existência da MAR 2, somente nas duas linhagens controle.

Neste artigo, realizamos uma tentativa de caracterização das MARs, num outro nível de complexidade da cromatina, através da determinação do enriquecimento com os marcadores epigenéticos de cromatina aberta (H4Ac) e de cromatina fechada (H3K9me3), nas linhagens controle não-cancerosas HB2 e MCF-10A, e nas linhagens cancerosas MDA-MB-231, T47D e MCF-7.

Além do estado epigenético da cromatina, foi verificada a possível ligação de proteínas e a ligação específica da proteína PARP-1 ligante às MARs (MARBP) na MAR 2, através de ensaios de gel *shift* (EMSA). Através da utilização de um programa de busca de sítios de ligação de fatores de transcrição, foram detectados sítios putativos, na sequência MAR 2, com os fatores de transcrição c/EBPbeta e c-myb, que poderiam ser interessantes elementos reguladores em *cis* da expressão gênica do *TP53* e demais genes flanqueadores.

MARs and the *TP53* gene domain in breast cells

Gilson C. Santos JR[1], Andréa C. S. Góes[2], Yegor Vassetzky[3], Claudia V. de Moura Gallo[1*]

[1]Departamento de Genética, Instituto de Biologia, Universidade do Estado do Rio de Janeiro (UERJ), Rio de Janeiro, 20550-013, Brasil.

[2]Departamento de Ensino de Ciências e Biologia, Universidade do Estado do Rio de Janeiro (UERJ), Rio de Janeiro, 20550-013, Brasil.

[3]Unité mixte de Recherche 8126 « Signalisation, noyaux et innovations en cancérologie», Centre Nacional de Recherche Scientifique, Institut de Cancérologie Gustave-Roussy, Université Paris-Sud 11, F-94805 Villejuif cedex, France.

*Corresponding author: cgallo8@yahoo.com

Laboratório de Biologia Molecular de Tumores (LBMT)

Universidade do Estado do Rio de Janeiro (UERJ)

Pavilhão Haroldo Lisboa da Cunha, sala 525/6

Rua São Francisco Xavier, 524, Rio de Janeiro, RJ, Brasil

CEP: 20550-013

Tel: +55+21+23340858

Key-words: p53, chromatin, loop domain, MAR, transcription, breast cancer, epigenetic modifications, histone, ChIP assay, EMSA, shift

Contract Grant sponsor: CAPES, CNPQ, CAPES-COFECUB

Abstract

In a previous work we determined nuclear matrix attachment sites (MARs) in the *TP53* gene domain in four breast cancer and two non-cancerous cell lines. We found that the *TP53* gene is localized inside a relatively small loop, encompassing 50 kb, delimited by two MARs, designated MARs 2 and 3 detected only in non-cancerous cell lines HB2 and MCF-10A (Goes et al. 2011). In the present paper we made an attempt to characterize these DNA elements in breast non-cancerous cell lines HB2 and MCF-10 and cancerous MCF-7, MDA-MB-231 and T47D, through the determination of epigenetic markers of euchromatin, H4Ac, and heterochromatin, H3K9me3. We further analyzed MAR 2 protein binding, and possible MAR 2 binding of the important MAR binding protein (MARBP), PARP-1, by Electrophoretic mobility Shift Assay (EMSA). We found that these chromatin epigenetic markers are differentially distributed through cell lines. Interestingly, MAR 2 presented a defined band-shift, which could represent trans-acting factor(s), involved in chromatin organization and function. Of note, using bioinformatics software, we found interesting transcription factors binding sites, such as for c/EBP-beta and c-myb, which could be cis-acting elements regulating *TP53* and neighboring genes expression. We describe a possible model for chromatin organization of *TP53* domain.

Introduction

Compartmentalization of chromatin is well defined by DNA loops delimited by nuclear S/MARs (Scaffold/Matrix Attachment Regions), which could be 20 to 200 kb long (Vassetzky, Hair, and Razin 2000). The S/MARs are responsible for DNA attachment to the nuclear matrix (NM) and are linked to cell replication and transcription. They may include Topoisomerase II binding sites (Eivazova et al. 2009; S. V. Razin, Vassetzky, and Hancock 1991) as well as other sequence motifs. Furthermore, NM are enriched in several transcription factors, which have been suggested to be MAR binding proteins (MARBPs) (Ottaviani et al. 2008; Wilson and Coverley 2013; Rivera-Mulia et al. 2011).

In other organization level, approximately 147 bp of DNA is wrapped on an octamer of four core histone proteins (H2A, H2B, H3 and H4), making up the basic unit of chromatin known as nucleosome. The N-terminal tail of histones is subject to several types of post-translational modifications which the two most important are acetylation and methylation of defined amino acids, usually a lysine. These histone modifications can affect the chromatin assembly making it permissible for proteins to modulate cellular processes such as transcription, repair, replication and genome stability (Choe et al. 2012; Budhavarapu, Chavez, and Tyler 2013; Terweij and Leeuwen 2013; Luo et al. 2008).

Histone acetylation and methylation are dynamic processes directed by histone acetyltransferases (HATs) and histone methyltransferases (HMTs). Histone H4 acetylation (H4Ac) is a hallmark of open chromatin or euchromatin and may be a sign of gene activation (Chicoine et al. 1986; O'Neill and Turner 1995; THORNE et al. 1990). It is generally decreased in breast cancer cell lines and tissues (Leroy et al. 2013; Bell et al. 2011). In contrast, histone H3 lysine 9 trimethylation (H3K9me3) is a hallmark of closed chromatin or constitutive heterochromatin and may denote gene repression (Hon et al. 2012; Baylin and Jones 2011).

In a recent paper, Keaton et al (Keaton et al. 2011) described that scaffold attachment regions (SARs) are associated with H4Ac enriched regions and Hendzel et al (Hendzel et al. 1994) reported that HATs are associated with

nuclear matrix. In addition, loops can be active or inactive through chromatin status between the MARs (Davie 1997).

However, literature reporting the interplay between MARs and chromatin status in breast cancer are still missing.

We have previously described MARs in the genomic domain of the tumor suppressor gene *TP53*, in several breast cell lines, using DNA arrays (Goes et al. 2011). We found that the chromatin organization among the cell lines was quite different and only in non-cancerous cells HB-2 two MARs were symmetrically disposed in relation to *TP53* P1 promoter, possibly constituting the borders of a chromatin loop. Interestingly, the MAR localized downstream to *TP53*, designed MAR 2, only detected in HB-2 cells, were confirmed by qPCR in HB-2 and MCF-10A. The present report presents data obtained from chromatin immunoprecipitation and electrophoretic mobility-shift assays performed with the main MARs detected in the *TP53* genomic domain. We believe that our results will help to better understand the *TP53* chromatin domain organization.

Methods

Cell lines

All cell lines were obtained from David Cappellen and Nancy Hynes (Friedrich Miescher Institute for BioMedical Research, Novartis Research Foundation, Basel, Switzerland). The human mammary carcinoma cell lines MDA-MB-231, T47D, and the HeLa cervix carcinoma cell line were cultured in DMEM medium supplemented with 10% horse serum, 0.5% penicillin/streptomycin and 1% glutamine. The human mammary carcinoma cell lines MCF7 and BT474 were cultured in RPMI medium supplemented with 10% horse serum, 0.5% penicillin/streptomycin and 1% glutamine. The control normal epithelial cell lines MCF10A and HB2 were cultured in DMEM medium supplemented with 10% horse serum, 0.5 µg/mL hydrocortisone, 10 µg/mL insulin, 0.5% penicillin/streptomycin and 1% glutamine.

ChIP assay

$25x10^6$ cells were cross-linked with 1% formaldehyde for 10 minutes in a rocking platform at room temperature. Cross-linking reaction was stopped with Glycine 0.125M diluted in 1X PBS. The cells were washed with ice-cold 1X PBS and resuspended in 1mL Lysis/Sonication cold buffer (1%SDS, 10mM EDTA and 50mM Tris-HCl pH 7.5) with fresh 0.5mM PMSF and 1X PIC (Protease Inhibitor Cocktail) and incubated for 30 minutes on ice. The lysates were homogenized with 10 strokes, centrifuged at 750xg for 5 minutes at 4°C and the supernatant was discarded. The pellet was resuspended in 350 µL of Lysis/Sonication cold buffer with freshly added 1mM PMSF and 1X PIC, sonicated on ice and centrifuged for 10 minutes with 2000xg at 4°C. The supernatant contains the extracted chromatin. Immunoprecipitation was carried out overnight at 4°C with constant agitation in an immunoprecipitation buffer (5mM Tris-HCl pH 8.0, 15mM NaCl, 1mM EDTA and 0.1% NP40) with 20 µg of chromatin, 750 µg of Protein G dynabeads #100.03D (Invitrogen®), 4 µg of antibodies H4 pan-acetyl (#39243, Active Motif®), tri-methyl H3K9 (#05-1242, Millipore®), normal rabbit IgG (#PP64B, Millipore®; control) and 1X PIC. All the immunoprecipitations were made with at 1:4 dilutions. The magnetic beads were washed 6 times with the immunoprecipitation buffer and the chromatin was eluted with the Lysis/sonication buffer for 15 minutes at room temperature with constant agitation. The magnetic beads were separated from eluted chromatin and the proteinase K digestion and reverse cross-link were done by 5.25X dilution with 0.2380M NaCl diluted in water, denatured at 95°C for 15 minutes, after 1 uL of RNAse A (10 µg/µL) was added and incubated at 37°C for 15 minutes and 1µL of proteinase K (10 µg/µL) was added and incubated at 67°C for 15 minutes. DNA was cleaned-up by the standard Phenol-Chloroform method and submitted to qPCR.

qPCR, was carried out using the standard Syber-Green method with the Mastermix (Roche®). All fold enrichment values of H4Ac and H3K9me3 are relative to the fold enrichment values of the β-actin gene region or the alpha-satellite region, respectively. All primers, synthesized by SIGMA®, are listed in 5' – 3' and F-forward/R-reverse:

MAR 1: F- GAGTGGGTGATTTCTACTGCT/R- AACTCCTCCCCCAGTCTTTTC;

MAR 2: F- CTGGCCGGAAATGTTTTCTA/R- GTGCCAGGAGCTGTTCTAGG;

MAR 3: F- GTCTGGAGCTATTTGAAAATG/ R- TGTCTTCCTGTGCCTGTAGTC;

MAR 4: F- GTCCTGCCCACTCCCTTCACC/R- CACCCCCAGTCTCTTTGTGCC;

TP53P1: F- GCGTGTCACCGTCGTGGAAAG/ R-GGAGCCTCGCAGGGGTTGATG;

B-actin gene region F-GACGTAGCACAGCTTCTCCT/R-GGGACCTGACTGACTACCTCAT;

Alpha-Satellite (#CS207313, Millipore®) F-CTGCACTACCTGAAGAGGAC/R-GATGGTTCAACACTCTTACA.

Chromatin extraction, immunoprecipitation and qPCR were done in triplicate and the error bars correspond the S.E.M. of three different experiments.

EMSA (Electrophoretic Mobility Shift Assay)

Starting from $2x10^5$ cells, we made whole cells lysates with ice-cold NENT buffer (150mM NaCl; 1mM EDTA; 50mM Tris-HCl pH 7.5; NP40 0.5%) with fresh 1X PIC. 25 pmoles of purified single-strand oligonucleotides 7 (non-MAR: CAATAAAGTCCTCTTGACAAATAAATATAAGCACATTTAAG) and 42 (MAR 2: AATAGAACATATTGATTTAAGGTTGTGAATTACAAGTTTA) (Sigma®) were radiolabeled with 10 U of T4 polynucleotide kinase (#EK0037, Fermentas®) and 10µCi of γP^{32} with incubation at 37°C for 1 hour and purified with Probe-Quant kit G-50 (GE®). The radiolabeled oligos 7 and 42 were incubated for 30 minutes at room temperature with 4 µg of whole cell protein extracts with binding buffer (10mM Tris-HCl pH 7.5; 0.1M NaCl; 1mM EDTA; 4% Glicerol; 1mM DTT) and fresh 1µg of Poly dI-dC (we also incubated without Poly dI-dC and did not observed any changes). After DNA-protein binding reaction, the complexes were submitted to 6% non-denaturing poly-acrylamide gel electrophoresis for one hour at 4°C, the gel was dried at GE® vacuum gel-dry system at 80°C in a filter paper and the radioactive filter paper was exposed with x-ray film for 24 hours at -80°C. After film revelation and

scanned, all densitometry analysis were made by Image J® software. The whole-cell protein extraction and EMSA were done in triplicate. Measure of the relative binding in different cell lines was done with the formula (band shift signal of each cell line/free probe signal) and error bars +/-correspond the S.E.M. of three different experiments. For super-shift assays, 1uL of PARP-1 (SC-53643, Millipore®) was added before or after DNA probe, followed by 30 minutes of room temperature binding reaction with whole-cell protein extracts, as described above. For antibody affinity control, we also made super-shift assays with anti-IgG (#PP64B, Millipore®) in the same conditions of described above.

Transcription factors binding sites search

Analysis of transcription factors binding sites was performed assessing http://alggen.lsi.upc.es/cgi-bin/promo_v3/promo/promoinit.cgi?dirDB=TF_8.3 (Messeguer et al. 2002; Farré et al. 2003).

Statistic analysis

All statistic data and graphics performed by GraphPad version 6.0 using unpaired t-test analyses with Welch's correction and 95% confidence interval.

Results and Discussion

Scaffold/Matrix Attachment Regions (S/MARs) have been described as cis-acting factors operating in DNA replication, transcription regulation and chromatin organization. Possibly it takes part in the coordination of these cellular processes (Trevilla-García and Aranda-Anzaldo 2011; Dijkwel and Hamlin 1988; Boulikas 1995). The tumor suppressor gene *TP53* is one of the most studied genes implicated in cancer and, although a huge knowledge of its post-translational regulation found in the literature (Muller and Vousden 2013; Khoury et al. 2013), its transcription control and genomic domain are not very well established (B. Wang et al. 2013). In a previous work we described MARs in a genomic region of 167 kb containing the *TP53* and neighboring genes, using different cell lines (Goes et al, 2011). In the present paper we concentrated our study in four MARs, namely MAR 1, 2, 3 and 4, with emphasis in MAR 2, which was just detected in the two analyzed non-

cancerous cell lines HB2 and MCF-10A. Figure 1A shows the organization of *TP53* gene domain region and the localization of the MARs.

Chromatin is composed of DNA and proteins, mostly histones, which are involved in genomic DNA organization in the nuclei. Histone alterations in N-terminal tail by acetylation, methylation or ubiquitylation may produce different levels of DNA compaction, leading to an open chromatin or euchromatin, permissive to protein factors access, or leading to a close chromatin or heterochromatin, repressive for the association of transcription factors (S. V Razin et al. 2004; Espinoza and Ren 2011; van Steensel 2011; Zuleger, Robson, and Schirmer 2011). These histone alterations may be tracked using chromatin immunoprecipitation assay (ChIP), and give an idea of the chromatin ambiance through the epigenetic profile at a genomic site, in normal and cancerous cells (Gargiulo and Minucci 2009; Dalvai and Bystricky 2010).

In order to determine the chromatin state at MARs, we performed ChIP assays to detect the enrichment of the euchromatin marker H4Ac and heterochromatin marker H3K9me3, in two non-cancerous cell lines: HB2 and MCF-10A, and in three cancerous cell lines: MCF-7, T47D and MDA-MB-231. Also, we did ChIP assays in *TP53* gene P1 promoter region (TP53P1) to check a possible influence of promoter chromatin status in *TP53* gene transcription level. As presented in Figure 1B, despite the important difference between H3K9me3 and H4Ac enrichment in all four MARs observed in MDA-MB-231 and MCF-10A cells, we could not identify a pattern of histone markers enrichment between the non-cancerous and cancerous cells. Moreover, enrichment levels were quite different among cell lines, suggesting that MARs are not linked to a defined chromatin state. Though, a recent report described an association of MARs to active histone marks, H3Ac and H4Ac, suggesting that they may prevent the spread of silencing chromatin (Majocchi, Aritonovska, and Mermod 2013). Surprisingly, TP53P1 presented a highly enrichment of heterochromatin marker H3K9me3 in MCF-7 and MDA-MB-231 cells. The highest enrichment of H3K9me3 in MCF-7 cells corroborates with lowest levels of *TP53* gene expression published earlier by our group (Goes et al. 2011).

In an attempt to characterize a possible activity linked to the non-cancerous cells on MAR 2, we assessed protein binding through a supershift analysis performed with antibody anti-PARP-1. Poly-ADP-ribose polymerase 1 or PARP-1 is a multifunctional enzyme, present in human cells nuclei. Aubin et al. 1983, reported that PARP-1 interfere in the chromatin organization, modifying histone H1 and facilitating local chromatin remodeling. Moreover, it's an important MARBP, implicated in breast cancer progression and heterochromatin maintenance (Zaalishvili et al. 2012; Barboro et al. 2012; Galande and Kohwi-Shigematsu 1999; Vidaković et al. 2005; T.-Y. Wang et al. 2010; Sjakste, Sjakste, and Vikmanis 2004; Thomas and Tulin 2013).

Surprisingly, as shown in Figure 2, anti-PARP-1 can bind to protein complexes of cancerous cells MDA-MB-231 and MCF-7, disabling MAR 2 probe binding. As MAR 2 was not detected in our earlier report on these cell lines, we can suggest that PARP-1 interaction has another role than MARBP, for MDA-MB-231 and MCF-7. In contrast, in non-cancerous MCF10A cell line, where MAR 2 was detected by qPCR, and cancerous cell line T47D (also lacking MAR 2 region), we did not detect PARP-1 binding. These results together, suggest that PARP-1 is not a MAR 2 binding protein, although it can act in a different fashion through binding in the MAR 2 region in MDA-MB-231 and MCF-7 cells. In addition, as all anti-PARP-1 binding reactions show intense binding in gel wells, we can suggest that PARP-1 can integrate larger protein complexes that still remain to be elucidated.

Figure 3 shows EMSA performed with total protein extracts from breast cell lines and MAR 2 as probe. Furthermore, we made analysis of a non-MAR Oligonucleotide (oligo 7) in order to compare the presence of protein complexes attached to DNA in a non-MAR probe. Interestingly, we could observe a single shifted band with MAR2 and several unspecific bands with oligo 7. This single band is more intense in the non-cancerous MCF-10A, although present in cancerous cells. This observation suggests that MAR 2 is subject to bind protein factors among the different breast cell lines (Figure 3).

Hence, with the possibility of trans-acting factors binding specifically at MAR 2, we performed a search of transcription factors binding sites using the MAR

2 oligonucleotide sequence. As presented in Figure 4, besides the AT-rich composition, a hallmark of MAR elements, 11 functional proteins were found to have putative binding sites. They are: GR-beta; GR-alpha; PR A; PR B; FOXP3; c-Myb; HOXD9; HOXD10; POU2F2 (Oct-2.1); C/EBP-alpha and C/EBP-beta (Figure 4). We will discuss some of these proteins in the light of published literature and importance for our work.

Octamer-binding 2 or Oct-2 is one of the members of the POU factors and was considered to be expressed only in B lymphocytes and neuronal cells (Latchman 1996). However, Dong and Zhou, 2007, demonstrated its expression in mouse mammary gland (Dong and Zhao 2007). Finally, it is now considered to be highly expressed in adult tissues. The octamer motif – ATGCAAAT – and close motifs are normally present in promoters and enhancers elements (Zhao 2013).

C/EBP-alpha and C/EBP-beta, are proteins of the CCAAT/enhancer-binding protein (C/EBP) family, involved in the control of cell proliferation and differentiation (Tsukada et al. 2011; Nerlov 2007). C/EBP-alpha is considered to be a tumor suppressor, promoting differentiation and blocking proliferation. In other hand, C/EBP-beta activities are less straightforward. It seems that C/EBP-beta inhibit or activate cell cycle progression, depending on the cellular context (Nerlov 2007). This transcription factor acts through protein-protein interactions with its own molecules (homodimer) or with a different protein molecule (heterodimer). One of these cooperative interactions occurs with the protein c-myb, with a crucial role in myeloid differentiation (Tahirov et al. 2002; Tsukada et al. 2011).

Very interestingly, we have found a clear palindrome, characteristic of c/EBP-beta DNA binding sites, in the MAR2 sequence with a high score of similarity with c/EBP-beta published sites. Moreover, 6 base pairs away, it came out in evidence a DNA binding site for c-myb that, as already mentioned, may interact with c/EBP-beta (Tahirov et al. 2002).

c-myb proteins constitute a superfamily of sequence-specific transcription factors encoded by the proto-oncogene c-MYB. These protein factors are very important in plants and in mammals it plays a key role in proliferation control,

regulating several different molecular pathways. The over-expression of c-myb has been described in cancers with an association with aggressiveness, including breast cancer (Zhou and Ness 2011).

Our results point to a possible active role of c/EBP binding at MAR 2 in the expression of *TP53* and neighboring genes. As described in Goes et al. 2011, the expression of *TP53* and other studied genes were up-regulated in HB2 cells. Conversely, we performed RT-qPCR with MCF10A cells, which presented MAR 2, assessed by qPCR, and found that *TP53* transcription level was not that high, presenting approximately 5X less transcription than HB2.

Binding of c/EBP complexes in a MAR element in normal and in cancerous cells, may differently induce genes, including the nearby *TP53*, leading to a normal cell growth or not.

Robinson et al, 1998 have demonstrated, using c/EBP-beta-deficient mice, that c/EBP-beta is essential for normal growth and differentiation of the mammary gland. Bundy and Sealy, 2003, have shown that the over-expression of LAP2, a c/EBP-beta isoform, in MCF10A cells, leads to epithelial–mesenchymal transition and transformation. A more profound analysis of the protein complexes found in EMSA experiments is currently under investigation in our laboratories, but our work with MAR2 by EMSA data through different lineage protein cells extracts are encouraging. We believe that this DNA sequence is an interesting functional element and that our data will help to better understand the mechanisms of *TP53* regulation and breast cancer development. Figure 5 presents the chromatin loop organization model, illustrating only loops with *TP53* and flanking gene *ATP1B2* domains, limited by described MARs (Goes et al. 2011) together with chromatin status of described MARs and *TP53* P1 promoter region (TP53P1), resuming our findings. This model allows the visualization of different levels of chromatin organization (MARs and histone epigenetic modifications linked to open/closed chromatin), acting on transcription levels in different cell lines. Also, from this model, we could illustrate there is no association between chromatin status (blue/red bars) and loop/MARs presence, neither normal breast cells nor cancer breast cell lines.

References

Aubin, R J, A Fréchette, G de Murcia, P Mandel, A Lord, G Grondin, and G G Poirier. 1983. "Correlation Between Endogenous Nucleosomal hyper(ADP-Ribosyl)ation of Histone H1 and the Induction of Chromatin Relaxation." *The EMBO Journal* 2 (10) (January): 1685–93. http://www.pubmedcentral.nih.gov/articlerender.fcgi?artid=555344&tool=pmcentrez&rendertype=abstract.

Barboro, Paola, Erica Repaci, Cristina D'Arrigo, and Cecilia Balbi. 2012. "The Role of Nuclear Matrix Proteins Binding to Matrix Attachment Regions (Mars) in Prostate Cancer Cell Differentiation." *PloS One* 7 (7) (January): e40617. doi:10.1371/journal.pone.0040617. http://www.pubmedcentral.nih.gov/articlerender.fcgi?artid=3394767&tool=pmcentrez&rendertype=abstract.

Baylin, Stephen B, and Peter A Jones. 2011. "A Decade of Exploring the Cancer Epigenome - Biological and Translational Implications." *Nature Reviews. Cancer* 11 (10) (October): 726–34. doi:10.1038/nrc3130. http://dx.doi.org/10.1038/nrc3130.

Bell, Oliver, Vijay K Tiwari, Nicolas H Thomä, and Dirk Schübeler. 2011. "Determinants and Dynamics of Genome Accessibility." *Nature Reviews. Genetics* 12 (8) (August): 554–64. doi:10.1038/nrg3017. http://www.ncbi.nlm.nih.gov/pubmed/21747402.

Boulikas, T. 1995. "Chromatin Domains and Prediction of MAR Sequences." *International Review of Cytology* 162A (January): 279–388. http://www.ncbi.nlm.nih.gov/pubmed/8575883.

Budhavarapu, Varija N, Myrriah Chavez, and Jessica K Tyler. 2013. "How Is Epigenetic Information Maintained through DNA Replication?" *Epigenetics & Chromatin* 6 (1): 32. doi:10.1186/1756-8935-6-32. http://www.epigeneticsandchromatin.com/content/6/1/32.

Chicoine, L G, I G Schulman, R Richman, R G Cook, and C D Allis. 1986. "Nonrandom Utilization of Acetylation Sites in Histones Isolated from Tetrahymena. Evidence for Functionally Distinct H4 Acetylation Sites." *The Journal of Biological Chemistry* 261 (3) (January 25): 1071–6. http://www.ncbi.nlm.nih.gov/pubmed/3080415.

Choe, Moon Kyung, Chang-Pyo Hong, Jihwan Park, Seong Hye Seo, and Tae-Young Roh. 2012. "Functional Elements Demarcated by Histone Modifications in Breast Cancer Cells." *Biochemical and Biophysical Research Communications* 418 (3) (February 17): 475–82. doi:10.1016/j.bbrc.2012.01.042. http://www.ncbi.nlm.nih.gov/pubmed/22285863.

Dalvai, Mathieu, and Kerstin Bystricky. 2010. "The Role of Histone Modifications and Variants in Regulating Gene Expression in Breast Cancer." *Journal of Mammary Gland Biology and Neoplasia* 15 (1) (March): 19–33. doi:10.1007/s10911-010-9167-z. http://www.ncbi.nlm.nih.gov/pubmed/20131086.

Davie, J R. 1997. "Nuclear Matrix, Dynamic Histone Acetylation and Transcriptionally Active Chromatin." *Molecular Biology Reports* 24 (3) (August): 197–207. http://www.ncbi.nlm.nih.gov/pubmed/9291093.

Dijkwel, P a, and J L Hamlin. 1988. "Matrix Attachment Regions Are Positioned Near Replication Initiation Sites, Genes, and an Interamplicon Junction in the Amplified Dihydrofolate Reductase Domain of Chinese Hamster Ovary Cells." *Molecular and Cellular Biology* 8 (12) (December): 5398–409. http://www.pubmedcentral.nih.gov/articlerender.fcgi?artid=365642&tool=pmcentrez&rendertype=abstract.

Dong, Bing, and Feng-Qi Zhao. 2007. "Expression of the Oct-2 Transcription Factor in Mouse Mammary Gland and Cloning and Characterization of a Novel Oct-2 Isoform." *Cell and Tissue Research* 328 (3) (June): 595–606. doi:10.1007/s00441-006-0368-0. http://www.ncbi.nlm.nih.gov/pubmed/17285328.

Eivazova, Elvira R, Aleksey Gavrilov, Iryna Pirozhkova, Andrei Petrov, Olga V Iarovaia, Sergey V Razin, Marc Lipinski, and Yegor S Vassetzky. 2009. "Interaction in Vivo Between the Two Matrix Attachment Regions Flanking a Single Chromatin Loop." *Journal of Molecular Biology* 386 (4) (March 6): 929–37. doi:10.1016/j.jmb.2008.12.022. http://www.ncbi.nlm.nih.gov/pubmed/19118562.

Espinoza, Celso a, and Bing Ren. 2011. "Mapping Higher Order Structure of Chromatin Domains." *Nature Genetics* 43 (7) (July): 615–6. doi:10.1038/ng.869. http://www.ncbi.nlm.nih.gov/pubmed/21709679.

Farré, Domènec, Romà Roset, Mario Huerta, José E Adsuara, Llorenç Roselló, M Mar Albà, and Xavier Messeguer. 2003. "Identification of Patterns in Biological Sequences at the ALGGEN Server: PROMO and MALGEN." *Nucleic Acids Research* 31 (13) (July 1): 3651–3.

http://www.pubmedcentral.nih.gov/articlerender.fcgi?artid=169011&tool=pmcentrez&rendertype=abstract.

Galande, S, and T Kohwi-Shigematsu. 1999. "Poly(ADP-Ribose) Polymerase and Ku Autoantigen Form a Complex and Synergistically Bind to Matrix Attachment Sequences." *The Journal of Biological Chemistry* 274 (29) (July 16): 20521–8. http://www.ncbi.nlm.nih.gov/pubmed/10400681.

Gargiulo, Gaetano, and Saverio Minucci. 2009. "Epigenomic Profiling of Cancer Cells." *The International Journal of Biochemistry & Cell Biology* 41 (1) (January): 127–35. doi:10.1016/j.biocel.2008.07.021. http://www.ncbi.nlm.nih.gov/pubmed/18771747.

Goes, Andrea C S, David Cappellen, Gilson C Santos, Iryna Pirozhkova, Marc Lipinski, Yegor Vassetzky, and Claudia V de Moura-Gallo. 2011. "Loop Domain Organization of the P53 Locus in Normal and Breast Cancer Cells Correlates with the Transcriptional Status of the TP53 and the Neighboring Genes." *Journal of Cellular Biochemistry* 112 (8) (August): 2072–81. doi:10.1002/jcb.23129. http://www.ncbi.nlm.nih.gov/pubmed/21465532.

Hendzel, M J, J M Sun, H Y Chen, J B Rattner, and J R Davie. 1994. "Histone Acetyltransferase Is Associated with the Nuclear Matrix." *The Journal of Biological Chemistry* 269 (36): 22894–22901. http://www.ncbi.nlm.nih.gov/pubmed/8077241.

Hon, Gary C, R David Hawkins, Otavia L Caballero, Christine Lo, Ryan Lister, Mattia Pelizzola, Armand Valsesia, et al. 2012. "Global DNA Hypomethylation Coupled to Repressive Chromatin Domain Formation and Gene Silencing in Breast Cancer." *Genome Research* 22 (2) (February): 246–58. doi:10.1101/gr.125872.111. http://www.pubmedcentral.nih.gov/articlerender.fcgi?artid=3266032&tool=pmcentrez&rendertype=abstract.

Keaton, Mignon a, Christopher M Taylor, Ryan M Layer, and Anindya Dutta. 2011. "Nuclear Scaffold Attachment Sites Within ENCODE Regions Associate with Actively Transcribed Genes." *PloS One* 6 (3) (January): e17912. doi:10.1371/journal.pone.0017912. http://www.pubmedcentral.nih.gov/articlerender.fcgi?artid=3056778&tool=pmcentrez&rendertype=abstract.

Khoury, Marie P, Virginie Marcel, Kenneth Fernandes, Alexandra Diot, David P Lane, and Jean-christophe Bourdon. 2013. "Detecting and Quantifying P53 Isoforms at mRNA Level in Cell Lines and Tissues." In *Methods in Molecular Biology (Clifton, N.J.)*, edited by Sumitra Deb and Swati Palit Deb, 962:1–14. Totowa, NJ: Humana Press. doi:10.1007/978-1-62703-236-0_1. http://link.springer.com/10.1007/978-1-62703-236-0.

Latchman, D S. 1996. "The Oct-2 Transcription Factor." *The International Journal of Biochemistry & Cell Biology* 28 (10) (October): 1081–3. http://www.ncbi.nlm.nih.gov/pubmed/8930131.

Leroy, Gary, Peter A Dimaggio, Eric Y Chan, Barry M Zee, M Andres Blanco, Barbara Bryant, Ian Z Flaniken, et al. 2013. "A Quantitative Atlas of Histone Modification Signatures from Human Cancer Cells." *Epigenetics & Chromatin* 6 (1) (January): 20. doi:10.1186/1756-8935-6-20. http://www.epigeneticsandchromatin.com/content/6/1/20.

Luo, XG, S Guo, Yu Guo, and CL Zhang. 2008. "Histone Modification and Breast Cancer." In *Breast Cancer - Focusing Tumor Microenvironment, Stem Cells and Metastasis*, 15:321–342. doi:10.5772/24308. http://www.intechopen.com/source/pdfs/24888/InTech-Histone_modification_and_breast_cancer.pdf.

Majocchi, Stefano, Elena Aritonovska, and Nicolas Mermod. 2013. "Epigenetic Regulatory Elements Associate with Specific Histone Modifications to Prevent Silencing of Telomeric Genes." *Nucleic Acids Research* (8) (September 25): 1–12. doi:10.1093/nar/gkt880. http://www.ncbi.nlm.nih.gov/pubmed/24071586.

Messeguer, X., R. Escudero, D. Farre, O. Nunez, J. Martinez, and M.M. Alba. 2002. "PROMO: Detection of Known Transcription Regulatory Elements Using Species-Tailored Searches." *Bioinformatics* 18 (2) (February 1): 333–334. doi:10.1093/bioinformatics/18.2.333. http://bioinformatics.oxfordjournals.org/content/18/2/333.

Muller, Patricia A J, and Karen H Vousden. 2013. "P53 Mutations in Cancer." *Nature Cell Biology* 15 (1) (January): 2–8. doi:10.1038/ncb2641. http://dx.doi.org/10.1038/ncb2641.

Nerlov, Claus. 2007. "The C/EBP Family of Transcription Factors: a Paradigm for Interaction Between Gene Expression and Proliferation Control." *Trends in Cell Biology* 17 (7) (July): 318–24. doi:10.1016/j.tcb.2007.07.004. http://www.ncbi.nlm.nih.gov/pubmed/17658261.

O'Neill, L P, and B M Turner. 1995. "Histone H4 Acetylation Distinguishes Coding Regions of the Human Genome from Heterochromatin in a Differentiation-Dependent but Transcription-Independent Manner." *The EMBO Journal* 14 (16) (August 15): 3946–57.

http://www.pubmedcentral.nih.gov/articlerender.fcgi?artid=394473&tool=pmcentrez&rendertype=abstract.

Ottaviani, Diego, Elliott Lever, Petros Takousis, and Denise Sheer. 2008. "Anchoring the Genome." *Genome Biology* 9 (1) (January): 201. doi:10.1186/gb-2008-9-1-201. http://genomebiology.com/2008/9/1/201.

Razin, S.V., Y.S. Vassetzky, and R. Hancock. 1991. "Nuclear Matrix Attachment Regions and Topoisomerase II Binding and Reaction Sites in the Vicinity of a Chicken DNA Replication Origin." *Biochemical and Biophysical Research Communications* 177 (1): 265–270. http://www.sciencedirect.com/science/article/pii/0006291X9191977K.

Razin, Sergey V, Andrei Petrov, Alan Hair, and Yegor S Vassetzky. 2004. "Chromatin Domains and Territories: Flexibly Rigid." *Critical Reviews in Eukaryotic Gene Expression* 14 (1-2) (January): 79–88. http://www.ncbi.nlm.nih.gov/pubmed/15104529.

Rivera-Mulia, Juan Carlos, Rolando Hernández-Muñoz, Federico Martínez, and Armando Aranda-Anzaldo. 2011. "DNA Moves Sequentially Towards the Nuclear Matrix During DNA Replication in Vivo." *BMC Cell Biology* 12 (1) (January): 3. doi:10.1186/1471-2121-12-3. http://www.pubmedcentral.nih.gov/articlerender.fcgi?artid=3037911&tool=pmcentrez&rendertype=abstract.

Sjakste, Nikolajs, Tatjana Sjakste, and Uldis Vikmanis. 2004. "ROLE OF THE NUCLEAR MATRIX PROTEINS IN MALIGNANT." *Experimental Oncology* 26 (3): 170–178.

Tahirov, Tahir H, Ko Sato, Emi Ichikawa-Iwata, Motoko Sasaki, Taiko Inoue-Bungo, Masaaki Shiina, Kazumi Kimura, et al. 2002. "Mechanism of c-Myb-C/EBP Beta Cooperation from Separated Sites on a Promoter." *Cell* 108 (1) (January 11): 57–70. http://www.ncbi.nlm.nih.gov/pubmed/11792321.

Terweij, Marit, and Fred van Leeuwen. 2013. "Histone Exchange: Sculpting the Epigenome." *Frontiers in Life Science* (October 9): 1–17. doi:10.1080/21553769.2013.838193. http://dx.doi.org/10.1080/21553769.2013.838193.

Thomas, Colin, and Alexei V Tulin. 2013. "Poly-ADP-Ribose Polymerase: Machinery for Nuclear Processes." *Molecular Aspects of Medicine* 34 (6) (December): 1124–37. doi:10.1016/j.mam.2013.04.001. http://www.ncbi.nlm.nih.gov/pubmed/23624145.

THORNE, Alan W., Daniel KMICIEK, Keith MITCHELSON, Pierre SAUTIERE, and Colyn CRANE-ROBINSON. 1990. "Patterns of Histone Acetylation." *European Journal of Biochemistry* 193 (3) (November): 701–713. doi:10.1111/j.1432-1033.1990.tb19390.x. http://doi.wiley.com/10.1111/j.1432-1033.1990.tb19390.x.

Trevilla-García, Claudia, and Armando Aranda-Anzaldo. 2011. "Cell-Type-Specific Organization of Nuclear DNA into Structural Looped Domains." *Journal of Cellular Biochemistry* 112 (2) (February): 531–40. doi:10.1002/jcb.22943. http://www.ncbi.nlm.nih.gov/pubmed/21268074.

Tsukada, Junichi, Yasuhiro Yoshida, Yoshihiko Kominato, and Philip E Auron. 2011. "The CCAAT/enhancer (C/EBP) Family of Basic-Leucine Zipper (bZIP) Transcription Factors Is a Multifaceted Highly-Regulated System for Gene Regulation." *Cytokine* 54 (1) (April): 6–19. doi:10.1016/j.cyto.2010.12.019. http://www.ncbi.nlm.nih.gov/pubmed/21257317.

Van Steensel, Bas. 2011. "Chromatin: Constructing the Big Picture." *The EMBO Journal* 30 (10) (May 18): 1885–95. doi:10.1038/emboj.2011.135. http://www.pubmedcentral.nih.gov/articlerender.fcgi?artid=3098493&tool=pmcentrez&rendertype=abstract.

Vassetzky, Y S, A Hair, and S V Razin. 2000. "Rearrangement of Chromatin Domains in Cancer and Development." *Journal of Cellular Biochemistry. Supplement* Suppl 35 (January): 54–60. http://www.ncbi.nlm.nih.gov/pubmed/11389532.

Vidaković, Melita, Mario Koester, Sandra Goetze, Silke Winkelmann, Martin Klar, Goran Poznanović, and Juergen Bode. 2005. "Co-Localization of PARP-1 and Lamin B in the Nuclear Architecture: a Halo-Fluorescence- and Confocal-Microscopy Study." *Journal of Cellular Biochemistry* 96 (3) (October 15): 555–68. doi:10.1002/jcb.20516. http://www.ncbi.nlm.nih.gov/pubmed/16052477.

Wang, B, D Niu, T H Lam, Z Xiao, and E C Ren. 2013. "Mapping the P53 Transcriptome Universe Using P53 Natural Polymorphs." *Cell Death and Differentiation* (September 27). doi:10.1038/cdd.2013.132. http://dx.doi.org/10.1038/cdd.2013.132.

Wang, Tian-Yun, Zhong-Min Han, Yu-Rong Chai, and Jun-He Zhang. 2010. "A Mini Review of MAR-Binding Proteins." *Molecular Biology Reports* 37 (7) (October): 3553–60. doi:10.1007/s11033-010-0003-8. http://www.ncbi.nlm.nih.gov/pubmed/20174991.

Wilson, Rosemary H C, and Dawn Coverley. 2013. "Relationship Between DNA Replication and the Nuclear Matrix." *Genes to Cells : Devoted to Molecular & Cellular Mechanisms* 18 (1) (January): 17–31. doi:10.1111/gtc.12010.

http://www.pubmedcentral.nih.gov/articlerender.fcgi?artid=3564400&tool=pmcentrez&rendertype=abstract.

Zaalishvili, G, E Zaldastanishvili, M Karapetian, and T Zaalishvili. 2012. "Increased PARP-1 Levels in Nuclear Matrix Isolated from Heat Shock Treated Rat Liver." *Biochemistry. Biokhimii͡a* 77 (1) (January): 105–10. doi:10.1134/S0006297912010130. http://www.ncbi.nlm.nih.gov/pubmed/22339640.

Zhao, Feng-Qi. 2013. "Octamer-Binding Transcription Factors: Genomics and Functions." *Frontiers in Bioscience (Landmark Edition)* 18 (January): 1051–71. http://www.ncbi.nlm.nih.gov/pubmed/23747866.

Zhou, Ye, and Scott A Ness. 2011. "Myb Proteins: Angels and Demons in Normal and Transformed Cells." *Frontiers in Bioscience (Landmark Edition)* 16 (January): 1109–31. http://www.pubmedcentral.nih.gov/articlerender.fcgi?artid=3570128&tool=pmcentrez&rendertype=abstract.

Zuleger, Nikolaj, Michael I Robson, and Eric C Schirmer. 2011. "The Nuclear Envelope as a Chromatin Organizer." *Nucleus (Austin, Tex.)* 2 (5): 339–49. doi:10.4161/nucl.2.5.17846. http://www.pubmedcentral.nih.gov/articlerender.fcgi?artid=3322583&tool=pmcentrez&rendertype=abstract.

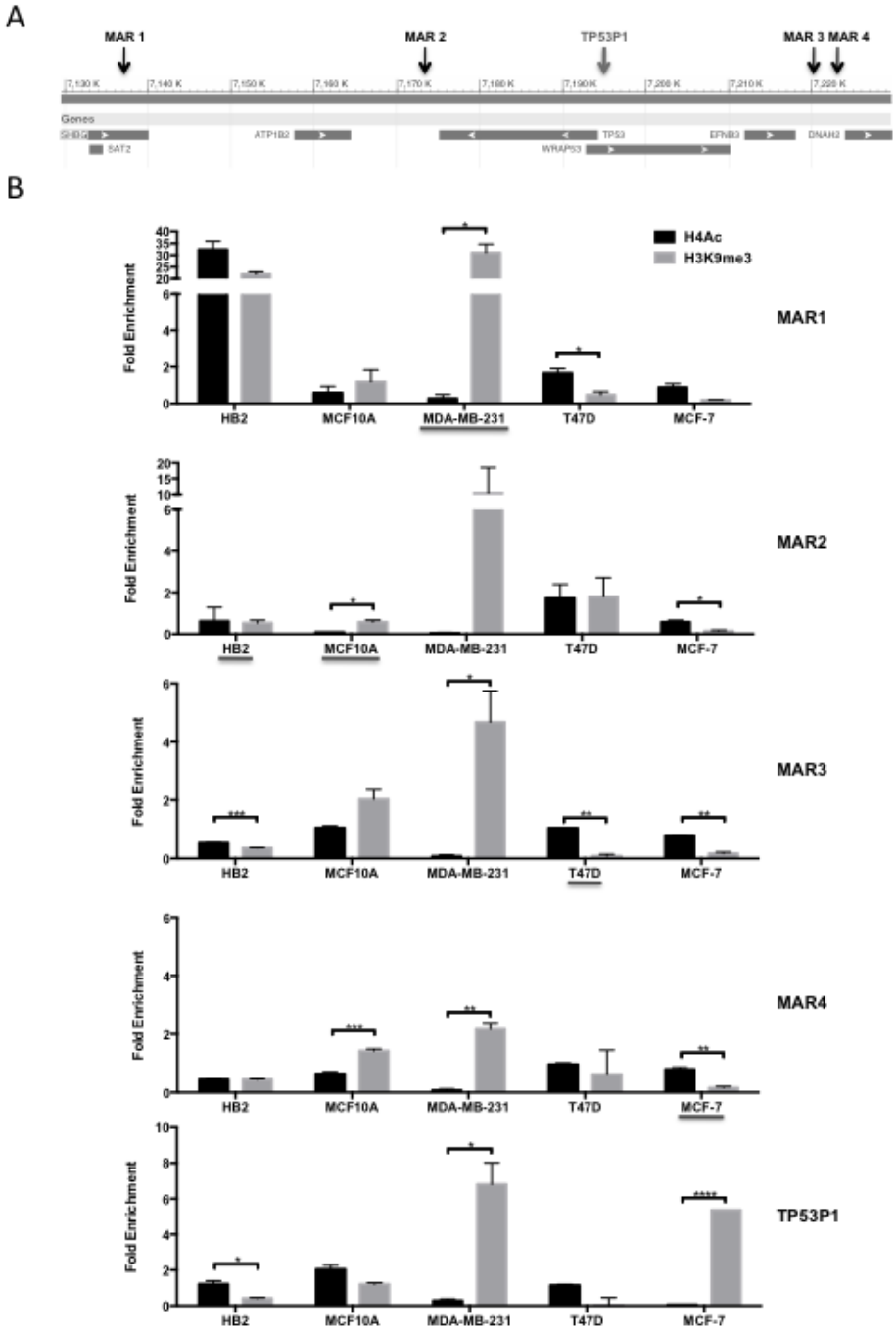

Figure 1 – Chromatin state of MARs and TP53P1 promoter region in *TP53* gene domain. (A) *TP53* genomic region organization based on NCBI database: NT_010718.16:7.1M-7.2M (94Kbs+), covering the 167kb genomic domain at the 17p13.1 chromosomal region. Genes are represented by horizontal bars and arrows indicate the four analyzed MARs (black); P1 promoter region of *TP53* gene (gray). (B) ChIP assay of MARs, indicating the enrichment of euchromatin marker H4Ac (relative to beta-actin gene region) and heterochromatin marker H3K9me3 (relative do alfa-satellite gene region). Underline indicates cell line where MAR was described. Error bars correspond to +/-S.E.M. from 3 different experiments. *p<0.05; **p<0.005; ***p<0.0005.

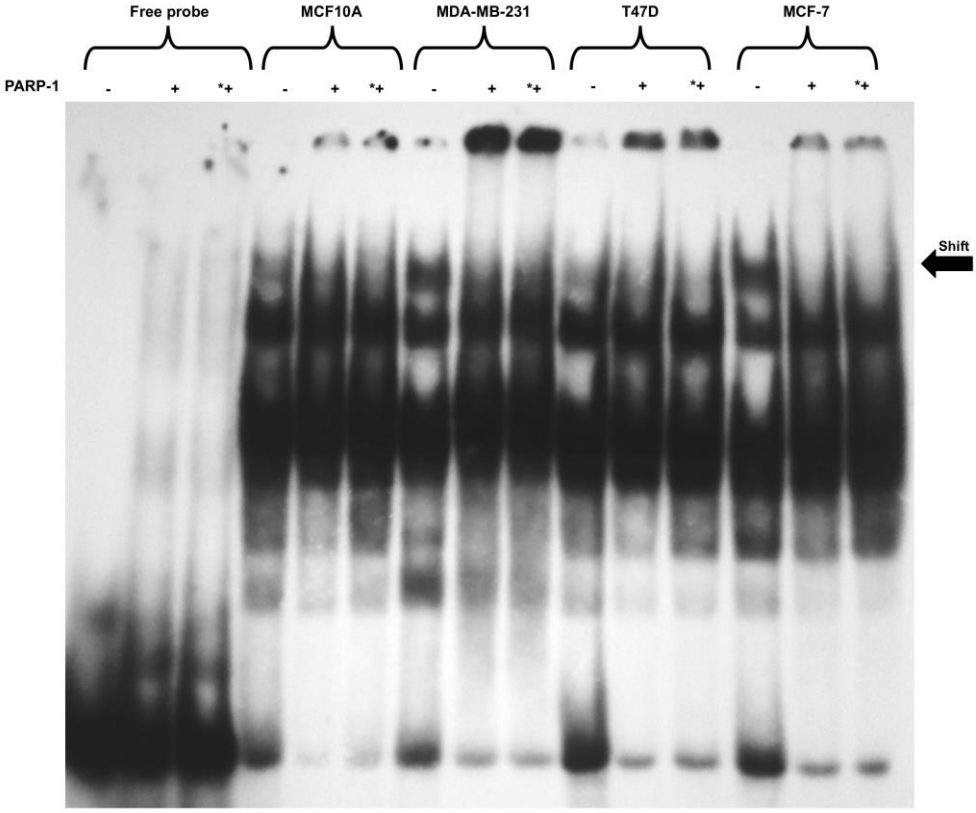

Figure 2 – **PARP-1 binding on MAR2.** Supershift assay of MAR 2 with the MARBP (MAR Binding Protein) PARP-1. Whole cell protein extracts were incubated with: +Radiolabeled DNA probe for 30 minutes, and addition of 1ug of anti-PARP-1, followed by 30 minutes of incubation; *+Anti-PARP-1 for 30 minutes and addition of DNA probe, followed by 30 minutes of incubation. MDA-MB-231 and MCF-7 cells showed a completely fade of upper band, indicated by a bold arrow, in the right. The experiment was performed in triplicate.

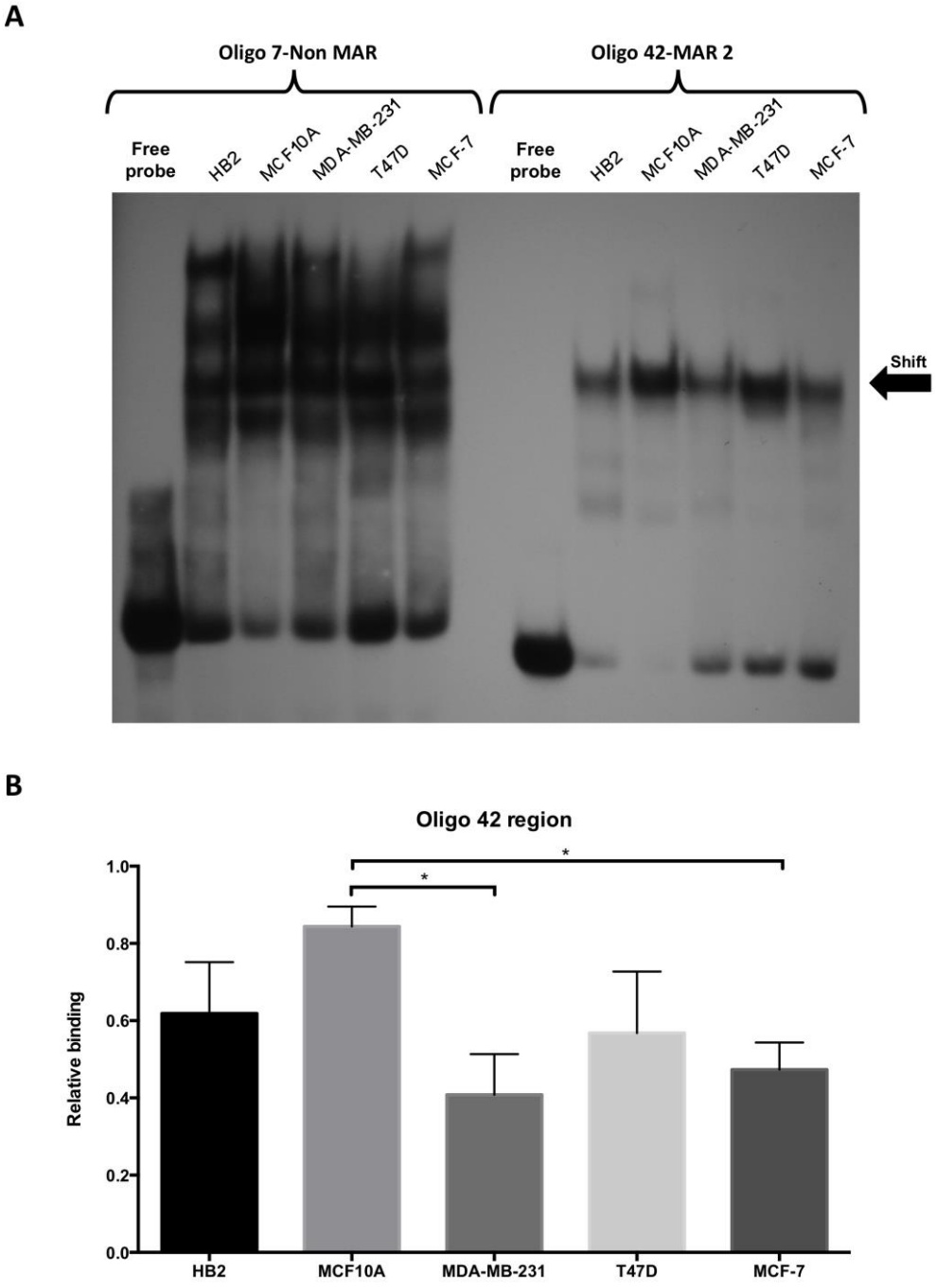

Figure 3 – MAR2 and Non-MAR protein binding. (A) The gel corresponds to EMSA (Electrophoretic Mobility Shift Assay) and the right black arrow highlights the band shift. The whole-cells lysates of HB2, MCF10A, MDA-MB-231, T47D and MCF-7, were incubated with oligos 7 (non-MAR) and 42 (MAR 2). Oligos number were accordingly our previous work (Goes et al. 2011). (B) The graphic below shows the percentage of relative binding by densitometry analysis (band shift - free probe), assessed by ImageJ 1.47 version software, for MAR2 (oligo 42 region). Error bars correspond to +/-S.E.M. from 3 different experiments. *p<0.05.

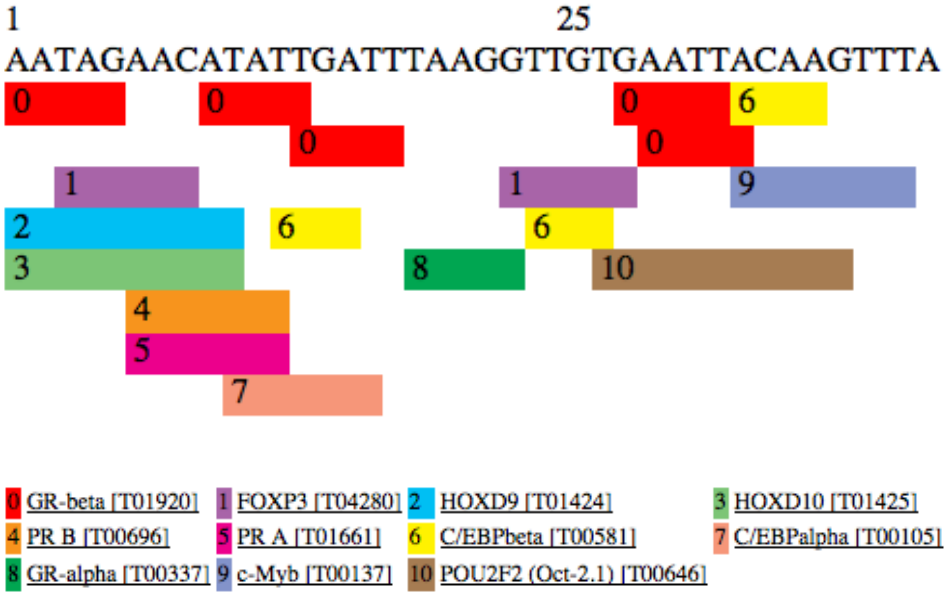

Figure 4 – Schematic representation of putative cis-acting factors in MAR2 sequence. Analysis of transcription factors binding sites was performed assessing: http://alggen.lsi.upc.es/cgibin/promo_v3/promo/promoinit.cgi?dirDB=TF_8.3. (Messeguer et al. 2002; Farré et al. 2003).

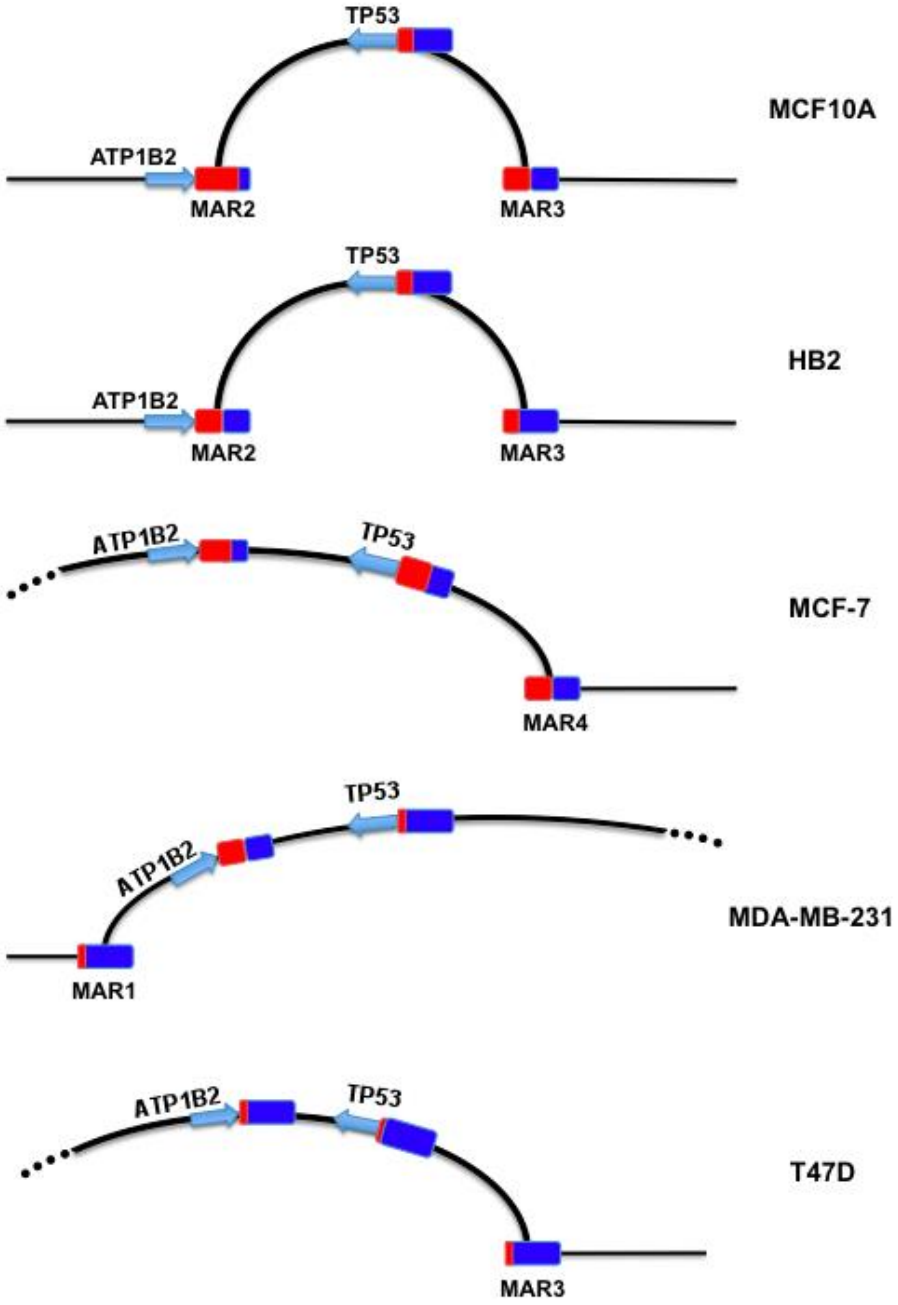

Figure 5 – **Loop domain organization model of *TP53* gene through detected MARs and chromatin markers**. Bars correspond to H4Ac enrichment (blue) and H3K9me3 enrichment (red), at MAR1, MAR2, MAR3, MAR4 and TP53P1. As our previous model (Goes et al. 2011), loops are restricted by MARs and we used four points when the limits of loops were unknown. Blue arrows represent *ATP1B2* and *TP53* genes with transcription direction.

5.3 **Artigo III:** ***Epigenetic modifications, chromatin distribution and TP53 transcription in a model of breast cancer progression***

Neste artigo, foram descritas alterações epigenéticas chaves para a progressão tumoral mamária, através de 4 linhagens que constituem a série 21T (H16N2, 21PT, 21NT e 21MT1). Estas linhagens são originárias da mesma paciente, paciente 21, e mimetizam diferentes estágios de desenvolvimento tumoral mamário, desde o tecido normal até o metastático invasivo.

Dentre as alterações epigenéticas foram verificadas a metilação global genômica, a expressão global dos marcadores epigenéticos nas histonas H4Ac, H3K9me3 e H3K27me3, a distribuição nuclear dos marcadores H4Ac e H3K9me3, a expressão de RNAm de importantes genes relacionados às modificações epigenéticas analisadas, e o enriquecimento dos marcadores epigenéticos H4Ac e H3K9me3, na região promotora do importante gene supressor de tumor *TP53*, ao longo da progressão do câncer mamário.

Os resultados obtidos mostraram de forma mais aparente nas células de mama metastáticas, uma hipometilação global genômica, hipoacetilação global e acumulação de heterocromatina pericêntrica. Também foi possível sugerir que estas alterações epigenéticas estariam ocorrendo em sinergia somente nos últimos estágios de progressão metastática.

Epigenetic modifications, chromatin distribution and *TP53* transcription in a model of breast cancer progression

Gilson C. Santos JR[1,3], Ana P. A. da Silva[1], Lucas Feldman[1], Grasiella M. Ventura[2], Yegor Vassetzky[3,4], Claudia V. de Moura Gallo[1*]

[1]Departamento de Genética, Universidade do Estado do Rio de Janeiro, Instituto de Biologia Roberto Alcantara Gomes, Rio de Janeiro, 20550-013, Brazil.

[2]Instituto de Ciências Biologicas, Universidade Federal do Rio de Janeiro (UFRJ).

[3]Université Paris-Sud 11 CNRS UMR 8126 «Signalisation, noyaux et innovations en cancérologie», Institut de Cancérologie Gustave-Roussy, Université Paris-Sud 11, F-94805 Villejuif cedex, France.

[4]N.K. Koltzov Institute of Developmental Biology, Russian Academy of Sciences, 117334 Moscow, Russia .

*Corresponding author: cgallo8@yahoo.com
Laboratório de Biologia Molecular de Tumores (LBMT)
Universidade do Estado do Rio de Janeiro (UERJ)
Pavilhão Haroldo Lisboa da Cunha, sala 525/6
Rua São Francisco Xavier, 524, Rio de Janeiro, RJ, Brasil
CEP: 205550-013
Tel: +55+21+23340858

To be submitted to: **Molecular Cancer**

Abstract

Background: Breast cancer is the most common aggressive cancer type in women. Inherited and acquired mutations as well as epigenetic alterations act together in breast carcinogenesis and tumor progression. The 21T series, a series of 4 breast cell lines originating from the same patient and representative of the breast tumor progression stages is a suitable model to investigate epigenetic alterations and their influences upon gene expression during breast tumor progression. We aimed to characterize epigenetic aspects of the 21T series and further analyze the transcription expression of the tumor suppressor *TP53*.

Results: We detected a global genomic hypomethylation profile in the cancerous 21NT and 21MT1, ductal carcinoma in-situ and invasive metastatic carcinoma, respectively. The analysis of histone modification markers showed an important global decrease of the active chromatin mark H4Ac in the metastatic 21MT1 relative to the other cell lines while the repressive marks H3K9Me3 and H3K27Me3 global expression was not significantly altered through tumor progression. The mRNA expression of key enzymes for DNA methylation and histone modification is consistent with the observed genomic hypomethylation and histone hypoacetylation. An increase of DNMT3A/B expression at the initial stages of oncogenesis and decrease of DNMT1 and HAT1 expression at the final stages were detected. Using a confocal immunofluorescent assay we observed that H4Ac is mostly located at the periphery and the repressive mark H3K9Me3 at the center of 21NT and 21MT1 cells nuclei. *TP53* P1 promoter in 21T series was found to be in an open state, with a relatively high enrichment of H4Ac. The *TP53* transcription level was found to be similar in all the 21T cell lines.

Conclusions: We have detected epigenetic alterations (global genome hypomethylation, global hypoacetylation and accumulation of pericentric heterochromatin) in metastatic breast cancer. They may act in a synergic fashion at late stages of breast cancer progression.

Background

Breast cancer is the most frequent cancer among women and ranks among the top five cancer killers, according to the World Health Organization (http://www.who.int/mediacentre/factsheeets/fs297/en; 2013). Inherited and acquired mutations in genetic material as well as epigenetic changes contribute to breast cancer progression and development [1, 2]. DNA methylation is one of the most studied types of epigenetic modification, and is generally implicated in gene silencing [3]. DNA methyltransferases (DNMTs) constitute a family of enzymes involved in those activities and its members, DNMT1, 2, 3A and 3B, seems to cooperate to maintain the methylation status of the genomic DNA or introduce *de novo* methyl groups [4]. Modification of histones, leading to chromatin changes, is also a relevant aspect of the epigenetic control of gene expression, e.g. activation or repression of genes involved in DNA repair, cell cycle and cancer progression [2, 5, 6]. Histone acetyl-transferases (HATs) catalyze reversible acetylation of histones which are linked to open chromatin and gene activation. HAT1 (KAT1) is the founding member of a superfamily of HATs and is responsible for acetylation of histone H4, H4Ac, [7, 8] a signal or marker of transcriptional active chromatin or euchromatin. Inversely, histone deacetylases (HDACs) control histone deacetylation levels and make histones more permissive to others modifications, being an important mean of chromatin remodeling [9]. Histone methyl-transferases (HMTs) catalyze reversible methylation of histones and can be linked to open or closed chromatin regions [10]. One of the HMTs, SUV39H1, is responsible for tri-methylation of histone H3 lysine 9 (H3K9me3), a strong marker of constitutive, transcriptional inactive, heterochromatin [11]. A decrease of global DNA methylation and hypermethylation of some crucial control gene promoters have been described as important features of cancer cells [5, 12, 13]. Chromatin remodeling has been also observed during carcinogenesis [14]. Understanding how these mechanisms act is very important and cell models of cancer progression help this task. In breast cancer, several cell models are

from the same patient: H16N2, representative of adjacent non-tumoral breast cells; 21PT, representative of Atypical Ductal Hyperplasia (ADH) cells; 21NT of Ductal Carcinoma *In Situ* (DCIS) and 21MT1 of Invasive Metastatic Carcinoma (IMC) [20]. This is an exceptional model to study breast cancer progression, including epigenetic alterations; however, the epigenetic changes occurring in this model of tumor progression remain unknown. In the present paper we have characterized epigenetic changes in the 21T series in relation with transcription of the master tumor suppressor gene *TP53*.

Results

Global genome hypomethylation in malignant breast cancer cells

It is generally accepted that one of the features of malignant cells is a genomic hypomethylation status [12]. Therefore, to characterize the DNA methylation profile of each cell line of the 21T series, we determined the relative global genomic methylation. Total genomic DNA was separated in two parts. One part was digested with a methylation sensitive *HpaII* restriction endonuclease, another with a methylation insensitive *MspI*. The digested DNA was run on agarose gels, and the intensities of *HpaII*- and *MspI*-digested DNA, relative to intact genomic DNAs was compared using Image J® software. The percentage of relative global genomic methylation was calculated using the following formula: (HpaII - MspI) x 100/genomic DNA. The non-cancerous H16N2 and the hyperplasic 21PT had ~30% of relative global genome methylation, while cancerous 21NT and the metastatic 21MT1 had a significantly lower global methylation level, ~15% (Figure 1).

Global decrease of active chromatin marker H4Ac in metastatic cells

To study chromatin remodeling during the progression to breast cancer, we determined global expression of markers of chromatin organization, H4Ac, a marker of active chromatin and H3K9Me3 and H3K27Me3, markers of repressive chromatin using Western-blot analysis. Whole-cells proteins were extracted from 21T cell lines, separated in 15% SDS-PAGE, and incubated with anti-H4Ac, anti-H3K72me3, anti-H3K9me3 antibodies as well as with anti-totalH3 (loading control). Relative abundance of these markers was calculated relative to anti-totalH3. Figure 2, shows a progressive decrease in total H4Ac observed between the non-cancerous H16N2 and the cancer cell lines. The metastatic 21MT1 had the lowest level of H4Ac. The global levels of H3K9Me3 and H3K27Me3 increased from the non-cancerous to cancer

Expression of key genes linked to epigenetic modifications in the 21T series cell lines

We have next used RT-qPCR to analyze mRNA levels of enzymes linked to the epigenetic modifications observed during breast cancer progression, DNMT1, DNMT3A/B, SUV39H1 and HAT1 in the 21T cell series (Table 1). From non-cancerous H16N2 to hyperplasic 21PT stage, the mRNA levels of the analyzed enzymes were up-regulated, with the exception of DNMT1 which was strongly down-regulated ($p=0.0416$). In contrast to the initial step of breast cancer progression, from non-cancerous 21PT to cancerous 21NT cells, DNMT1 was up-regulated ($p=0.0103$), but DNMT3B was down-regulated ($p=0.0011$). Finally, from cancerous 21NT to metastatic 21MT1, DNMT1, DNMT3A and HAT1 were down-regulated ($p=0.0103$, $p=0.0060$ and $p=0.0087$, respectively). Thus, high levels of genomic methylation at initial stages of oncogenesis may be due to an increase of DNMT3A/B mRNA expression while a decrease in global DNA methylation and global histone H4 acetylation during cancer progression may be linked to a decrease in DNMT1 and HAT1 mRNA levels at the final stages of metastatic progression.

Accumulation of pericentric heterochromatin at advanced stages of breast cancer progression

Having determined the expression of the global histone modification marks H4Ac and H3K9Me3 in the 21T series cell lines, we have next investigated the nuclear distribution of these markers during breast cancer progression confocal immunofluorescence. Briefly, fixed cells on round coverslips, were blocked in 3% PBS/BSA, incubated with primary antibodies anti-H4Ac and anti-H3K9me3 and incubated with secondary antibodies conjugated with Alexa Fluor 488 and 555 for H3K9Me3 and H4Ac, respectively. Nuclei were stained with DAPI. From 110 to 400 nuclei in 30 fields were analyzed by confocal microscopy. Nuclear markers distributions of histone marks were

located at the nuclear periphery in all cell lines, although it was less present in aggressive cells; this distribution was more pronounced in the metastatic 21MT1 (Figure 2A). H3K9me3 showed to be differently distributed among the cell lines, being progressively more central in the 21NT and MT1 cancerous cell lines. Hence, we have observed a redistribution of H3K9me3 in nuclei during cancer progression.

Homogeneous *TP53* transcription and open chromatin state of P1 promoter during breast cancer progression

To check the possible influence of the observed chromatin alterations during breast cancer progression in gene regulation, we decided to analyze the chromatin state of the *TP53* P1 promoter and transcription of the master regulator gene *TP53* in 21T series. We have used ChIP followed by qPCR to analyze chromatin markers H4Ac (fold enrichment relative to β-actin gene region) and H3K9Me3 (fold enrichment relative to alpha-satellite region) at the *TP53* promoter 1. The promoter was enriched in H4Ac indicating an open local chromatin organization, permissive to *TP53* transcription in all 21T cell lines (Figure 4A). We have next used RT-qPCR to quantify *TP53* mRNA levels in these cells. The *TP53* transcriptional levels were not statistically different among the cell lines of the 21T series, in agreement with the H4Ac ChIP data (Figure 4B).

Discussion

Breast cancer is a heterogeneous disease and one of the most common aggressive cancer types in women. Despite intensive research efforts, the causes of breast cancer development and aggressiveness are far from being revealed. Recently, alterations in the cell genome and epigenome were found to contribute to cancer progression [14, 21, 22].

Breast cancer cell lines have been established to help understand different and numerous stages of breast cancer development *in vitro*, with a relatively good correlation with the disease *in vivo* [23–25]. The 21T series, comprising the H16N2; 21PT; 21NT; 21MT1 cell lines was isolated from the same patient with an infiltrating carcinoma (IDC). With the exception of H16N2, the cells are HER-2 positive and *TP53* mutated (c.96_97ins1) [18, 26]. This cell series represents the progression of a human breast cancer in three stages: 1- from adjacent Non-cancerous (N) to Atypical Ductal Hyperplasia (ADH); 2- from ADH to Ductal Carcinoma *in situ* (DCIS); 3- from DCIS to Invasive Metastatic Carcinoma (IMC).

In the present paper we aimed to characterize the epigenetic aspects of the 21T series and also study whether the observed molecular alterations could influence transcription of the key tumor suppressor *TP53*. We then performed analysis of global genomic DNA methylation; mRNA expression of key enzymes of DNA methylation (DNMT1, DNMT3A/3B) and histone modification (SUV39H1 and HAT1); active (H4Ac) and repressive (H3K9Me3) chromatin markers expression and their nuclear distribution. We will discuss below our results in the light of the different stages of breast cancer progression.

From the non-cancerous H16N2 to ADH 21PT, the global genomic methylation did not statistically change, remaining at high levels. DNA methylation enzymes DNMT1 and DNMT3A/B were transcriptionally down and up-regulated, respectively. These results suggest that higher levels of global genomic methylation at the initial stage of breast cancer progression are maintained by DNMT3A/B rather than DNMT1, as mRNA expression

From ADH 21PT to DCIS 21NT cells, a highly significant decrease of global methylation was detected. However, DNMT1 and DNMT3B were oppositely regulated with an increase and a decrease in their mRNA levels, respectively. As observed at the previous stage, we could not detect significant alterations in global expression of histone epigenetic modification marks, but the nuclear distribution of the repressive marker H3K9me3 was more concentrated in the center of the cell nuclei in DCIS. This is the first report of heterochromatic changes through loss of peripheral and gain of pericentric heterochromatin, from hyperplasic to cancerous non-metastatic breast cells, despite earlier reports of pericentric heterochromatin accumulation from non-cancerous to metastatic breast cells [27].

From DCIS 21NT to IMC 21MT1 cells, the global genomic methylation was not altered and we detected an important decrease of *DNMT1*, *DNMT3A* and *HAT1* genes transcription as well as a global decrease of H4Ac expression with a high concentration of repressive/heterochromatin marker H3K9me3 in pericentric regions, in agreement with the published data [27]. Global genomic hypomethylation and higher levels of H3K9me3 were also linked to malignant melanocyte metastatic transformation [28]. However, in the case of melanocytes, lower DNMT1 transcription levels were found exclusively in non-cancerous melanocytes and higher DNMT3A transcription levels only in metastatic melanoma [28]. The inverse correlation of transcription levels between DNMT1 and DNMT3A/B that we have observed in normal versus cancerous non-metastatic breast cell lines, could suggest a compensatory role of these enzymes in breast cancer progression. The global hypoacetylation of histone H4, possibly due to low transcription levels of HAT1 that we have observed in the 21MT1 metastatic breast cell line, could silence or reduce the expression levels of tumor suppressor genes [9] and lead to deficient homologous recombination repair [29].

Having studied the global changes in chromatin organization, we analyzed the expression level of the key transcriptional regulator gene *TP53* as well as chromatin organization by ChIP on *TP53* gene P1 promoter region.

in the promoter region P1 as well as the homogeneous expression of *TP53* gene through breast cancer progression, reinforces that the protein p53 may be preferentially regulated by post-translational modifications [30]. Of note, cancerous cells of 21T series present p53 protein loss due to a frame-shift mutation [19].

Our results reinforce the link of key epigenetic alterations, as global genomic hypomethylation, global hypoacetylation and accumulation of pericentric heterochromatin in metastatic breast cancer, as described elsewhere [9, 14, 27, 31]. In addition, based in our results, we suggest that these key epigenetic phenotypes manifest in a synergic fashion at later stages of metastatic breast cancer progression. The key epigenetic modifications we have observed during breast cancer progression could be essential to change the 'epigenetic state' of differentiated cells into a less differentiated state characteristic of metastatic cells [32].

Methods

Cell culture

The 21T cell series (21PT, 21NT and 21MT1) were kindly provided by Dr. Pierre Hainaut (International Agency for Research on Cancer), Lyon, France) and the H16N2 by Dr. Vimla Band (Department of Genetics, Cell Biology and Anatomy; University of Nebraska Medical Center). Cells were cultured in α-MEM medium (#12-169F, Lonza®) supplemented with l-glutamine 4mM (Gibco®), 10% fetal bovine serum (Gibco®), 10ug/ml insulin (Sigma®), 0,5ug/ml hydrocortisone (Sigma®), 20ng/ml EGF (Sigma®), 1X anti-anti (antibiotic-antimycotic, Gibco®) and 10ug/ml ciprofloxacin at 37°C in a humidified atmosphere at 5% CO_2. Cells counting and viability were carried out on Moxi Z Mini (Orflo®). All the 21T cell lines were genotyped to confirm their allelic profile. Cultures were routinely checked for mycoplasma contamination.

Determination of the global methylation levels by digestion of genomic DNA with restriction enzymes *MspI* and *HpaII*

Genomic DNA from 21T series cells was extracted and purified using Invisorb Spin Tissue Kit (Invitek®) and quantified using NanoDrop 2000 (Thermo Scientific®). 3 μg of DNA was digested with 30 units of either a methylation sensitive *HpaI* restriction endonuclease, or with a methylation insensitive *MspII* (New England Biolabs®) for 16 hours at 37°C, followed by addition of 30 units more for 1 hour and heat inactivation for 20 minutes at 65°C. The samples were run on in 1% agarose gel electrophoresis and stained with ethidium bromide. The percentage of relative global genomic methylation was measured by comparing band intensities of digested and intact genomic DNA using ImageJ software and then calculated using the following formula: (HpaII - MspI) x 100/genomic DNA, as described elsewhere [28].

Western Blot

Cells were washed twice with ice-cold 1X PBS and lysed with a buffer containing 150mM NaCl, 1mM EDTA, 50mM Tris-HCl (pH 7.5), 0.5% NP-40

and a protease inhibitor cocktail (Roche). Samples were incubated on ice for 30 minutes. Protein extracts (10ug) were heat denatured and separated by SDS-PAGE. Proteins were transferred to a nitrocellulose membrane (BioRad®), blocked for 1 hour with 5% non-fat dry milk in TBST (136mM NaCl, 2.6mM KCl, 24mM Tris-HCl pH 7.4 and 0,1% Tween 20) and incubated for 1 hour with the following primary human antibodies diluted 1:4000 in TBST: H4 pan-acetyl (#39243, Active Motif®), tri-methyl H3K4 (#07-473, Millipore®), tri-methyl H3K9 (#05-1242, Millipore®), tri-methyl H3K27 (#17-622, Millipore®) and total H3 (#4620, Cell Signalling®). The signals were visualized by chemoluminescence using the Immobilion Western kit (#WBKLS0500, Millipore®) after incubation with the secondary horseradish-peroxidase conjugated antibodies (KPL®).

mRNA expression analysis

Total RNA was isolated using Trizol (Life Technologies®). cDNA synthesis and real-time PCR analysis with gene-specific primers were carried out using the GoTaq 2-Step RT-qPCR System (Promega®) according to the manufacturer's instruction. RT-qPCR was carried out on the 7500 Real-time PCR system (Applied Biosystems®). The housekeeping *β-actin* gene was used as the internal control and the PCR products was measured by SYBR Green. The primers (Eurofins MWG Operon®) used were as follows (F-Forward; R-Reverse):

DNMT1- F: CCTTGGAGAACGGTGCTCAT / R: CTTAGCCTCTCCATCGGACT;
DNMT3A- F: AGAAGTGTACACGGACATGTGG/ R: AGGAGATGCAGATGTCCTCAAT;
DNMT3B- F:CATCAAAGTTTCTGCTGCTCAC / R: CAAAGATCCTTTCGAGCTCAGT;
SUV39H1- F: ATGGAGTACGTGGGAGAGATCA / R: TCTTGTGGCAAAGAAAGCGATG;
HAT1- F: CGTGGATGATGAAAGATGGCAC / R: TTTTGGATGGATCTTCCGCTGT.

Immunofluorescence, confocal microscopy and image analysis

Cells were grown on round coverslips inside a 24-well test plate, then they were fixed in a 4% paraformaldehyde solution for 10 minutes, rinsed with PBS 1X and permeabilized with 0,5% Triton X-100 for 10 minutes. After, they were washed 3 times with PBS 1X, followed by 30 minutes of incubation with 5mM Ammonium Chloride. They were rinsed then with 1% PBS/BSA solution

and incubated in 3% PBS/BSA solution for 30 minutes. After the fixation process, the cells were incubated with the primary antibodies diluted 1:200 in 1% PBS/BSA (anti-H3K9me3 and anti-H4Ac, the same used for Western Blot) for 16 hours, rinsed with 1% PBS/BSA, blocked for 30 minutes in 3% PBS/BSA and then were incubated with the secondary antibodies (Alexa Fluor 488 #A21202 for H3K9Me3 and Alexa Fluor 555 #A31572 for H4Ac) for 2 hours in the dark. After that, cells were washed with 1% PBS/BSA and 1X PBS; and incubated with DAPI (1:3000 in 1%PBS/BSA) for 5 minutes in the dark. After washing with PBS 1X, the coverslips were inverted onto glass slides with mounting medium (SlowFade - Antifade kit, Invitrogen®) and were analyzed under Leica® TCS SP5 AOBS confocal laser microscope equipped with a 63X oil immersion objective. Data acquisition was made in triplicate in three different experiments, with 30 fields for each slide by counting 110-400 nuclei per each cell line. Nuclear markers distributions were detected through plotting the means of each pixel in a diametral ROI designed for each nuclei, with Leica Application Suite Advanced Fluorescence Lite 2.4.1® software. Each graphic point corresponds to fluorescence intensity of a single pixel. All fields were analyzed with Leica Application Suite Advanced Fluorescence Lite 2.4.1® software.

ChIP assay

$25x10^6$ cells were cross-linked with 1% formaldehyde for 10 minutes in a rocking platform at room temperature. Cross-linking reaction was stopped with Glycine 0.125M diluted in 1X PBS. The cells were washed with ice-cold 1X PBS and resuspended in 1mL Lysis/Sonication cold buffer (1%SDS, 10mM EDTA and 50mM Tris-HCl pH 7.5) with fresh 0.5mM PMSF and 1X PIC (Protease Inhibitor Cocktail) and incubated for 30 minutes on ice. The lysates were homogenized with 10 strokes, centrifuged at 750xg for 5 minutes at 4˚C and the supernatant was discarded. The pellet was resuspended in 350 µL of Lysis/Sonication cold buffer with freshly added 1mM PMSF and 1X PIC, sonicated on ice and centrifuged for 10 minutes with 2000xg at 4˚C. The supernatant contains the extracted chromatin. Immunoprecipitation was carried out overnight at 4˚C with constant agitation in an immunoprecipitation buffer (5mM Tris-HCl pH 8.0, 15mM NaCl, 1mM EDTA and 0.1% NP40) with

20 µg of chromatin, 750 µg of Protein G dynabeads #100.03D (Invitrogen®), 4 µg of antibodies H4 pan-acetyl (#39243, Active Motif®), tri-methyl H3K9 (#05-1242, Millipore®), normal rabbit IgG (#PP64B, Millipore®; control) and 1X PIC. All the immunoprecipitations were made with at 1:4 dilutions. The magnetic beads were washed 6 times with the immunoprecipitation buffer and the chromatin was eluted with the Lysis/sonication buffer for 15 minutes at room temperature with constant agitation. The magnetic beads were separated from eluted chromatin and the proteinase K digestion and reverse cross-link were done as described above. DNA was cleaned-up by the standard Phenol-Chloroform method and submitted to qPCR.

qPCR, was carried out using the standard Syber-Green method with the Mastermix (Roche®). All fold enrichment values of H4Ac and H3K9me3 are relative to the fold enrichment values of the β-actin gene region or the alpha-satellite region, respectively. All primers, synthesized by SIGMA®, are listed in 5' – 3' and F-forward/R-reverse:

TP53P1 F- GCGTGTCACCGTCGTGGAAAG/ R-GGAGCCTCGCAGGGGTTGATG;

B-actin gene region F- GACGTAGCACAGCTTCTCCT/ R-GGGACCTGACTGACTACCTCAT;

Alpha-Satellite (#CS207313, Millipore®) F-CTGCACTACCTGAAGAGGAC/R-GATGGTTCAACACTCTTACA.

All Chromatin extraction, immunoprecipitation and qPCR were done in triplicate and the error bars correspond the S.E.M. of three different experiments.

Statistical analysis

All statistics were made by Graphpad® software 6.0, with 95% of CI, using non-parametric t-test. All error bars represent S.E.M. (standard error of the mean).

Additional files

Additional file 1: Table S1

Competing interests

The authors declare that there are no conflicts of interest.

Acknowledgements

We thank Dr. Pierre Hainaut and Dr. Vilma Band for the gift of cell lines. The research in YV lab was funded by grants from Fondation de France, Institute National de Cancer (INCa) and CAPES-COFECUB.

Authors' contributions

Santos GC-Jr carried out all the experiments, result analysis and drafted the manuscript. APAS carried out cell cultures, immunofluorescence, confocal microscopy and image analysis. GMV participated in the immunofluorescence, confocal microscopy and image analysis. LF participated in the DNA global methylation assays and mRNA expression assays. YV participated in the study design, support concerning technical questions and critical revision of manuscript. CVMG conceived the study, participated in its design and coordination, and wrote the manuscript. All authors read and approved the final manuscript.

References

1. Stefansson O a, Esteller M: **Epigenetic Modifications in Breast Cancer and Their Role in Personalized Medicine.** *Am. J. Pathol.* 2013, **183**:1–12.
2. Albert M, Helin K: **Histone methyltransferases in cancer.** *Semin. Cell Dev. Biol.* 2010, **21**:209–20.
3. Jones P a: **Functions of DNA methylation: islands, start sites, gene bodies and beyond.** *Nat. Rev. Genet.* 2012, **13**:484–92.
4. Denis H, Ndlovu MN, Fuks F: **Regulation of mammalian DNA methyltransferases: a route to new mechanisms.** *EMBO Rep.* 2011, **12**:647–56.
5. Akhavan-Niaki H, Samadani AA: **DNA Methylation and Cancer Development: Molecular Mechanism.** *Cell Biochem. Biophys.* 2013.
6. Badeaux AI, Shi Y: **Emerging roles for chromatin as a signal integration and storage platform.** *Nat. Rev. Mol. Cell Biol.* 2013, **14**:211–24.
7. Yuan H, Marmorstein R: **Histone acetyltransferases: Rising ancient counterparts to protein kinases.** *Biopolymers* 2013, **99**:98–111.
8. Luo X, Guo S, Guo Y, Zhang C: **Histone Modification and Breast Cancer**. In *Breast Cancer - Focus. Tumor Microenviron. Stem cells Metastasis*. 2008, **15**:321–342.
9. Di Cerbo V, Schneider R: **Cancers with wrong HATs: the impact of acetylation.** *Brief. Funct. Genomics* 2013, **12**:231–43.
10. Greer EL, Shi Y: **Histone methylation: a dynamic mark in health, disease and inheritance.** *Nat. Rev. Genet.* 2012, **13**:343–57.
11. Rice JC, Briggs SD, Ueberheide B, Barber CM, Shabanowitz J, Hunt DF, Shinkai Y, Allis CD: **Histone methyltransferases direct different degrees of methylation to define distinct chromatin domains.** *Mol. Cell* 2003, **12**:1591–8.

12. Hon GC, Hawkins RD, Caballero OL, Lo C, Lister R, Pelizzola M, Valsesia A, Ye Z, Kuan S, Edsall LE, Camargo AA, Stevenson BJ, Ecker JR, Bafna V, Strausberg RL, Simpson AJ, Ren B: **Global DNA hypomethylation coupled to repressive chromatin domain formation and gene silencing in breast cancer.** *Genome Res.* 2012, **22**:246–58.
13. Park SY, Kwon HJ, Lee HE, Ryu HS, Kim S-W, Kim JH, Kim IA, Jung N, Cho N-Y, Kang GH: **Promoter CpG island hypermethylation during breast cancer progression.** *Virchows Arch.* 2011, **458**:73–84.
14. Locke WJ, Clark SJ: **Epigenome remodelling in breast cancer: insights from an early in vitro model of carcinogenesis.** *Breast Cancer Res.* 2012, **14**:215.
15. Chakrabarti A, Verbridge S, Stroock AD, Fischbach C, Varner JD: **Multiscale models of breast cancer progression.** *Ann. Biomed. Eng.* 2012, **40**:2488–500.
16. Ethier SP: **Human breast cancer cell lines as models of growth regulation and disease progression.** *J. Mammary Gland Biol. Neoplasia* 1996, **1**:111–21.
17. Kern FG, McLeskey SW, Zhang L, Kurebayashi J, Liu Y, Ding IY, Kharbanda S, Chen D, Miller D, Cullen K: **Transfected MCF-7 cells as a model for breast-cancer progression.** *Breast Cancer Res. Treat.* 1994, **31**:153–65.
18. Band V, Zajchowski D, Swisshelm K, Trask D, Kulesa V, Cohen C, Connolly J, Sager R: **Tumor Progression in Four Mammary Epithelial Cell Lines Derived from the Same Patient Tumor Progression in Four Mammary Epithelial Cell Lines Derived from the Same Patient**. *Cancer Res.* 1990, **50**:7351–7357.
19. Liu XL, Band H, Gao Q, Wazer DE, Chu Q, Band V: **Tumor cell-specific loss of p53 protein in a unique in vitro model of human breast tumor progression.** *Carcinogenesis* 1994, **15**:1969–73.
20. Souter LH, Andrews JD, Zhang G, Cook AC, Postenka CO, Al-Katib W, Leong HS, Rodenhiser DI, Chambers AF, Tuck AB: **Human 21T breast epithelial cell lines mimic breast cancer progression in vivo and in vitro and show stage-specific gene expression patterns.** *Lab. Invest.* 2010, **90**:1247–58.
21. Baylin SB, Jones PA: **A decade of exploring the cancer epigenome - biological and translational implications.** *Nat. Rev. Cancer* 2011, **11**:726–34.
22. Schweiger M-R, Barmeyer C, Timmermann B: **Genomics and epigenomics: new promises of personalized medicine for cancer patients.** *Brief. Funct. Genomics* 2013.
23. Vargo-Gogola T, Rosen JM: **Modelling breast cancer: one size does not fit all.** *Nat. Rev. Cancer* 2007, **7**:659–72.
24. Perou CM, Sørlie T, Eisen MB, van de Rijn M, Jeffrey SS, Rees CA, Pollack JR, Ross DT, Johnsen H, Akslen LA, Fluge O, Pergamenschikov A, Williams C, Zhu SX, Lønning PE, Børresen-Dale AL, Brown PO, Botstein D: **Molecular portraits of human breast tumours.** *Nature* 2000, **406**:747–52.
25. Neve RM, Chin K, Fridlyand J, Yeh J, Baehner FL, Fevr T, Clark L, Bayani N, Coppe J-P, Tong F, Speed T, Spellman PT, DeVries S, Lapuk A, Wang NJ, Kuo W-L, Stilwell JL, Pinkel D, Albertson DG, Waldman FM, McCormick F, Dickson RB, Johnson MD, Lippman M, Ethier S, Gazdar A, Gray JW: **A collection of breast cancer cell lines for the study of functionally distinct cancer subtypes.** *Cancer Cell* 2006, **10**:515–27.
26. Band V, Sager R: **Neoplastic Transformation in Human Cell Culture**. In *Neoplast. Transform. Hum. Cell Cult.* 25th edition. edited by Rhim JS, Dritschilo A Totowa, NJ: Humana Press; 1991:169–178.

27. Carone DM, Lawrence JB: **Heterochromatin instability in cancer: from the Barr body to satellites and the nuclear periphery.** *Semin. Cancer Biol.* 2013, **23**:99–108.
28. Mologhoni F, Cruz AT, Meliso FM, Morais AS, Souza CF, Xander P, Bischof JM, Costa FF, Soares MB, Liang G, Jones P a., Jasiulionis MG: **Epigenetic reprogramming as a key contributor to melanocyte malignant transformation**. *Epigenetics* 2011, **6**:450–464.
29. Yang X, Li L, Liang J, Shi L, Yang J, Yi X, Zhang D, Han X, Yu N, Shang Y: **Histone acetyltransferase 1 promotes homologous recombination in DNA repair by facilitating histone turnover.** *J. Biol. Chem.* 2013, **288**:18271–82.
30. Dehart CJ, Chahal JS, Flint SJ, Perlman DH: **Extensive post-translational modification of active and inactivated forms of endogenous p53.** *Mol. Cell. Proteomics* 2013:M113.030254–.
31. Suzuki J, Chen Y-Y, Scott GK, Devries S, Chin K, Benz CC, Waldman FM, Hwang ES: **Protein acetylation and histone deacetylase expression associated with malignant breast cancer progression.** *Clin. Cancer Res.* 2009, **15**:3163–71.
32. Halley-Stott RP, Gurdon JB: **Epigenetic memory in the context of nuclear reprogramming and cancer.** *Brief. Funct. Genomics* 2013, **12**:164–73.

Tables

Table 1. Expression of key genes responsible for epigenetic modifications in 21T series cell lines.

Genes	H16N2	21PT	21NT	21MT1
DNMT1	0.045552300	0.004120244	0.0389197100	0.0033738800
DNMT3A	0.000246858	0.003024751	0.0013899000	0.0001814570
DNMT3B	0.000175841	0.008179488	0.0000875218	0.0002220440
SUV39H1	0.000002911	0.000367855	0.0008094410	0.0001528890
HAT1	0.000245947	0.029841590	0.0448822600	0.0000071696

-RT-qPCR analysis relative to β-actin gene.

Supplementary Table 1. Fold expression change of key genes responsible for epigenetic modifications in each cancer progression stage.

Through unpaired T-test with Welch's correction, we could compare the genes expression values (table 1), for each breast cancer progression stage, as shown in supplementary Table 1 (the table shows only fold change values with p-value <0.05).

H16N2 to 21PT

Genes		Fold change		*p* value
SUV39H1		126.3672278		0.0005
HAT1		121.3334133		0.0073
DNMT3B		46.51638696		0.0008
DNMT3A		12.2529997		0.0296
DNMT1		0.09045084		0.0416

21PT to 21NT

Genes		Fold change		*p* value
DNMT1		9.445971161		0.0103
DNMT3B		0.010700156		0.0011

21NT to 21MT1

Genes		Fold change		*p* value
DNMT3A		0.130553997		0.0060
DNMT1		0.086688219		0.0103
HAT1		0.000159743		0.0087

H16N2 to 21NT

Genes		Fold change		*p* value
HAT1		182.4875441		0.0088
DNMT3A		5.630362395		0.0028

H16N2 to 21MT1

Genes		Fold change		*p* value
DNMT1		0.07406607		0.0405

-RT-qPCR analysis relative to β-actin gene.

Figure 1

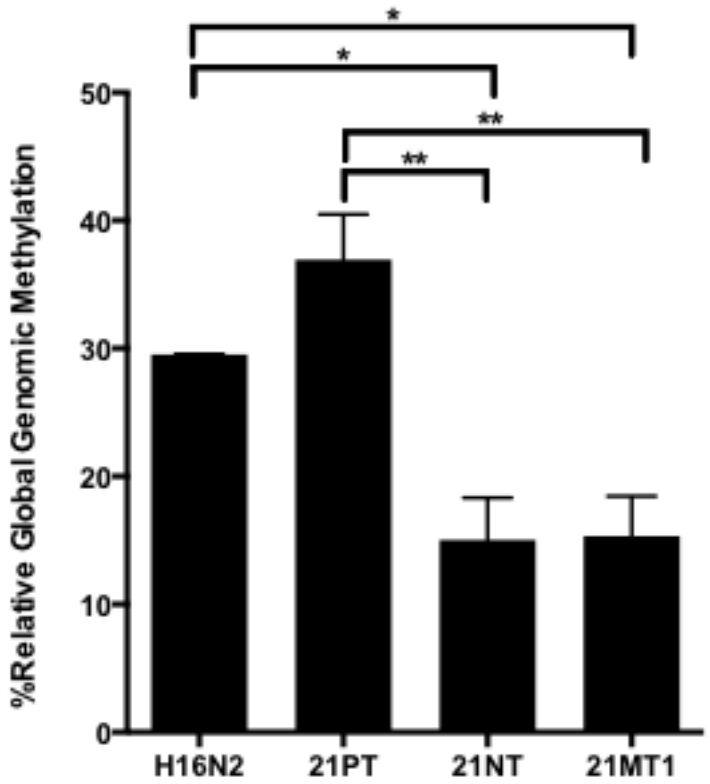

Figure 1. Relative global genomic methylation levels of the 21T cell lines. Relative global genomic methylation of the non-cancerous cells (H16N2), atypical ductal hyperplasia stage (21PT), ductal “in situ” (21NT) and metastatic carcinoma (21MT1). The global genomic methylation was estimated using *HpaII* and *MspI* restriction endonucleases as described in Materials and Methods. Error bars represent S.E.M. of four different experiments; t-test: *p<0.05;**p<0.005.

Figure 2

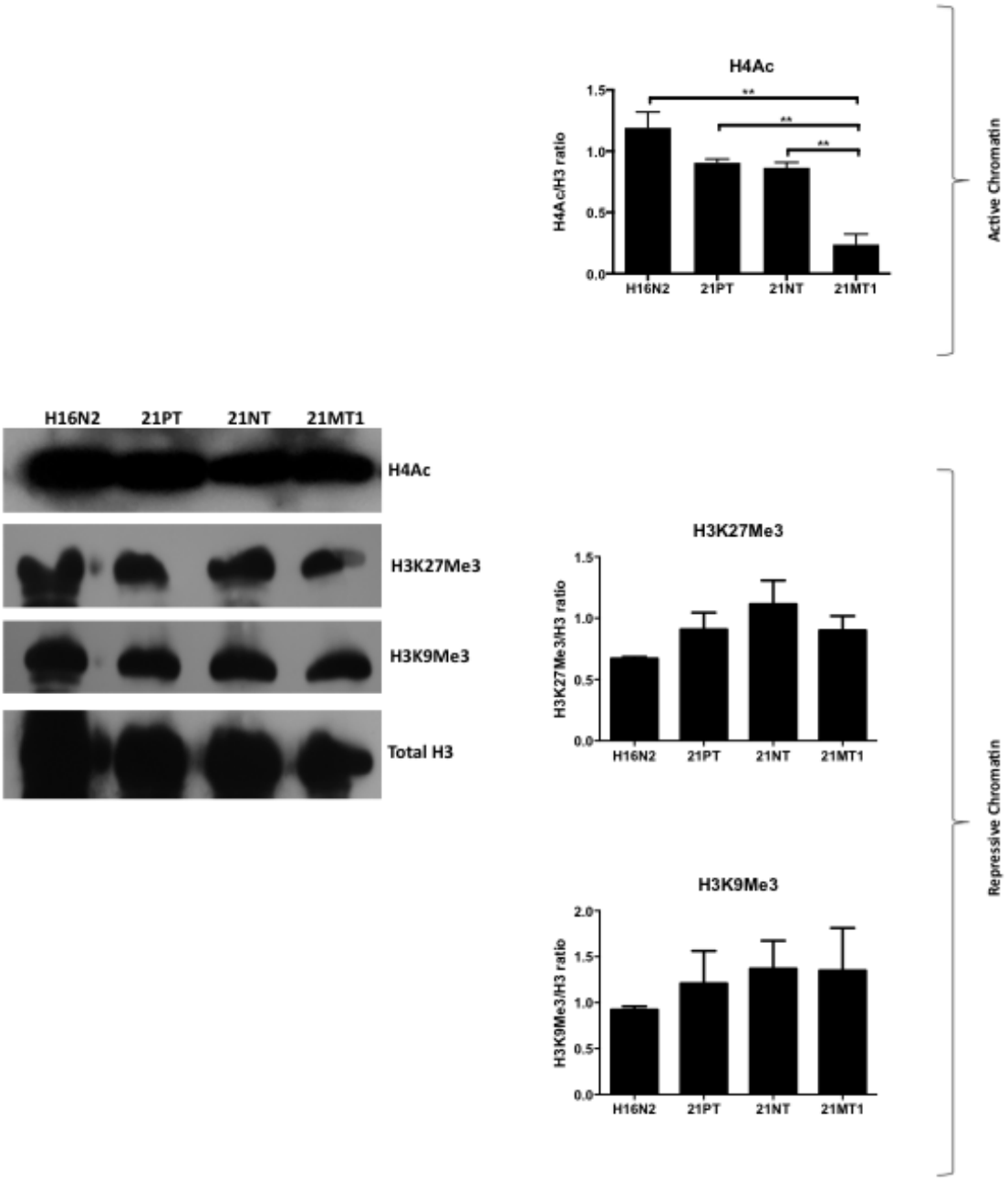

Figure 2. Histone markers H4Ac, H3K9Me3 and H3K27Me3 expression in breast tumor progression. Western Blot analysis of active histone marks H4Ac and the repressive marks H3K9Me3 and H3K27Me3 in non-cancerous (H16N2), atypical ductal hyperplasia (21PT); ductal in-situ carcinoma (21NT); metastatic carcinoma (21MT1) cell lines. Total H3 expression was used as a control. All charts represent the ratio between histone marks and the total H3 histone **P<0,005; *P<0,05; Statistical test: one-way ANOVA with Bonferroni post-test.

Figure 3

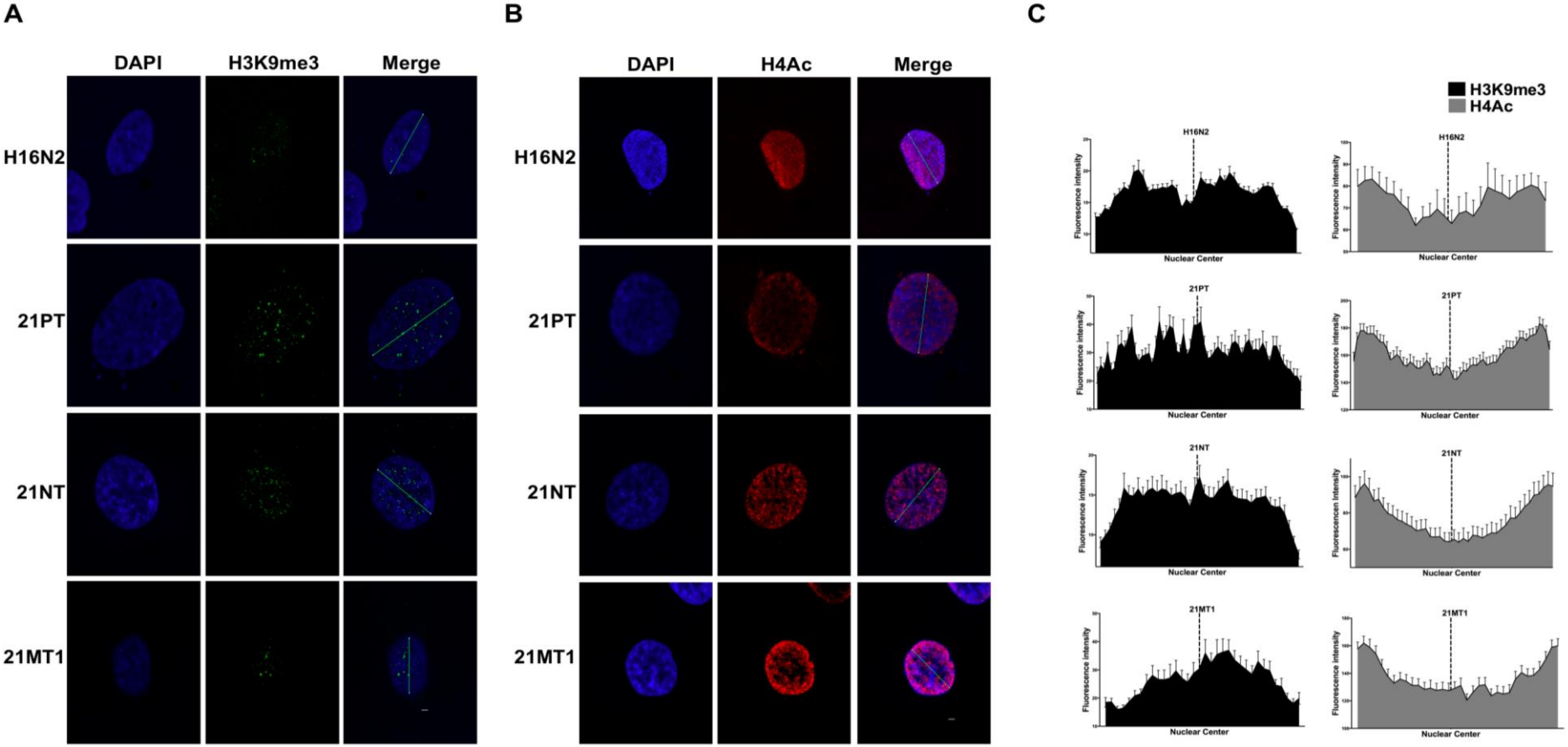

Figure 3. Nuclear distribution of chromatin markers H3K9me3 and H4Ac during breast tumor progression. Representative confocal nuclear cell images for each 21T cell line: **(A)** H3K9me3 (green); **(B)** H4Ac (red). **(C)** H3K9me3 (dark) and H4Ac (gray) fluorescence intensity distribution. Each abscissa point represents a single pixel of a diametral nuclear ROI, the bold grid line indicates the nuclear center position and the ordinate represents the fluorescence intensity in arbitrary units. For graphic markers distribution, confocal image analysis was evaluated by fluorescent intensity pixels of the markers H3K9me3 and H4Ac, in a diametral nuclear ROI, for 110-400 nuclei (30 fields) for each 21T cell line. Each error bar represents S.E.M. of fluorescent intensity pixels. Scale bar = 2 μM.

Figure 4

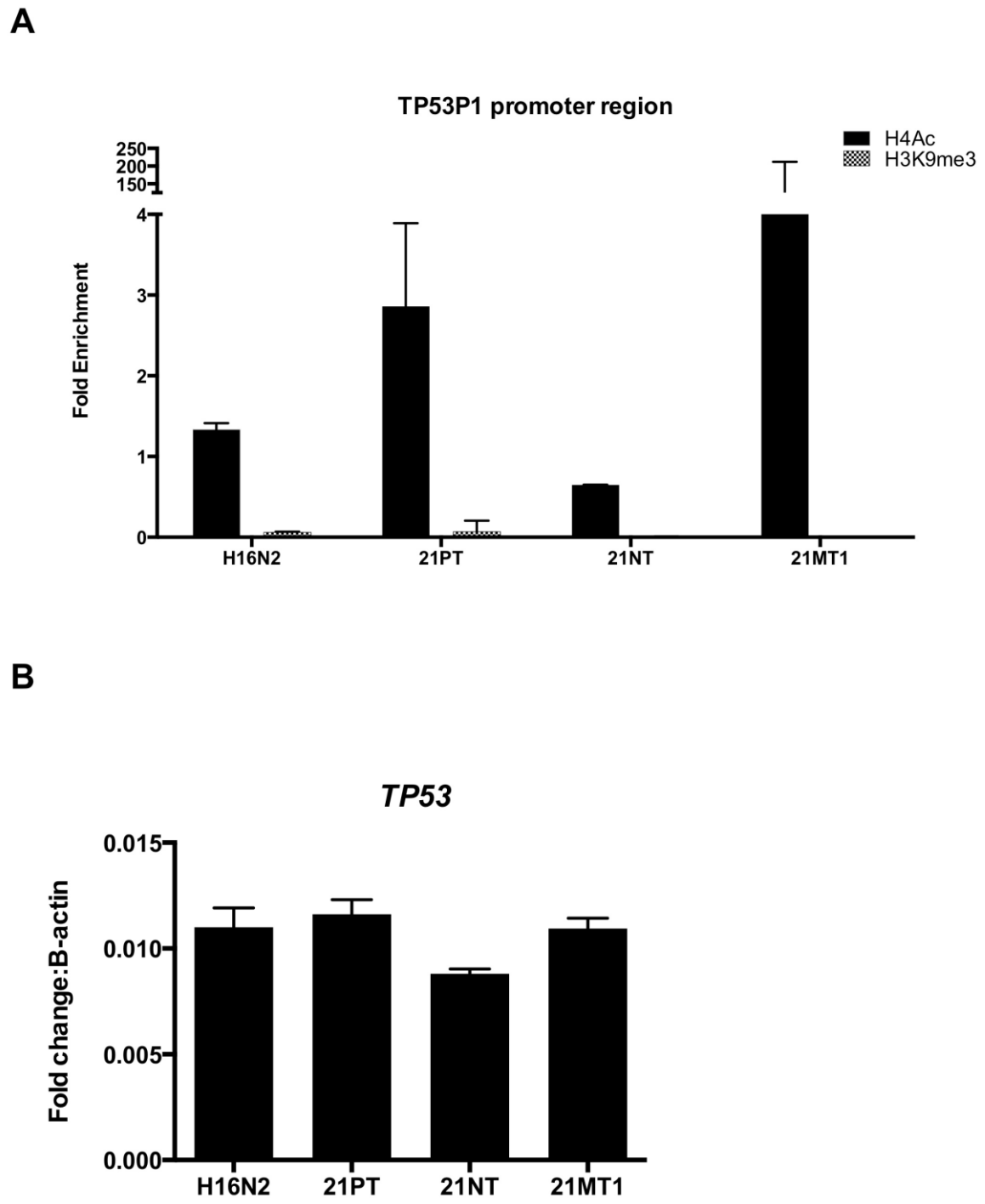

Figure 4. Chromatin state at the promoter P1 and *TP53* transcription during tumor progression. ChIP assay of *TP53* promoter P1 in (**A**) tumor progression (21T series). (**B**) Relative *TP53* transcription levels measured by RT-qPCR in 21T series. Error bars represent S.E.M. of three independent experiments.

6 **DISCUSSÃO**

Ao longo deste trabalho, que compreende 1 artigo publicado, 1 artigo em análise e outro em preparação, foram descritos os sítios no DNA fixados à matriz nuclear, chamados MARs, e, em outros níveis de compactação da cromatina, as modificações epigenéticas possivelmente associadas ao desenvolvimento do câncer de mama.

Para as análises da cromatina, foram utilizadas 3 linhagens normais (HB2, MCF10A e H16N2), 3 linhagens tumorais não-metastáticas (BT-474, HeLa, 21NT), 4 linhagens tumorais metastáticas (MDA-MB-231, T47D, MCF-7 e 21MT1) e 1 linhagem hiperplásica (21PT), somando 11 linhagens. Este grande número de linhagens possibilitou uma importante descrição dos principais mecanismos que atuam na organização da cromatina nos diferentes estágios, e características, da progressão tumoral mamária.

No artigo I, foi investigado pela primeira vez o papel dos sítios de fixação à matriz nuclear, na regulação do gene *TP53*, no câncer de mama, e os resultados obtidos mostraram uma interessante distribuição *in vivo* das MARs nas linhagens tumorais mamárias.

O *loop* relativamente menor, 50kb, verificado na linhagem normal HB2, e confirmado também na linhagem normal MCF10A (através de qPCR), foi um resultado interessante, uma vez que estudos anteriores, mostraram que o tamanho relativo do *loop* é menor nas células tumorais, comparando com células controle normais (160,161).

O fato de cada linhagem analisada, ter apresentado um perfil de MARs diferente, é compatível com a extensa variabilidade de fenótipos existentes nas linhagens tumorais mamárias (162). Apesar da grande variabilidade de MARs, a região de estudo, 17p13.1, apresentou uma baixa quantidade de MARs, que está de acordo com estudos anteriores, onde foi mostrado uma correlação inversa entre quantidade de genes e o número de MARs, nos cromossomos 14, 15, 16, 17 e 18 (60,163).

Através de RT-qPCR, verificamos que os níveis transcricionais estão correlacionados negativamente com o tamanho do *loop* de cromatina, e o gene *TP53* e os flanqueadores, estão mais expressos na linhagem controle HB2 do que

nas linhagens tumorais mamárias. Este resultado está de acordo com estudos anteriores que mostraram que a formação dos loops favorece a transcrição (47,164,165).

Vale a pena ressaltar ainda, que no artigo I foi detectada a MAR2, somente nas células normais HB2 e MCF10A (através de qPCR). Esta importante MAR2, foi estudada no artigo II, onde foi descrito uma intensa, e altamente específica, ligação de complexos protéicos nesta região, através de ensaios de gel-shift, na linhagem normal MCF10A, ao comparar com as outras linhagens tumorais. Também, no mesmo artigo II, verificamos através de ensaios de imunoprecipitação da cromatina (ChIP assays), que a MAR2 apresenta um significativo maior enriquecimento do marcador de cromatina fechada, H3K9me3, somente na linhagem normal MCF10A, em relação a linhagem HB2.

Os resultados obtidos nos artigos I e II, reforçam o papel da MAR2 como um putativo receptor de fatores transcricionais ou acentuassomos. Apesar da intensa ligação de proteínas na MAR2, esta região apresentou um significativo maior enriquecimento do marcador H3K9me3, na linhagem MCF10A, diferente da HB2, que apresentou um equilíbrio no enriquecimento dos marcadores H4Ac e H3K9me3. Acreditamos que este fenômeno observado na MCF10A, pode ser global e exclusivo desta linhagem, pois se repete em quase todas as regiões genômicas analisadas.

No artigo II, 45% das MARs detectadas nas linhagens HB2, MCF10A, MDA-MB-231, T47D e MCF-7, apresentaram um balanceamento dos marcadores de cromatina aberta (H4Ac) e fechada (H3K9me3). Em contraste, 25% e 30% das MARs, apresentaram um significativo maior enriquecimento de H3K9me3 e H4Ac, respectivamente.

A partir dos resultados obtidos no artigo II, foi possível detectar que os marcadores epigenéticos da cromatina apresentam uma distribuição diferente nas MARs 1, 2, 3 e 4, para cada linhagem celular. Também, verificamos que a MAR2, apresentou uma ligação específica de proteínas, que pode representar a atuação de fatores envolvidos na organização e funcionamento da cromatina.

Apesar da utilização dos extratos totais de proteínas de linhagens celulares no artigo II, também foi utilizado, nos ensaios de gel *shift*, extratos de proteínas nucleares e citoplasmáticos, porém sem muito sucesso. Na figura 5 (APÊNDICE A), é possível visualizar a qualidade e a grande diferença no perfil de proteínas obtido através do extrato total de proteínas de linhagens celulares. Também foram

realizados ensaios de gel shift na ausência do competidor Poli-dIdC, conforme mostra a figura 6 (APÊNDICE B), que surpreendentemente não apresentou alterações, corroborando a grande especificidade das proteínas à MAR2.

Foram realizados ensaios de ChIP com extratos celulares provenientes das 12 linhagens (caracterizadas na Tabela 1) com os marcadores H4Ac, H3K9me3 e os marcadores, H3K4me3 (relacionado à regiões promotoras ativas) e H3K27me3 (relacionado à heterocromatina facultativa), para as 4 MARs, e para as 4 regiões não-MARs (promotores P1 e P2 do gene *TP53*, e oligos 62 e 64). Entretanto, foram inseridos no artigo II, somente os resultados de ChIP com os marcadores H4Ac e H3K9me3 nas linhagens MCF10A, HB2, T47D, MDA-MB-231 e MCF-7, para as 4 MARs descritas anteriormente no artigo I (142), e no artigo III, foram inseridos somente os resultados de ChIP com os mesmos marcadores nas linhagens da série 21T para a região promotora P1 do gene *TP53.*

O estado da cromatina na região promotora do gene *TP53* (TP53P1), analisado no artigo II, está de acordo com os níveis transcricionais do gene *TP53*, nas linhagem normal HB2 e na tumoral MCF-7, descritos no artigo I. A linhagem MCF-7, com menor expressão do gene *TP53*, apresenta um grande enriquecimento do marcador H3K9me3, e a alta expressão do gene *TP53*, na linhagem HB2, é corroborada pelo maior enriquecimento do marcador H4Ac.

O fato de os níveis transcricionais do gene *TP53* corroborarem com o estado da cromatina na região promotora P1 do gene *TP53*, em algumas linhagens, nos permite sugerir que o gene *TP53* pode ser regulado, nestas linhagens, através de modificações epigenéticas na cromatina, em sua região promotora P1. O fato das outras linhagens não corroborarem os resultados, pode indicar que existem outros fenômenos influenciando a transcrição do gene *TP53*.

Apesar de não detectarmos uma correlação entre um estado da cromatina específico e as MARs, ou entre as células normais e cancerosas, um estudo recente verificou uma correlação entre a presença de MARs com os marcadores de cromatina aberta H3Ac e H4Ac (166).

O fato do anticorpo anti-PARP-1 se ligar no complexo de proteínas nas linhagens MDA-MB-231 e MCF-7 (ambas não possuem a MAR2), bloqueando a ligação com sonda de DNA de mesma seqüência da MAR2 (descrita no artigo I), conforme a Figura 2 do artigo II, pode sugerir que a proteína ligante à matriz nuclear (MARBP) PARP-1 não faz parte do complexo de proteínas que atuam na ancoragem

do DNA à matriz nuclear, mas a ligação da PARP-1 ao DNA nestas linhagens, possui outras funções.

Através de uma plataforma computacional via web (http://alggen.lsi.upc.es/cgi-bin/promo_v3/promo/promoinit.cgi?dirDB=TF_8.3), foi possível realizarmos uma busca por putativos fatores transcricionais que poderiam ter afinidade à MAR2. Foram detectados 11 putativos sítios de ligação para as proteínas GR-beta, GR-alpha, PR A, PR B, FOXP3, c-Myb, HOXD9, HOXD10, POU2F2 (Oct-2.1), C/EBP-alpha e C/EBP-beta (conforme a Figura 4, artigo II).

A identificação e caracterização das proteínas responsáveis pela ancoragem à MAR2, será de extrema importância para o melhor entendimento do papel dos sítios de fixação à matriz nuclear, e sua influência na transcrição gênica no câncer.

Nos artigos I e II, o estudo da cromatina no câncer de mama, foi realizado através da descrição dos sítios de fixação à matriz nuclear e caracterização do importante sítio MAR2, detectado somente nas linhagens normais mamárias HB2 e MCF10A. Entretanto, no artigo III, o estudo da cromatina foi realizado através da descrição e caracterização, das principais alterações epigenéticas que ocorrem ao longo da progressão tumoral mamária, e suas possíveis influências na transcrição do gene supressor de tumor *TP53*, através da série 21T.

No artigo III, analisamos o estado da metilação global genômica, os níveis transcricionais dos genes relacionados à metilação no DNA (DNMT1, DNMT3A e DNMT3B), trimetilação na lisina 9 da histona H3 (SUV39H1), acetilação na histona H4 (HAT1), a expressão global e a distribuição nuclear, dos marcadores de eucromatina H4Ac e heterocromatina H3K9me3, ao longo da progressão tumoral mamária na série 21T.

No decorrer da progressão metastática mamária, verificamos a ocorrência de hipometilação global genômica, hipoacetilação global e acumulação de heterocromatina pericentromérica, todos fenômenos já descritos em artigos anteriores (133,167–169), porém foram descritos pela primeira vez na série 21T.

O possível papel compensatório das enzimas DNMTs 1 e 3A/B nos estágios iniciais de desenvolvimento do tumor mamário, da linhagem H16N2 para a linhagem 21PT, na manutenção dos altos níveis de metilação global genômica (observados à nível transcricional), é um interessante campo de estudo e a realização de ensaios de western blot, poderia ser o próximo passo para analisar estas enzimas à nível traducional.

A organização da cromatina é parte integrante das medidas de morfologia nuclear, que incluem também, o tamanho do núcleo, formato e ploidia. Entretanto, dada a importância destas medidas de morfologia nuclear no diagnóstico do câncer, é ainda surpreendente a carência de conhecimento detalhado dos eventos moleculares intrínsecos que podem ocasionar estas alterações na célula (170).

Conforme descrito recentemente, as regiões ricas em genes estão localizadas, na maior parte no centro do núcleo em células linfoblastóides (171). Portanto, o aumento no tamanho dos *loops* de cromatina (relacionados a regiões ricas em genes), junto à maior concentração de heterocromatina no centro do núcleo, observado nas células tumorais mamárias metastáticas, pode sugerir que a maior parte dos genes localizados nos *loops* pericêntricos estão sendo regulados negativamente no processo de metástase.

O aumento no número de *loops* também pode ocorrer na diferenciação celular, conduzindo a ativação ou aumento da expressão de determinados genes, antes inativos na periferia nuclear e associados à lamina nuclear (LADs). A ativação dos genes na diferenciação celular, está associada à existência de LADs e enriquecimento do marcador H3K4me3, especificamente na região promotora destes genes (172).

Apesar da expressão gênica depender da topologia da cromatina e da localização do gene numa região nuclear permissiva a sua transcrição, ainda não é conhecido se a ativação da transcrição é anterior ou posterior ao alargamento do *loop* ou se é um fenômeno totalmente independente (8).

Além do posicionamento nuclear dos *loops* de cromatina, a expressão gênica também é regulada através da ligação, por complementaridade de base, de RNAs não codificantes no RNAm. Estes RNAs não codificantes, são denominados micro-RNAs e dependendo do grau de complementaridade, podem atuar na repressão da tradução, e degradação (173,174) ou até aumento da tradução no RNAm alvo (175). Em virtude destas características, os micro-RNAs têm sido implicados nos diversos tipos de câncer, principalmente os de origem mamária (176–179).

A família de micro-RNAs miR-29, apresenta uma afinidade pela região 3’-UTR dos genes DNMT3A e DNMT3B, regulando negativamente a expressão destes (180,181), e indiretamente a do gene DNMT1 (182). Durante o período de doutoramento realizado em nosso laboratório, a Dra. Luiza Stankevicins descreveu uma significativa alta expressão dos micro-RNAs miR-29a-c (aproximadamente na

ordem de aproximadamente entre 3,0-3,8X), na linhagem metastática 21MT1 ao comparar com a linhagem normal H16N2 (dados ainda não publicados).

Apesar da grande afinidade da família do miR-29 pelas DNMTs3A/B, é possível sugerir que a baixa expressão de RNAm da DNMT1, descrita no artigo II, poderia estar associada à alta expressão do miR-29a-c, na linhagem 21MT1 ao comparar com a linhagem H16N2. Isto poderia sugerir que os miRs-29a-c podem regular negativamente a DNMT1, em detrimento das DNMTs 3A/3B, o que poderia conduzir a hipometilação global genômica na progressão do carcinoma mamário.

Contudo, ao longo desta tese, foram descritas alterações intrínsecas na cromatina em diferentes níveis de complexidade que ocorrem no câncer de mama. Estas alterações cromatinianas, foram caracterizadas através do estudo dos sítios de fixação à matriz nuclear e do “estado epigenético”. Além do mais, este trabalho corrobora estudos anteriores, que verificaram que estas alterações são definidas na fase de menor diferenciação celular, determinando o destino diferenciado da célula, através de um “canalículo de desenvolvimento”, como sulcos existentes em declives, por onde pedras (células), ao rolarem de uma montanha, poderiam entrar e seguir (68,183–186).

CONCLUSÃO

a) Os loops de cromatina, na região de domínio do gene *TP53*, podem influenciar a transcrição do gene *TP53*, e dos genes flanqueadores, em linhagens celulares normais e tumorais mamárias. Com isto, podemos concluir que o gene TP53 é regulado através de ancoragem de sítios de fixação à matriz nuclear, flanqueando a região de domínio deste gene.

b) As MARs não estão associadas a um estado específico da cromatina, e a MAR2, detectada nas células normais mamárias, possui uma intensa e altamente específica, ligação de complexos de proteínas. Isto pode indicar que o estado da cromatina e os sítios de fixação à matriz nuclear são fenômenos independentes. A indentificação das proteínas que participam especificamente na ancoragem à matriz nuclear, nas células normais MCF10A e HB2, vai ser de grande importância no futuro.

c) Drásticas alterações epigenéticas ocorrem na cromatina, no decorrer da progressão tumoral mamária, tais como: Hipometilação global genômica, hipoacetilação global e redistribuição da heterocromatina para o centro do núcleo. Entretanto, ao longo da progressão tumoral, o gene supressor de tumor *TP53*, possui uma expressão homogênea, concomitante com o estado de cromatina aberta no promotor P1.

REFERÊNCIAS

1. Rajapakse I, Groudine M. On emerging nuclear order. J. Cell Biol. 2011 Mar 7 [Acesso em 2013 Aug 6];192(5):711–21.Disponível em: http://www.jcb.org/cgi/doi/10.1083/jcb.201010129

2. Martins RP, Finan JD, Guilak F, Lee D a. Mechanical regulation of nuclear structure and function. Annu. Rev. Biomed. Eng. 2012 Jan [Acesso em 2013 Aug 16];14(May):431–55.Disponível em: http://www.pubmedcentral.nih.gov/articlerender.fcgi?artid=3575008&tool=pmcentrez&rendertype=abstract

3. Woodcock CLF, Frado L-LY. Ultrastructure of Chromatin Subunits during Unfolding, Histone Depletion, and Reconstitution. Cold Spring Harb. Symp. Quant. Biol. 1978 Jan 1 [Acesso em 2013 Oct 10];42(0):43–55. Disponível em: http://symposium.cshlp.org/content/42/43.short

4. Olins AL, Olins DE. Spheroid chromatin units (v bodies). Science [Internet]. 1974 Jan 25 [Acesso em 2013 Sep 30];183(4122):330–2. Disponível em: http://www.ncbi.nlm.nih.gov/pubmed/4128918

5. Belmont AS, Bruce K. Visualization of G1 chromosomes: a folded, twisted, supercoiled chromonema model of interphase chromatid structure. J. Cell Biol. 1994 Oct [Acesso em 2013 Sep 30];127(2):287–302. Disponível em: http://www.pubmedcentral.nih.gov/articlerender.fcgi?artid=2120203&tool=pmcentrez&rendertype=abstract

6. Gerchman SE, Ramakrishnan V. Chromatin higher-order structure studied by neutron scattering and scanning transmission electron microscopy. Proc. Natl. Acad. Sci. U. S. A. 1987 Nov [Acesso em 2013 Sep 30];84(22):7802–6. Disponível em: http://www.pubmedcentral.nih.gov/articlerender.fcgi?artid=299397&tool=pmcentrez&rendertype=abstract

7. Finch JT, Klug A. Solenoidal model for superstructure in chromatin. Proc. Natl. Acad. Sci. U. S. A. 1976 Jun [Acesso em 2013 Sep 30];73(6):1897–901. Disponível em: http://www.pubmedcentral.nih.gov/articlerender.fcgi?artid=430414&tool=pmcentrez&rendertype=abstract

8. Hübner MR, Eckersley-Maslin M a, Spector DL. Chromatin organization and transcriptional regulation. Curr. Opin. Genet. Dev. 2013 Apr [Acesso em 2013 Aug 12];23(2):89–95. Disponível em: http://www.ncbi.nlm.nih.gov/pubmed/23270812

9. Nelson D, Cox M. Principles of Biochemistry. Sixth. Shultz L, Moran S, Tontonoz M, editors. New York: Macmillan higher education; 2013. p. 994–5.

10. Nossal NG, Franklin JL, Kutter E, Drake JW. Anecdotal, historical and critical commentaries on genetics. Gisela Mosig. Genetics. 2004 Nov [Acesso em 2013 Oct 11];168(3):1097–104. Disponível em: http://www.pubmedcentral.nih.gov/articlerender.fcgi?artid=1448785&tool=pmcentrez&rendertype=abstract

11. Filion GJ, van Bemmel JG, Braunschweig U, Talhout W, Kind J, Ward LD, et al. Systematic protein location mapping reveals five principal chromatin types in Drosophila cells. Cell. 2010 Oct 15 [Acesso em 2013 Sep 19];143(2):212–24. Disponível em: http://www.pubmedcentral.nih.gov/articlerender.fcgi?artid=3119929&tool=pmcentrez&rendertype=abstract

12. Ernst J, Kellis M. Discovery and characterization of chromatin states for systematic annotation of the human genome. Nat. Biotechnol. Nature Publishing Group; 2010 Aug [Acesso em 2013 Sep 17];28(8):817–25. Disponível em: http://www.pubmedcentral.nih.gov/articlerender.fcgi?artid=2919626&tool=pmcentrez&rendertype=abstract

13. Németh A, Längst G. Genome organization in and around the nucleolus. Trends Genet. 2011 Apr [Acesso em 2013 Aug 6];27(4):149–56. Disponível em: http://www.ncbi.nlm.nih.gov/pubmed/21295884

14. Guelen L, Pagie L, Brasset E, Meuleman W, Faza MB, Talhout W, et al. Domain organization of human chromosomes revealed by mapping of nuclear lamina interactions. Nature. 2008 Jun 12 [Acesso em 2013 Aug 7];453(7197):948–51. Disponível em: http://www.ncbi.nlm.nih.gov/pubmed/18463634

15. Kumaran RI, Thakar R, Spector DL. Chromatin dynamics and gene positioning. Cell. 2008 Mar 21 [Acesso em 2013 Sep 23];132(6):929–34. Disponível em: http://www.pubmedcentral.nih.gov/articlerender.fcgi?artid=2898133&tool=pmcentrez&rendertype=abstract

16. Mekhail K, Seebacher J, Gygi SP, Moazed D. Role for perinuclear chromosome tethering in maintenance of genome stability. Nature. 2008 Dec 4 [Acesso em 2013 Oct 11];456(7222):667–70. Disponível em: http://www.pubmedcentral.nih.gov/articlerender.fcgi?artid=2596277&tool=pmcentrez&rendertype=abstract

17. Vogelstein B, Pardoll DM, Coffey DS. Supercoiled loops and eucaryotic DNA replication. Cell. 1980 Nov [Acesso em 2013 Oct 11];22(1):79–85. Disponível em: http://linkinghub.elsevier.com/retrieve/pii/0092867480901567

18. Singh G. Mathematical model to predict regions of chromatin attachment to the nuclear matrix. Nucleic Acids Res. 1997 Apr 1 [Acesso em 2013 Oct 11];25(7):1419–25. Disponível em: http://nar.oxfordjournals.org/content/25/7/1419

19. Buongiorno-Nardelli M, Micheli G, Carrĩ MT, Marilley M. A relationship between replicon size and supercoiled loop domains in the eukaryotic genome. Nature. Nature Publishing Group; 1982 Jul 1 [Acesso em 2013 Oct 11];298(5869):100–2. Disponível em: http://www.nature.com/nature/journal/v298/n5869/pdf/298100a0.pdf

20. Bode J, Goetze S, Heng H, Krawetz SA, Benham C. From DNA structure to gene expression: mediators of nuclear compartmentalization and dynamics. Chromosome Res. 2003 Jan [Acesso em 2013 Oct 11];11(5):435–45. Disponível em: http://www.ncbi.nlm.nih.gov/pubmed/12971720

21. Berezney R, Coffey DS. Identification of a nu1. Berezney R, Coffey DS. Identification of a nuclear protein matrix. Biochem. Biophys. Res. Commun. 1974 Oct 23 [Acesso em 2013 Oct 11];60(4):1410–7. Disponível em: http://www.ncbi.nlm.nih.gov/pubmed/4214419

22. Mirkovitch J, Mirault ME, Laemmli UK. Organization of the higher-order chromatin loop: specific DNA attachment sites on nuclear scaffold. Cell. 1984 Nov [Acesso em 2013 Oct 11];39(1):223–32. Disponível em: http://www.ncbi.nlm.nih.gov/pubmed/6091913

23. Jackson D, Cook P. Visualization of a filamentous nucleoskeleton with a 23nm axial repeat. EMBO J. 1988;7(12):3667–77.

24. Jackson D a, Cook PR. A general method for preparing chromatin containing intact DNA. EMBO J. 1985 Apr;4(4):913–8. Disponível em: http://www.pubmedcentral.nih.gov/articlerender.fcgi?artid=554279&tool=pmcentrez&rendertype=abstract

25. Cook PR. A general method for preparing intact nuclear DNA. EMBO J. 1984 Aug;3(8):1837–42. Disponível em: http://www.pubmedcentral.nih.gov/articlerender.fcgi?artid=557606&tool=pmcentrez&rendertype=abstract

26. Nickerson JA, Krockmalnic G, Wan KM, Penman S. The nuclear matrix revealed by eluting chromatin from a cross-linked nucleus. Proc. Natl. Acad. Sci. U. S. A. 1997 Apr 29 [Acesso em 2013 Oct 14];94(9):4446–50. Disponível em: http://www.pubmedcentral.nih.gov/articlerender.fcgi?artid=20742&tool=pmcentrez&rendertype=abstract

27. Albrethsen J, Knol JC, Jimenez CR. Unravelling the nuclear matrix proteome. J. Proteomics. Elsevier B.V.; 2009 Feb 15 [Acesso em 2013 Aug 14];72(1):71–81. Disponível em: http://www.ncbi.nlm.nih.gov/pubmed/18957335

28. Coffey DS. Nuclear Matrix Proteins as Proteomic Markers of Preneoplastic and Cancer Lesions : Commentary re: G. Brunagel et al., Nuclear Matrix Protein Alterations Associated with Colon Cancer Metastasis to the Liver. Clin. Cancer Res., 8: 3039-3045, 2002. Clin. Cancer Res. 2002 Oct 1 [Acesso em 2013 Oct

14];8(10):3031–3. Disponível em: http://clincancerres.aacrjournals.org/content/8/10/3031.long

29. Nickerson J. Experimental observations of a nuclear matrix. J. Cell Sci. 2001 Feb 1 [Acesso em 2013 Oct 14];114(3):463–74. Disponível em: http://jcs.biologists.org/content/114/3/463.abstract

30. Sabbatino VE. Biología Celular y Humana. [Acesso em 2013 Oct 14]. Disponível em: http://www.genomasur.com/BCH/BCH_libro/capitulo_03.htm

31. Vaughn JP, Dijkwel PA, Mullenders LHF, Hamlin JL. Replication forks are associated with the nuclear matrix. 1990;18(8):1965–9.

32. Girard-Reydet C, Grégoire D, Vassetzky Y, Méchali M. DNA replication initiates at domains overlapping with nuclear matrix attachment regions in the xenopus and mouse c-myc promoter. Gene. 2004 May 12 [Acesso em 2013 Aug 24];332:129–38. Disponível em: http://www.ncbi.nlm.nih.gov/pubmed/15145062

33. Berrios M, Osheroff N, Fisher PA. In situ localization of DNA topoisomerase II, a major polypeptide component of the Drosophila nuclear matrix fraction. Proc. Natl. Acad. Sci. U. S. A. 1985 Jun [Acesso em 2013 Oct 14];82(12):4142–6. Disponível em: http://www.pubmedcentral.nih.gov/articlerender.fcgi?artid=397951&tool=pmcentrez&rendertype=abstract

34. Cockerill PN, Garrard WT. Chromosomal loop anchorage of the kappa immunoglobulin gene occurs next to the enhancer in a region containing topoisomerase II sites. Cell. 1986 Jan 31 [Acesso em 2013 Oct 14];44(2):273–82. Disponível em: http://www.ncbi.nlm.nih.gov/pubmed/3002631

35. Ottaviani D, Lever E, Takousis P, Sheer D. Anchoring the genome. Genome Biol. 2008 Jan [Acesso em 2013 Sep 23];9(1):201. Disponível em: http://genomebiology.com/2008/9/1/201

36. Benham C, Kohwi-Shigematsu T, Bode J. Stress-induced duplex DNA destabilization in scaffold/matrix attachment regions. J. Mol. Biol. 1997 [Acesso em 2013 Oct 14];274(2):181–96. Disponível em: http://www.sciencedirect.com/science/article/pii/S0022283697913851

37. Evans K, Ott S, Hansen A, Koentges G, Wernisch L. A comparative study of S/MAR prediction tools. BMC Bioinformatics. 2007 Jan [Acesso em 2013 Sep 26];8(1):71. Disponível em: http://www.biomedcentral.com/1471-2105/8/71

38. Petrov A, Allinne J, Pirozhkova I, Laoudj D, Lipinski M, Vassetzky YS. A nuclear matrix attachment site in the 4q35 locus has an enhancer-blocking activity in vivo: implications for the facio-scapulo-humeral dystrophy. Genome Res. 2008 Jan [Acesso em 2013 Aug 29];18(1):39–45. Disponível em: http://www.pubmedcentral.nih.gov/articlerender.fcgi?artid=2134777&tool=pmcentrez&rendertype=abstract

39. Pogo BGT, Allfrey VG, Mirsky AE. Rna synthesis and histone acetylation during the course of gene activation in lymphocytes. Proc. Natl. Acad. Sci. U. S. A. 1966;55:805–12.

40. Phi-Van L, von Kries JP, Ostertag W, Strätling WH. The chicken lysozyme 5' matrix attachment region increases transcription from a heterologous promoter in heterologous cells and dampens position effects on the expression of transfected genes. Mol. Cell. Biol. 1990 May;10(5):2302–7. Disponível em: http://www.pubmedcentral.nih.gov/articlerender.fcgi?artid=360577&tool=pmcentrez&rendertype=abstract

41. Klehr D, Maass K, Bode J. Scaffold-attached regions from the human interferon .beta. domain can be used to enhance the stable expression of genes under the control of various promoters. Biochemistry. American Chemical Society; 1991 Feb [Acesso em 2013 Oct 14];30(5):1264–70. Disponível em: http://dx.doi.org/10.1021/bi00219a015

42. Auten J, Agarwal M, Chen J, Sutton R, Plavec I. Effect of scaffold attachment region on transgene expression in retrovirus vector-transduced primary T cells and macrophages. Hum. Gene Ther. Mary Ann Liebert, Inc.; 1999 May 20 [Acesso em 2013 Oct 14];10(8):1389–99. Disponível em: http://online.liebertpub.com/doi/abs/10.1089/10430349950018058?journalCode=hum

43. Jenuwein T, Forrester WC, Fernández-Herrero LA, Laible G, Dull M, Grosschedl R. Extension of chromatin accessibility by nuclear matrix attachment regions. Nature. 1997 Jan 16 [Acesso em 2013 Oct 14];385(6613):269–72. Disponível em: http://www.ncbi.nlm.nih.gov/pubmed/9000077

44. Hart CM, Laemmli UK. Facilitation of chromatin dynamics by SARs. Curr. Opin. Genet. Dev. 1998 [Acesso em 2013 Oct 14];8(5):519–25. Disponível em: http://www.sciencedirect.com/science/article/pii/S0959437X98800051

45. Forrester WC, van Genderen C, Jenuwein T, Grosschedl R. Dependence of enhancer-mediated transcription of the immunoglobulin mu gene on nuclear matrix attachment regions. Science. 1994 Aug 26 [Acesso em 2013 Oct 14];265(5176):1221–5. Disponível em: http://www.ncbi.nlm.nih.gov/pubmed/8066460

46. Cockerill PN, Yuen MH, Garrard WT. The enhancer of the immunoglobulin heavy chain locus is flanked by presumptive chromosomal loop anchorage elements. J. Biol. Chem. 1987 Apr 15;262(11):5394–7. Disponível em: http://www.ncbi.nlm.nih.gov/pubmed/3031052

47. Rivera-Mulia JC, Hernández-Muñoz R, Martínez F, Aranda-Anzaldo A. DNA moves sequentially towards the nuclear matrix during DNA replication in vivo. BMC Cell Biol. BioMed Central Ltd; 2011 Jan [Acesso em 2013 Aug 14];12(1):3. Disponível em:

http://www.pubmedcentral.nih.gov/articlerender.fcgi?artid=3037911&tool=pmcentrez&rendertype=abstract

48. Castillo-Mora RC, Aranda-Anzaldo A. Reorganization of the DNA-nuclear matrix interactions in a 210 kb genomic region centered on c-myc after DNA replication in vivo. J. Cell. Biochem. 2012 Jul [Acesso em 2013 Aug 16];113(7):2451–63. Disponível em: http://www.ncbi.nlm.nih.gov/pubmed/22396210

49. Iarovaia O V, Akopov SB, Nikolaev LG, Sverdlov ED, Razin S V. Induction of transcription within chromosomal DNA loops flanked by MAR elements causes an association of loop DNA with the nuclear matrix. Nucleic Acids Res. 2005 Jan [Acesso em 2013 Oct 15];33(13):4157–63. Disponível em: http://www.pubmedcentral.nih.gov/articlerender.fcgi?artid=1180747&tool=pmcentrez&rendertype=abstract

50. Ostermeier GC. Nuclear matrix association of the human -globin locus utilizing a novel approach to quantitative real-time PCR. Nucleic Acids Res. 2003 Jun 15 [Acesso em 2013 Aug 16];31(12):3257–66. Disponível em: http://nar.oxfordjournals.org/lookup/doi/10.1093/nar/gkg424

51. Benyajati C, Worcel A. Isolation, characterization, and structure of the folded interphase genome of Drosophila melanogaster. Cell. 1976 Nov [Acesso em 2013 Oct 15];9(3):393–407. Disponível em: http://www.ncbi.nlm.nih.gov/pubmed/825231

52. Marsden MP, Laemmli UK. Metaphase chromosome structure: evidence for a radial loop model. Cell. 1979 Aug [Acesso em 2013 Oct 15];17(4):849–58. Disponível em: http://www.ncbi.nlm.nih.gov/pubmed/487432

53. Boulikas T. Chromatin domains and prediction of MAR sequences. Int. Rev. Cytol. 1995 Jan [Acesso em 2013 Oct 15];162A:279–388. Disponível em: http://www.ncbi.nlm.nih.gov/pubmed/8575883

54. Heng HHQ, Goetze S, Ye CJ, Liu G, Stevens JB, Bremer SW, et al. Chromatin loops are selectively anchored using scaffold/matrix-attachment regions. J. Cell Sci. 2004 Mar 1 [Acesso em 2013 Aug 16];117(Pt 7):999–1008. Disponível em: http://www.ncbi.nlm.nih.gov/pubmed/14996931

55. Djeliova V, Russev G, Anachkova B. Dynamics of association of origins of DNA replication with the nuclear matrix during the cell cycle. Nucleic Acids Res. 2001 Aug 1;29(15):3181–7. Disponível em: http://www.pubmedcentral.nih.gov/articlerender.fcgi?artid=55821&tool=pmcentrez&rendertype=abstract

56. Ortega JM, DePamphilis ML. Nucleoskeleton and initiation of DNA replication in metazoan cells. J. Cell Sci. 1998 Dec 18 [Acesso em 2013 Oct 15];111 (Pt 2:3663–73. Disponível em: http://www.ncbi.nlm.nih.gov/pubmed/9819357

57. Ottaviani D, Lever E, Takousis P, Sheer D. Anchoring the genome. Genome Biol. 2008 Jan [Acesso em 2013 Sep 11];9(1):201. Disponível em: http://www.pubmedcentral.nih.gov/articlerender.fcgi?artid=2395230&tool=pmcentrez&rendertype=abstract

58. Frouin I, Montecucco A, Spadari S, Maga G. DNA replication: a complex matter. EMBO Rep. 2003 Jul [Acesso em 2013 Oct 15];4(7):666–70. Disponível em: http://www.pubmedcentral.nih.gov/articlerender.fcgi?artid=1326325&tool=pmcentrez&rendertype=abstract

59. Linnemann AK, Platts AE, Krawetz S a. Differential nuclear scaffold/matrix attachment marks expressed genes. Hum. Mol. Genet. 2009 Feb 15 [Acesso em 2013 Aug 13];18(4):645–54. Disponível em: http://www.pubmedcentral.nih.gov/articlerender.fcgi?artid=2638830&tool=pmcentrez&rendertype=abstract

60. Linnemann AK, Krawetz S a. Silencing by nuclear matrix attachment distinguishes cell-type specificity: association with increased proliferation capacity. Nucleic Acids Res. 2009 May [Acesso em 2013 Sep 11];37(9):2779–88. Disponível em: http://www.pubmedcentral.nih.gov/articlerender.fcgi?artid=2685086&tool=pmcentrez&rendertype=abstract

61. Bode J, Schlake T, Ríos-Ramírez M, Mielke C, Stengert M, Kay V, et al. Scaffold/matrix-attached regions: structural properties creating transcriptionally active loci. Int. Rev. Cytol. 1995 Jan [Acesso em 2013 Oct 15];162A:389–454. Disponível em: http://www.ncbi.nlm.nih.gov/pubmed/8575884

62. Kramer JA, Krawetz SA. Nuclear matrix interactions within the sperm genome. J. Biol. Chem. 1996 May 17 [Acesso em 2013 Oct 15];271(20):11619–22. Disponível em: http://www.ncbi.nlm.nih.gov/pubmed/8662749

63. Weber M, Hagège H, Murrell A, Brunel C, Reik W, Cathala G, et al. Genomic imprinting controls matrix attachment regions in the Igf2 gene. Mol. Cell. Biol. 2003 Dec [Acesso em 2013 Oct 15];23(24):8953–9. Disponível em: http://www.pubmedcentral.nih.gov/articlerender.fcgi?artid=309645&tool=pmcentrez&rendertype=abstract

64. Wong S-P, Harbottle RP. Genetic modification of dividing cells using episomally maintained S/MAR DNA vectors. Mol. Ther. Nucleic Acids 2013 Jan [Acesso em 2013 Aug 17];2(April):e115. Disponível em: http://www.ncbi.nlm.nih.gov/pubmed/23941867

65. Wilson RHC, Coverley D. Relationship between DNA replication and the nuclear matrix. Genes Cells. 2013 Jan [Acesso em 2013 Oct 9];18(1):17–31. Disponível em: http://www.pubmedcentral.nih.gov/articlerender.fcgi?artid=3564400&tool=pmcentrez&rendertype=abstract

66. Wang T-Y, Han Z-M, Chai Y-R, Zhang J-H. A mini review of MAR-binding proteins. Mol. Biol. Rep. 2010 Oct [Acesso em 2013 Aug 16];37(7):3553–60. Disponível em: http://www.ncbi.nlm.nih.gov/pubmed/20174991

67. Nakagawa S, Prasanth K V. eXIST with matrix-associated proteins. Trends Cell Biol. Elsevier Ltd; 2011 Jun [Acesso em 2013 Aug 16];21(6):321–7. Disponível em: http://www.ncbi.nlm.nih.gov/pubmed/21392997

68. Berger SL, Kouzarides T, Shiekhattar R, Shilatifard A. An operational definition of epigenetics. Genes Dev. 2009 Apr 1 [Acesso em 2013 Sep 26];23(7):781–3. Disponível em: http://www.ncbi.nlm.nih.gov/pubmed/19339683

69. Goldberg AD, Allis CD, Bernstein E. Epigenetics: a landscape takes shape. Cell. 2007 Feb 23 [Acesso em 2011 Jul 17];128(4):635–8. Disponível em: http://www.ncbi.nlm.nih.gov/pubmed/17320500

70. Mutskov VJ, Farrell CM, Wade PA, Wolffe AP, Felsenfeld G. The barrier function of an insulator couples high histone acetylation levels with specific protection of promoter DNA from methylation. Genes Dev. 2002 Jun 15 [Acesso em 2013 Oct 17];16(12):1540–54. Disponível em: http://www.pubmedcentral.nih.gov/articlerender.fcgi?artid=186352&tool=pmcentrez&rendertype=abstract

71. O'Neill LP, Turner BM. Histone H4 acetylation distinguishes coding regions of the human genome from heterochromatin in a differentiation-dependent but transcription-independent manner. EMBO J. 1995 Aug 15 [Acesso em 2013 Oct 17];14(16):3946–57. Disponível em: http://www.pubmedcentral.nih.gov/articlerender.fcgi?artid=394473&tool=pmcentrez&rendertype=abstract

72. Hebbes TR, Clayton AL, Thorne AW, Crane-Robinson C. Core histone hyperacetylation co-maps with generalized DNase I sensitivity in the chicken beta-globin chromosomal domain. EMBO J. 1994 Apr 15 [Acesso em 2013 Oct 17];13(8):1823–30. Disponível em: http://www.pubmedcentral.nih.gov/articlerender.fcgi?artid=395022&tool=pmcentrez&rendertype=abstract

73. Davie JR. Nuclear matrix, dynamic histone acetylation and transcriptionally active chromatin. Mol. Biol. Rep. 1997 Aug;24(3):197–207. Disponível em: http://www.ncbi.nlm.nih.gov/pubmed/9291093

74. Couppez M, Martin-Ponthieu A, Sautière P. Histone H4 from cuttlefish testis is sequentially acetylated. Comparison with acetylation of calf thymus histone H4. J. Biol. Chem. 1987 Feb 25 [Acesso em 2013 Oct 17];262(6):2854–60. Disponível em: http://www.ncbi.nlm.nih.gov/pubmed/3818624

75. Thorne Aw, Kmiciek D, Mitchelson K, Sautiere P, Crane-Robinson C. Patterns of histone acetylation. Eur. J. Biochem. 1990 Nov [Acesso em 2013 Oct 17];193(3):701–13. Disponível em: http://doi.wiley.com/10.1111/j.1432-1033.1990.tb19390.x

76. Chicoine LG, Schulman IG, Richman R, Cook RG, Allis CD. Nonrandom utilization of acetylation sites in histones isolated from Tetrahymena. Evidence for functionally distinct H4 acetylation sites. J. Biol. Chem. 1986 Jan 25 [Acesso em 2013 Oct 17];261(3):1071–6. Disponível em: http://www.ncbi.nlm.nih.gov/pubmed/3080415

77. Clarke DJ, O'Neill LP, Turner BM. Selective use of H4 acetylation sites in the yeast Saccharomyces cerevisiae. Biochem. J. 1993 Sep 1 [Acesso em 2013 Oct 17];294(2):557–61. Disponível em: http://www.pubmedcentral.nih.gov/articlerender.fcgi?artid=1134491&tool=pmcentrez&rendertype=abstract

78. Baylin SB, Jones PA. A decade of exploring the cancer epigenome - biological and translational implications. Nat. Rev. Cancer. 2011 Oct [Acesso em 2013 Oct 17];11(10):726–34. Disponível em: http://www.pubmedcentral.nih.gov/articlerender.fcgi?artid=3307543&tool=pmcentrez&rendertype=abstract

79. Yuan H, Marmorstein R. Histone acetyltransferases: Rising ancient counterparts to protein kinases. Biopolymers. 2013 Feb [Acesso em 2013 Aug 27];99(2):98–111. Disponível em: http://www.ncbi.nlm.nih.gov/pubmed/23175385

80. Kouzarides T. Chromatin modifications and their function. Cell. 2007 Feb 23 [Acesso em 2013 Oct 17];128(4):693–705. Disponível em: http://www.ncbi.nlm.nih.gov/pubmed/17320507

81. Gómez Acuña LI, Fiszbein A, Alló M, Schor IE, Kornblihtt AR. Connections between chromatin signatures and splicing. Wiley Interdiscip. Rev. RNA. 2013 [Acesso em 2013 Oct 17];4(1):77–91. Disponível em: http://www.ncbi.nlm.nih.gov/pubmed/23074139

82. Ferrari KJ, Pasini D. Regulation and function of DNA and histone methylations. Curr. Pharm. Des. 2013 Jan;19(4):719–33. Disponível em: http://www.ncbi.nlm.nih.gov/pubmed/23016854

83. Greer EL, Shi Y. Histone methylation: a dynamic mark in health, disease and inheritance. Nat. Rev. Genet. Nature Publishing Group; 2012 May [Acesso em 2013 Aug 9];13(5):343–57. Disponível em: http://www.ncbi.nlm.nih.gov/pubmed/22473383

84. Hu S, Cheng L, Wen B. Large chromatin domains in pluripotent and differentiated cells Bivalent Domains Functional Heterogeneity in PSC Cultures Open Chromatin Structure in Pluripotent. 2012;9:48–53.

85. Peters AHFM, Kubicek S, Mechtler K, O'Sullivan RJ, Derijck AAHA, Perez-Burgos L, et al. Partitioning and plasticity of repressive histone methylation states in mammalian chromatin. Mol. Cell. 2003 Dec [Acesso em 2013 Sep

17];12(6):1577–89. Disponível em: http://www.ncbi.nlm.nih.gov/pubmed/14690609

86. Bernstein BE, Mikkelsen TS, Xie X, Kamal M, Huebert DJ, Cuff J, et al. A bivalent chromatin structure marks key developmental genes in embryonic stem cells. Cell. 2006 Apr 21 [Acesso em 2013 Oct 20];125(2):315–26. Disponível em: http://www.ncbi.nlm.nih.gov/pubmed/16630819

87. Zhao XD, Han X, Chew JL, Liu J, Chiu KP, Choo A, et al. Whole-genome mapping of histone H3 Lys4 and 27 trimethylations reveals distinct genomic compartments in human embryonic stem cells. Cell Stem Cell. 2007 Sep 13 [Acesso em 2013 Oct 20];1(3):286–98. Disponível em: http://www.ncbi.nlm.nih.gov/pubmed/18371363

88. Munari F, Soeroes S, Zenn HM, Schomburg A, Kost N, Schröder S, et al. Methylation of lysine 9 in histone H3 directs alternative modes of highly dynamic interaction of heterochromatin protein hHP1β with the nucleosome. J. Biol. Chem. 2012 Sep 28 [Acesso em 2013 Aug 13];287(40):33756–65. Disponível em: http://www.ncbi.nlm.nih.gov/pubmed/22815475

89. Dambacher S, Hahn M, Schotta G. The compact view on heterochromatin. Cell Cycle. 2013 Aug 23;12(18):1–2. Disponível em: http://www.ncbi.nlm.nih.gov/pubmed/23974091

90. Jones P a. Functions of DNA methylation: islands, start sites, gene bodies and beyond. Nat. Rev. Genet. Nature Publishing Group; 2012 Jul [Acesso em 2013 Aug 6];13(7):484–92. Disponível em: http://www.ncbi.nlm.nih.gov/pubmed/22641018

91. Wolf SF, Jolly DJ, Lunnen KD, Friedmann T, Migeon BR. Methylation of the hypoxanthine phosphoribosyltransferase locus on the human X chromosome: implications for X-chromosome inactivation. Proc. Natl. Acad. Sci. U. S. A. 1984 May [Acesso em 2013 Oct 23];81(9):2806–10. Disponível em: http://www.pubmedcentral.nih.gov/articlerender.fcgi?artid=345159&tool=pmcentrez&rendertype=abstract

92. Hellman A, Chess A. Gene body-specific methylation on the active X chromosome. Science. 2007 Feb 23 [Acesso em 2013 Oct 23];315(5815):1141–3. Disponível em: http://www.sciencemag.org/content/315/5815/1141.abstract

93. Yoder JA, Walsh CP, Bestor TH. Cytosine methylation and the ecology of intragenomic parasites. Trends Genet. 1997 Aug [Acesso em 2013 Oct 23];13(8):335–40. Disponível em: http://www.ncbi.nlm.nih.gov/pubmed/9260521

94. Pradhan S, Talbot D, Sha M, Benner J, Hornstra L, Li E, et al. Baculovirus-mediated expression and characterization of the full-length murine DNA methyltransferase. Nucleic Acids Res. 1997 Nov 15 [Acesso em 2013 Oct 23];25(22):4666–73. Disponível em:

http://www.pubmedcentral.nih.gov/articlerender.fcgi?artid=147102&tool=pmcentrez&rendertype=abstract

95. Liu K, Wang YF, Cantemir C, Muller MT. Endogenous Assays of DNA Methyltransferases: Evidence for Differential Activities of DNMT1, DNMT2, and DNMT3 in Mammalian Cells In Vivo. Mol. Cell. Biol. 2003 Apr 15 [Acesso em 2013 Oct 23];23(8):2709–19. Disponível em: http://mcb.asm.org/cgi/doi/10.1128/MCB.23.8.2709-2719.2003

96. Okano M, Bell DW, Haber D a, Li E. DNA methyltransferases Dnmt3a and Dnmt3b are essential for de novo methylation and mammalian development. Cell. 1999 Oct 29;99(3):247–57. Disponível em: http://www.ncbi.nlm.nih.gov/pubmed/10555141

97. Suetake I, Shinozaki F, Miyagawa J, Takeshima H, Tajima S. DNMT3L stimulates the DNA methylation activity of Dnmt3a and Dnmt3b through a direct interaction. J. Biol. Chem. 2004 Jun 25 [Acesso em 2013 Oct 18];279(26):27816–23. Disponível em: http://www.ncbi.nlm.nih.gov/pubmed/15105426

98. Kareta MS, Botello ZM, Ennis JJ, Chou C, Chédin F. Reconstitution and mechanism of the stimulation of de novo methylation by human DNMT3L. J. Biol. Chem. 2006 Sep 8 [Acesso em 2013 Oct 23];281(36):25893–902. Disponível em: http://www.ncbi.nlm.nih.gov/pubmed/16829525

99. Holz-Schietinger C, Reich NO. The inherent processivity of the human de novo methyltransferase 3A (DNMT3A) is enhanced by DNMT3L. J. Biol. Chem. 2010 Sep 17 [Acesso em 2013 Oct 23];285(38):29091–100. Disponível em: http://www.pubmedcentral.nih.gov/articlerender.fcgi?artid=2937940&tool=pmcentrez&rendertype=abstract

100. Ooi SKT, Qiu C, Bernstein E, Li K, Jia D, Yang Z, et al. DNMT3L connects unmethylated lysine 4 of histone H3 to de novo methylation of DNA. Nature. 2007 Aug 9 [Acesso em 2013 Oct 23];448(7154):714–7. Disponível em: http://www.pubmedcentral.nih.gov/articlerender.fcgi?artid=2650820&tool=pmcentrez&rendertype=abstract

101. Fuks F, Hurd PJ, Deplus R, Kouzarides T. The DNA methyltransferases associate with HP1 and the SUV39H1 histone methyltransferase. Nucleic Acids Res. 2003 May 1 [Acesso em 2013 Oct 24];31(9):2305–12. Disponível em: http://www.pubmedcentral.nih.gov/articlerender.fcgi?artid=154218&tool=pmcentrez&rendertype=abstract

102. Lehnertz B, Ueda Y, Derijck AAHA, Braunschweig U, Perez-Burgos L, Kubicek S, et al. Suv39h-mediated histone H3 lysine 9 methylation directs DNA methylation to major satellite repeats at pericentric heterochromatin. Curr. Biol. 2003 Jul 15 [Acesso em 2013 Sep 10];13(14):1192–200. Disponível em: http://www.ncbi.nlm.nih.gov/pubmed/12867029

103. Eden S, Hashimshony T, Keshet I, Cedar H, Thorne AW. DNA methylation models histone acetylation. Nature. 1998 Aug 27 [Acesso em 2013 Oct 24];394(6696):842. Disponível em: http://dx.doi.org/10.1038/29680

104. Nan X, Ng HH, Johnson CA, Laherty CD, Turner BM, Eisenman RN, et al. Transcriptional repression by the methyl-CpG-binding protein MeCP2 involves a histone deacetylase complex. Nature. 1998 May 28 [Acesso em 2013 Oct 21];393(6683):386–9. Disponível em: http://www.ncbi.nlm.nih.gov/pubmed/9620804

105. Hashimshony T, Zhang J, Keshet I, Bustin M, Cedar H. The role of DNA methylation in setting up chromatin structure during development. Nat. Genet. 2003 Jun [Acesso em 2013 Oct 24];34(2):187–92. Disponível em: http://www.ncbi.nlm.nih.gov/pubmed/12740577

106. Carone DM, Lawrence JB. Heterochromatin instability in cancer: from the Barr body to satellites and the nuclear periphery. Semin. Cancer Biol. Elsevier Ltd; 2013 Apr [Acesso em 2013 Aug 16];23(2):99–108. Disponível em: http://www.ncbi.nlm.nih.gov/pubmed/22722067

107. Pageau GJ, Hall LL, Ganesan S, Livingston DM, Lawrence JB. The disappearing Barr body in breast and ovarian cancers. Nat. Rev. Cancer. Nature Publishing Group; 2007 Aug [Acesso em 2013 Oct 24];7(8):628–33. Disponível em: http://dx.doi.org/10.1038/nrc2172

108. Albert M, Helin K. Histone methyltransferases in cancer. Semin. Cell Dev. Biol. Elsevier Ltd; 2010 Apr [Acesso em 2013 Aug 16];21(2):209–20. Disponível em: http://www.ncbi.nlm.nih.gov/pubmed/19892027

109. Wang D, Zhou J, Liu X, Lu D, Shen C, Du Y, et al. Methylation of SUV39H1 by SET7/9 results in heterochromatin relaxation and genome instability. Proc. Natl. Acad. Sci. U. S. A. 2013 Apr 2 [Acesso em 2013 Sep 10];110(14):5516–21. Disponível em: http://www.ncbi.nlm.nih.gov/pubmed/23509280

110. Vaute O, Nicolas E, Vandel L, Trouche D. Functional and physical interaction between the histone methyl transferase Suv39H1 and histone deacetylases. Nucleic Acids Res. 2002 Jan 15 [Acesso em 2013 Sep 10];30(2):475–81. Disponível em: http://www.pubmedcentral.nih.gov/articlerender.fcgi?artid=99834&tool=pmcentrez&rendertype=abstract

111. Kang MY, Lee B Bin, Kim Y-H, Chang DK, Kyu Park S, Chun H-K, et al. Association of the SUV39H1 histone methyltransferase with the DNA methyltransferase 1 at mRNA expression level in primary colorectal cancer. Int. J. Cancer. 2007 Nov 15 [Acesso em 2013 Oct 28];121(10):2192–7. Disponível em: http://www.ncbi.nlm.nih.gov/pubmed/17657744

112. Di Micco R, Sulli G, Dobreva M, Liontos M, Botrugno O a, Gargiulo G, et al. Interplay between oncogene-induced DNA damage response and heterochromatin in senescence and cancer. Nat. Cell Biol. Nature Publishing

Group; 2011 Mar [Acesso em 2013 Aug 8];13(3):292–302. Disponível em: http://www.ncbi.nlm.nih.gov/pubmed/21336312

113. Min SK, Koh YH, Park Y, Kim HJ, Seo J, Park H-R, et al. Expression of HAT1 and HDAC1, 2, 3 in Diffuse Large B-Cell Lymphomas, Peripheral T-Cell Lymphomas, and NK/T-Cell Lymphomas. Korean J. Pathol. 2012 Apr [Acesso em 2013 Oct 28];46(2):142–50. Disponível em: http://www.pubmedcentral.nih.gov/articlerender.fcgi?artid=3479788&tool=pmcentrez&rendertype=abstract

114. Leroy G, Dimaggio PA, Chan EY, Zee BM, Blanco MA, Bryant B, et al. A quantitative atlas of histone modification signatures from human cancer cells. Epigenetics Chromatin. 2013 Jan [Acesso em 2013 Oct 20];6(1):20. Disponível em: http://www.epigeneticsandchromatin.com/content/6/1/20

115. Lebel EA, Boukamp P, Tafrov ST. Irradiation with heavy-ion particles changes the cellular distribution of human histone acetyltransferase HAT1. Mol. Cell. Biochem. 2010 Jun [cited 2013 Oct 28];339(1-2):271–84. Available from: http://www.ncbi.nlm.nih.gov/pubmed/20148353

116. Yoo CB, Jones P a. Epigenetic therapy of cancer: past, present and future. Nat. Rev. Drug Discov. 2006 Jan [Acesso em 2013 Aug 8];5(1):37–50. Disponível em: http://www.ncbi.nlm.nih.gov/pubmed/16485345

117. Sulewska A, Niklinska W, Kozlowski M, Minarowski L, Naumnik W, Niklinski J, et al. DNA methylation in states of cell physiology and pathology. Folia Histochem. Cytobiol. 2007 Jan [Acesso em 2013 Oct 29];45(3):149–58. Disponível em: http://www.ncbi.nlm.nih.gov/pubmed/17951162

118. Fryxell KJ, Zuckerkandl E. Cytosine deamination plays a primary role in the evolution of mammalian isochores. Mol. Biol. Evol. 2000 Sep [Acesso em 2013 Oct 29];17(9):1371–83. Disponível em: http://www.ncbi.nlm.nih.gov/pubmed/10958853

119. Rideout WM, Coetzee GA, Olumi AF, Jones PA. 5-Methylcytosine as an endogenous mutagen in the human LDL receptor and p53 genes. Science. 1990 Sep 14 [Acesso em 2013 Oct 29];249(4974):1288–90. Disponível em: http://www.ncbi.nlm.nih.gov/pubmed/1697983

120. Daniel FI, Cherubini K, Yurgel LS, de Figueiredo MAZ, Salum FG. The role of epigenetic transcription repression and DNA methyltransferases in cancer. Cancer. 2011 Mar 15 [Acesso em 2013 Oct 29];117(4):677–87. Disponível em http://www.ncbi.nlm.nih.gov/pubmed/20945317

121. Chekhun VF, Lukyanova NY, Kovalchuk O, Tryndyak VP, Pogribny IP. Epigenetic profiling of multidrug-resistant human MCF-7 breast adenocarcinoma cells reveals novel hyper- and hypomethylated targets. Mol. Cancer Ther. 2007 Mar [Acesso em 2013 Oct 29];6(3):1089–98. Disponível em: http://www.ncbi.nlm.nih.gov/pubmed/17363502

122. Yoder J a, Walsh CP, Bestor TH. Cytosine methylation and the ecology of intragenomic parasites. Trends Genet. 1997 Aug;13(8):335–40. Disponível em: http://www.ncbi.nlm.nih.gov/pubmed/9260521

123. Sharp AJ, Stathaki E, Migliavacca E, Brahmachary M, Montgomery SB, Dupre Y, et al. DNA methylation profiles of human active and inactive X chromosomes. Genome Res. 2011 Oct [Acesso em 2013 Oct 29];21(10):1592–600. Disponível em: http://www.pubmedcentral.nih.gov/articlerender.fcgi?artid=3202277&tool=pmcentrez&rendertype=abstract

124. Robertson KD. DNA methylation, methyltransferases, and cancer. Oncogene. 2001 May 28 [Acesso em 2013 Oct 29];20(24):3139–55. Disponível em: http://www.ncbi.nlm.nih.gov/pubmed/11420731

125. Barboro P, Repaci E, D'Arrigo C, Balbi C. The role of nuclear matrix proteins binding to matrix attachment regions (Mars) in prostate cancer cell differentiation. PLoS One. 2012 Jan [Acesso em 2013 Oct 5];7(7):e40617. Disponível em: http://www.pubmedcentral.nih.gov/articlerender.fcgi?artid=3394767&tool=pmcentrez&rendertype=abstract

126. Instituto Nacional do Câncer José Alencar Gomes da Silva. Estimativa 2012 : incidência de câncer no Brasil / Instituto Nacional de Câncer José Alencar Gomes da Silva. (CEDC) CGDAECDE, editor. Rio de Janeiro, RJ; 2011.

127. Hon GC, Hawkins RD, Caballero OL, Lo C, Lister R, Pelizzola M, et al. Global DNA hypomethylation coupled to repressive chromatin domain formation and gene silencing in breast cancer. Genome Res. 2012 Feb [Acesso em 2013 Aug 16];22(2):246–58. Disponível em: http://www.pubmedcentral.nih.gov/articlerender.fcgi?artid=3266032&tool=pmcentrez&rendertype=abstract

128. Stefansson O a, Esteller M. Epigenetic Modifications in Breast Cancer and Their Role in Personalized Medicine. Am. J. Pathol. American Society for Investigative Pathology; 2013 Jul 27 [Acesso em 2013 Aug 7];183(4):1–12. Disponível em: http://www.ncbi.nlm.nih.gov/pubmed/23899662

129. Fernandez AF, Assenov Y, Martin-Subero JI, Balint B, Siebert R, Taniguchi H, et al. A DNA methylation fingerprint of 1628 human samples. Genome Res. 2012 Feb [Acesso em 2013 Nov 1];22(2):407–19. Disponível em: http://www.pubmedcentral.nih.gov/articlerender.fcgi?artid=3266047&tool=pmcentrez&rendertype=abstract

130. Holm K, Hegardt C, Staaf J, Vallon-Christersson J, Jönsson G, Olsson H, et al. Molecular subtypes of breast cancer are associated with characteristic DNA methylation patterns. Breast Cancer Res. 2010 Jan;12(3):R36. Disponível em: http://www.pubmedcentral.nih.gov/articlerender.fcgi?artid=2917031&tool=pmcentrez&rendertype=abstract

131. Fang F, Turcan S, Rimner A, Kaufman A, Giri D, Morris LGT, et al. Breast cancer methylomes establish an epigenomic foundation for metastasis. Sci. Transl. Med. 2011 Mar 23 [Acesso em 2013 Oct 30];3(75):75ra25. Disponível em: http://www.pubmedcentral.nih.gov/articlerender.fcgi?artid=3146366&tool=pmcentrez&rendertype=abstract

132. Manuscript A. Comprehensive molecular portraits of human breast tumours. Nature. 2012 Oct 4 [Acesso em 2013 Oct 31];490(7418):61–70. Disponível em: http://www.pubmedcentral.nih.gov/articlerender.fcgi?artid=3465532&tool=pmcentrez&rendertype=abstract

133. Suzuki J, Chen Y-Y, Scott GK, Devries S, Chin K, Benz CC, et al. Protein acetylation and histone deacetylase expression associated with malignant breast cancer progression. Clin. Cancer Res. 2009 May 1 [Acesso em 2013 Nov 1];15(9):3163–71. Disponível em: http://www.pubmedcentral.nih.gov/articlerender.fcgi?artid=3746548&tool=pmcentrez&rendertype=abstract

134. Elsheikh SE, Green AR, Rakha E a, Powe DG, Ahmed R a, Collins HM, et al. Global histone modifications in breast cancer correlate with tumor phenotypes, prognostic factors, and patient outcome. Cancer Res. 2009 May 1 [Acesso em 2013 Aug 16];69(9):3802–9. Disponível em: http://www.ncbi.nlm.nih.gov/pubmed/19366799

135. Slee RB, Steiner CM, Herbert B-S, Vance GH, Hickey RJ, Schwarz T, et al. Cancer-associated alteration of pericentromeric heterochromatin may contribute to chromosome instability. Oncogene. Nature Publishing Group; 2012 Jul 5 [Acesso em 2013 Aug 16];31(27):3244–53. Disponível em: http://www.ncbi.nlm.nih.gov/pubmed/22081068

136. Pageau GJ, Hall LL, Ganesan S, Livingston DM, Lawrence JB. The disappearing Barr body in breast and ovarian cancers. Nat. Rev. Cancer. 2007 Aug [Acesso em 2013 Nov 1];7(8):628–33. Disponível em: http://www.ncbi.nlm.nih.gov/pubmed/17611545

137. Borah V, Shah PN, Ghosh SN, Sampat MB, Jussawalla DJ. Further studies on the prognostic importance of Barr body frequency in human breast cancer: with discussion on its probable mechanism. J. Surg. Oncol. 1980 Jan [Acesso em 2013 Nov 1];13(1):1–7. Disponível em: http://www.ncbi.nlm.nih.gov/pubmed/7351835

138. Spencer V a, Samuel SK, Davie JR. Altered profiles in nuclear matrix proteins associated with DNA in situ during progression of breast cancer cells. Cancer Res. 2001 Feb 15;61(4):1362–6. Disponível em: http://www.ncbi.nlm.nih.gov/pubmed/11245435

139. Sjakste N, Sjakste T, Vikmanis U. ROLE OF THE NUCLEAR MATRIX PROTEINS IN MALIGNANT. Exp. Oncol. 2004;26(3):170–8.

140. Yanagisawa J, Ando J, Nakayama J, Kohwi Y, Kohwi-shigematsu T. A Matrix Attachment Region (MAR) -binding Activity Due to a p114 Kilodalton Protein Is Found Only in Human Breast Carcinomas and Not in Normal and Benign Breast Disease Tissues Advances in Brief A Matrix Attachment Region (MAR) -binding Activity Due t. Cancer Res. 1996;56:457–62.

141. Han H-J, Russo J, Kohwi Y, Kohwi-Shigematsu T. SATB1 reprogrammes gene expression to promote breast tumour growth and metastasis. Nature. 2008 Mar 13 [Acesso em 2013 Nov 1];452(7184):187–93. Disponível em: http://www.ncbi.nlm.nih.gov/pubmed/18337816

142. Goes ACS, Cappellen D, Santos GC, Pirozhkova I, Lipinski M, Vassetzky Y, et al. Loop domain organization of the p53 locus in normal and breast cancer cells correlates with the transcriptional status of the TP53 and the neighboring genes. J. Cell. Biochem. 2011 Aug [Acesso em 2013 Dec 21];112(8):2072–81. Disponível em: http://www.ncbi.nlm.nih.gov/pubmed/21465532

143. Xing L, Hung M, Bonfiglio T, Hicks DG, Tang P. Breast Cancer : Basic and Clinical Research The Expression Patterns of ER , PR , HER2 , CK5 / 6 , EGFR , Ki-67 and AR by Immunohistochemical Analysis in Breast Cancer Cell Lines. Breast CancerBasic Clin. Res. 2010;4:35–41.

144. Maskarinec G, Pagano IS, Little MA, Conroy SM, Park S-Y, Kolonel LN. Mammographic density as a predictor of breast cancer survival: the Multiethnic Cohort. Breast Cancer Res. 2013 Jan 22 [Acesso em 2013 Nov 5];15(1):R7. Disponível em: http://breast-cancer-research.com/content/15/1/R7

145. Goh AM, Coffill CR, Lane DP. The role of mutant p53 in human cancer. J. Pathol. 2011 Jan;223(2):116–26. Disponível em: http://www.ncbi.nlm.nih.gov/pubmed/21125670

146. Petitjean A, Mathe E, Kato S, Ishioka C, Tavtigian S V, Hainaut P, et al. Impact of mutant p53 functional properties on TP53 mutation patterns and tumor phenotype: lessons from recent developments in the IARC TP53 database. Hum. Mutat. 2007 Jun [Acesso em 2013 Nov 3];28(6):622–9. Disponível em: http://www.ncbi.nlm.nih.gov/pubmed/17311302

147. Varna M, Bousquet G, Plassa L-F, Bertheau P, Janin A. TP53 status and response to treatment in breast cancers. J. Biomed. Biotechnol. 2011 Jan [Acesso em 2013 Aug 16];2011(i):284584. Disponível em: http://www.pubmedcentral.nih.gov/articlerender.fcgi?artid=3114547&tool=pmcentrez&rendertype=abstract

148. Coles C, Condie a, Chetty U, Steel CM, Evans HJ, Prosser J. P53 Mutations in Breast Cancer. Cancer Res. 1992 Oct 1;52(19):5291–8. Disponível em: http://www.ncbi.nlm.nih.gov/pubmed/1394133

149. Lowe J, Shatz M, Resnick M, Menendez D. Modulation of immune responses by the tumor suppressor p53. Biodiscovery. 2013 May 31 [Acesso em 2013 Nov 6];(8):1–12. Disponível em:

http://www.biodiscoveryjournal.co.uk/Article/10.7750/BioDiscovery.2013.8.2#.Ua0Nu0B95vA

150. Suzuki K, Matsubara H. Recent advances in p53 research and cancer treatment. J. Biomed. Biotechnol. 2011 Jan [Acesso em 2013 Aug 8];2011:978312. Disponível em: http://www.pubmedcentral.nih.gov/articlerender.fcgi?artid=3134396&tool=pmcentrez&rendertype=abstract

151. Machado-Silva A, Perrier S, Bourdon J-C. P53 Family Members in Cancer Diagnosis and Treatment. Semin. Cancer Biol. 2010 Feb [Acesso em 2013 Aug 17];20(1):57–62. Disponível em: http://www.ncbi.nlm.nih.gov/pubmed/20206267

152. Khoury MP, Marcel V, Fernandes K, Diot A, Lane DP, Bourdon J. Detecting and quantifying p53 isoforms at mRNA level in cell lines and tissues. In: Deb S, Deb SP, editors. Methods Mol. Biol. Totowa, NJ: Humana Press; 2013 [Acesso em 2013 Dec 18]. p. 1–14. Disponível em: http://link.springer.com/10.1007/978-1-62703-236-0

153. Band V, Zajchowski D, Stenman G, Morton CC, Kulesa V, Connolly J, et al. A newly established metastatic breast tumor cell line with integrated amplified copies of ERBB2 and double minute chromosomes. Genes. Chromosomes Cancer. 1989 Sep;1(1):48–58. Disponível em: http://www.ncbi.nlm.nih.gov/pubmed/2487147

154. Band V, Zajchowski D, Swisshelm K, Trask D, Kulesa V, Cohen C, et al. Tumor Progression in Four Mammary Epithelial Cell Lines Derived from the Same Patient Tumor Progression in Four Mammary Epithelial Cell Lines Derived from the Same Patient. Cancer Res. 1990;50:7351–7.

155. Souter LH, Andrews JD, Zhang G, Cook AC, Postenka CO, Al-Katib W, et al. Human 21T breast epithelial cell lines mimic breast cancer progression in vivo and in vitro and show stage-specific gene expression patterns. Lab. Invest. Nature Publishing Group; 2010 Aug [Acesso em 2013 Jun 9];90(8):1247–58. Disponível em: http://www.ncbi.nlm.nih.gov/pubmed/20458274

156. Liu XL, Band H, Gao Q, Wazer DE, Chu Q, Band V. Tumor cell-specific loss of p53 protein in a unique in vitro model of human breast tumor progression. Carcinogenesis. 1994 Sep;15(9):1969–73. Disponível em: http://www.ncbi.nlm.nih.gov/pubmed/7923592

157. Caradonna F, Luparello C. Cytogenetic characterization of HB2 epithelial cells from the human breast. In Vitro Cell. Dev. Biol. Anim. 2013 Aug 27 [Acesso em 2013 Nov 3]; Disponível em: http://www.ncbi.nlm.nih.gov/pubmed/23982912

158. Bartek J, Bartkova J, Kyprianou N, Lalani EN, Staskova Z, Shearer M, et al. Efficient immortalization of luminal epithelial cells from human mammary gland by introduction of simian virus 40 large tumor antigen with a recombinant retrovirus. Proc. Natl. Acad. Sci. U. S. A. 1991 May 1 [Acesso em 2013 Nov

3];88(9):3520–4. Disponível em: http://www.pubmedcentral.nih.gov/articlerender.fcgi?artid=51483&tool=pmcentrez&rendertype=abstract

159. Band V, Sager R. Neoplastic Transformation in Human Cell Culture. In: Rhim JS, Dritschilo A, editors. Neoplast. Transform. Hum. Cell Cult. 25th ed. Totowa, NJ: Humana Press; 1991 [Acesso em 2013 Nov 4]. p. 169–78. Disponível em: http://link.springer.com/10.1007/978-1-4612-0411-4

160. Linskens MH, Eijsermans A, Dijkwel PA. Comparative analysis of DNA loop length in nontransformed and transformed hamster cells. Mutat. Res. 1987 Jun [Acesso em 2014 Jan 3];178(2):245–56. Disponível em: http://www.ncbi.nlm.nih.gov/pubmed/3587255

161. Oberhammer F, Wilson JW, Dive C, Morris ID, Hickman JA, Wakeling AE, et al. Apoptotic death in epithelial cells: cleavage of DNA to 300 and/or 50 kb fragments prior to or in the absence of internucleosomal fragmentation. EMBO J. 1993 Sep [Acesso em 2014 Jan 3];12(9):3679–84. Disponível em: http://www.pubmedcentral.nih.gov/articlerender.fcgi?artid=413644&tool=pmcentrez&rendertype=abstract

162. Neve RM, Chin K, Fridlyand J, Yeh J, Baehner FL, Fevr T, et al. A collection of breast cancer cell lines for the study of functionally distinct cancer subtypes. Cancer Cell. Elsevier; 2006 Dec 1 [Acesso em 2013 Nov 7];10(6):515–27. Disponível em: http://www.cell.com/cancer-cell/fulltext/S1535-6108(06)00314-X

163. Linnemann AK, Platts AE, Krawetz S a. Differential nuclear scaffold/matrix attachment marks expressed genes. Hum. Mol. Genet. 2009 Feb 15;18(4):645–54. Disponível em: http://www.pubmedcentral.nih.gov/articlerender.fcgi?artid=2638830&tool=pmcentrez&rendertype=abstract

164. Wang L, Di L-J, Lv X, Zheng W, Xue Z, Guo Z-C, et al. Inter-MAR association contributes to transcriptionally active looping events in human beta-globin gene cluster. PLoS One. 2009 Jan [Acesso em 2013 Aug 16];4(2):e4629. Disponível em: http://www.pubmedcentral.nih.gov/articlerender.fcgi?artid=2645683&tool=pmcentrez&rendertype=abstract

165. Kadauke S, Blobel G a. Chromatin loops in gene regulation. Biochim. Biophys. Acta. Elsevier B.V.; 2009 Jan [Acesso em 2013 Aug 16];1789(1):17–25. Disponível em: http://www.pubmedcentral.nih.gov/articlerender.fcgi?artid=2638769&tool=pmcentrez&rendertype=abstract

166. Majocchi S, Aritonovska E, Mermod N. Epigenetic regulatory elements associate with specific histone modifications to prevent silencing of telomeric genes. Nucleic Acids Res. 2013 Sep 25 [Acesso em 2013 Nov 12];(8):1–12. Disponível em: http://www.ncbi.nlm.nih.gov/pubmed/24071586

167. Di Cerbo V, Schneider R. Cancers with wrong HATs: the impact of acetylation. Brief. Funct. Genomics. 2013 May [Acesso em 2013 Sep 2];12(3):231–43. Disponível em: http://www.ncbi.nlm.nih.gov/pubmed/23325510

168. Locke WJ, Clark SJ. Epigenome remodelling in breast cancer: insights from an early in vitro model of carcinogenesis. Breast Cancer Res. 2012 Nov 15 [Acesso em 2013 Nov 20];14(6):215. Disponível em: http://breast-cancer-research.com/content/14/6/215

169. Kern FG, McLeskey SW, Zhang L, Kurebayashi J, Liu Y, Ding IY, et al. Transfected MCF-7 cells as a model for breast-cancer progression. Breast Cancer Res. Treat. 1994 Jan [Acesso em 2013 Nov 19];31(2-3):153–65. Disponível em: http://www.ncbi.nlm.nih.gov/pubmed/7881095

170. Reddy KL, Feinberg AP. Higher order chromatin organization in cancer. Semin. Cancer Biol. Elsevier Ltd; 2013 Apr [Acesso em 2013 Dec 3];23(2):109–15. Disponível em: http://www.pubmedcentral.nih.gov/articlerender.fcgi?artid=3715089&tool=pmcentrez&rendertype=abstract

171. Bickmore W a, van Steensel B. Genome architecture: domain organization of interphase chromosomes. Cell. Elsevier Inc.; 2013 Mar 14 [Acesso em 2013 Aug 6];152(6):1270–84. Disponível em: http://www.ncbi.nlm.nih.gov/pubmed/23498936

172. Collas P, Lund EG, Oldenburg AR. Closing the (nuclear) envelope on the genome: How nuclear lamins interact with promoters and modulate gene expression. Bioessays. 2013 Nov 24 [Acesso em 2013 Nov 29];35:1–9. Disponível em: http://www.ncbi.nlm.nih.gov/pubmed/24272858

173. Bartel DP. MicroRNAs: genomics, biogenesis, mechanism, and function. Cell. 2004 Jan 23 [Acesso em 2013 Dec 11];116(2):281–97. Disponível em: http://www.ncbi.nlm.nih.gov/pubmed/14744438

174. Bartel B. MicroRNAs directing siRNA biogenesis. Nat. Struct. Mol. Biol. 2005 Jul [Acesso em 2013 Dec 17];12(7):569–71. Disponível em: http://dx.doi.org/10.1038/nsmb0705-569

175. Vasudevan S, Tong Y, Steitz JA. Switching from repression to activation: microRNAs can up-regulate translation. Science. 2007 Dec 21 [Acesso em 2013 Dec 13];318(5858):1931–4. Disponível em: http://www.sciencemag.org/content/318/5858/1931.short

176. Veeck J, Esteller M. Breast cancer epigenetics: from DNA methylation to microRNAs. J. Mammary Gland Biol. Neoplasia. 2010 Mar [Acesso em 2013 Sep 20];15(1):5–17. Disponível em: http://www.pubmedcentral.nih.gov/articlerender.fcgi?artid=2824126&tool=pmcentrez&rendertype=abstract

177. Lopez-Serra P, Esteller M. DNA methylation-associated silencing of tumor-suppressor microRNAs in cancer. Oncogene. Nature Publishing Group; 2012 Mar 29 [Acesso em 2013 Aug 16];31(13):1609–22. Disponível em: http://www.pubmedcentral.nih.gov/articlerender.fcgi?artid=3325426&tool=pmcentrez&rendertype=abstract

178. Ryan BM, Robles AI, Harris CC. Genetic variation in microRNA networks: the implications for cancer research. Nat. Rev. Cancer. Nature Publishing Group; 2010 Jun [Acesso em 2013 Dec 13];10(6):389–402. Disponível em: http://dx.doi.org/10.1038/nrc2867

179. Hannafon BN, Sebastiani P, de las Morenas A, Lu J, Rosenberg CL. Expression of microRNA and their gene targets are dysregulated in preinvasive breast cancer. Breast Cancer Res. BioMed Central Ltd; 2011 Jan [Acesso em 2013 Aug 16];13(2):R24. Disponível em: http://www.pubmedcentral.nih.gov/articlerender.fcgi?artid=3219184&tool=pmcentrez&rendertype=abstract

180. Fabbri M, Garzon R, Cimmino A, Liu Z, Zanesi N, Callegari E, et al. MicroRNA-29 family reverts aberrant methylation in lung cancer by targeting DNA methyltransferases 3A and 3B. Proc. Natl. Acad. Sci. U. S. A. 2007 Oct 2 [Acesso em 2013 Sep 20];104(40):15805–10. Disponível em: http://www.pnas.org/content/104/40/15805.short

181. Tatarinova T, Kerton O. DNA Methylation - From Genomics to Technology. Tatarinova T, Kerton O, editors. Croatia: InTech; 2012 [Acessado em 2013 Oct 17]. Disponível em: http://www.intechopen.com/books/dna-methylation-from-genomics-to-technology

182. Garzon R, Liu S, Fabbri M, Liu Z, Heaphy CEA, Callegari E, et al. MicroRNA-29b induces global DNA hypomethylation and tumor suppressor gene reexpression in acute myeloid leukemia by targeting directly DNMT3A and 3B and indirectly DNMT1. Blood. 2009 Jun 18 [Acessado em 2013 Dec 7];113(25):6411–8. Disponível em: http://www.pubmedcentral.nih.gov/articlerender.fcgi?artid=2710934&tool=pmcentrez&rendertype=abstract

183. Gilbert SF. Epigenetic landscaping: Waddington’s use of cell fate bifurcation diagrams. Biol. Philos. 1991 Apr [Acessado em 2013 Oct 16];6(2):135–54. Disponível em: http://link.springer.com/10.1007/BF02426835

184. Waddington CH. The epigenotype. 1942. Int. J. Epidemiol. 2012 Feb [Acessado em 2013 Dec 12];41(1):10–3. Disponível em: http://www.ncbi.nlm.nih.gov/pubmed/22186258

185. Halley-Stott RP, Gurdon JB. Epigenetic memory in the context of nuclear reprogramming and cancer. Brief. Funct. Genomics. 2013 May [Acessado em 2013 Aug 8];12(3):164–73. Disponível em: http://www.pubmedcentral.nih.gov/articlerender.fcgi?artid=3662891&tool=pmcentrez&rendertype=abstract

186. Devinoy E, Rijnkels M. Epigenetics in mammary gland biology and cancer. J. Mammary Gland Biol. Neoplasia. 2010 Mar [Acessado em 2013 Aug 16];15(1):1–4. Disponível em: http://www.ncbi.nlm.nih.gov/pubmed/20148294

APÊNDICE A **–** Gel SDS com extrato total de proteínas das linhagens celulares

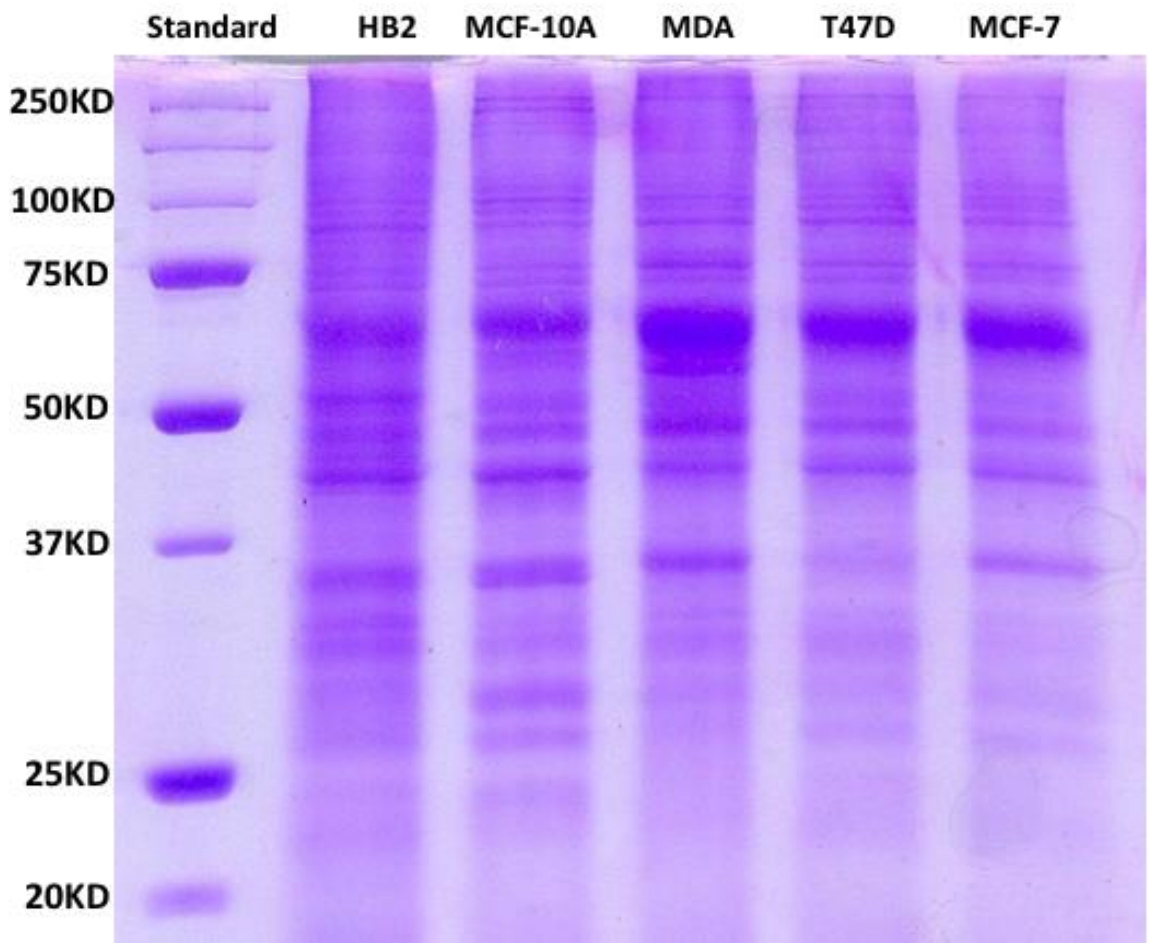

Figura 5. Gel SDS-PAGE com extrato total de proteínas das linhagens celulares. Gel SDS-PAGE 8% corado com azul de coomasie, motrando a heterogeneidade do extrato total de proteínas das linhagens celulares. A definição das bandas mostra a boa qualidade do extrato. Standard: Padrão de peso de proteínas não-corado (Protein Precision Plus; Bio-Rad®). KD- KiloDalton.

APÊNDICE B – Gel Shift com e sem a adição de Poli dI-dC

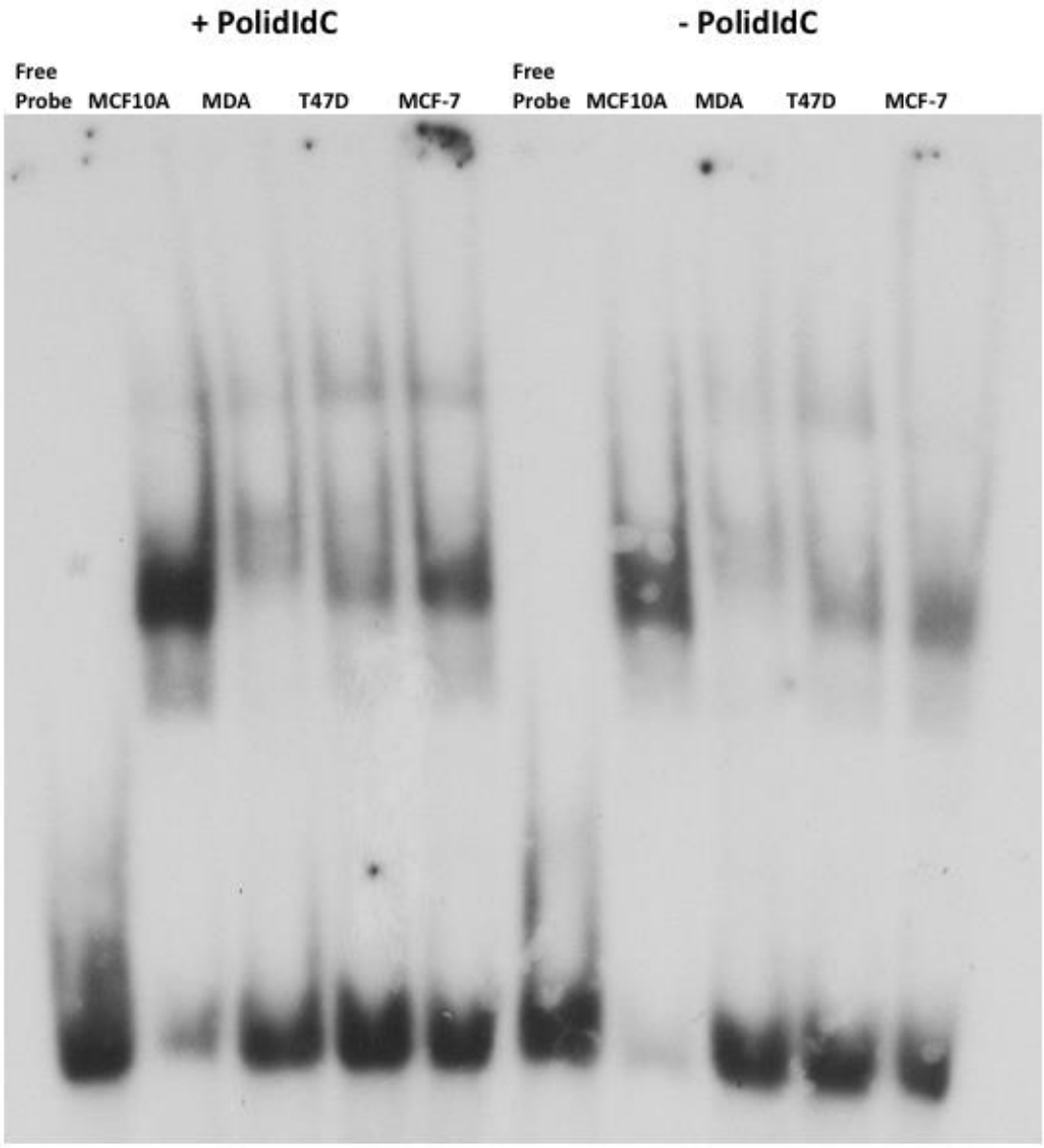

Figura 6. Gel shift com e sem a adição do competidor Poli dI-dC. Ensaio de gel shift com e sem a adição de 1ug do competidor Poli dI-dC. A ausência do competidor não muda o perfil de ligação altamente específico das proteínas à MAR2.

ANEXO – Artigo IV - Genomic instability at the 13q31 locus and somatic mtDNA mutation in the D-loop site correlate with tumor aggressiveness in sporadic Brazilian breast cancer cases

Este artigo foi elaborado durante o período de doutoramento, onde também foram realizadas todas as análises estatísticas. Entretanto, todos os experimentos foram realizados durante o período de mestrado.

CLINICS 2012;67(10):1181-1190 DOI:10.6061/clinics/2012(10)10

CLINICAL SCIENCE

Genomic instability at the 13q31 locus and somatic mtDNA mutation in the D-loop site correlate with tumor aggressiveness in sporadic Brazilian breast cancer cases

Gilson Costa dos Santos-Jr,[I] Andréa Carla de Souza Góes,[I] Humberto de Vitto,[II] Carla Cristina Moreira,[I] Elizabeth Avvad,[III] Franklin David Rumjanek,[II] Claudia Vitoria de Moura Gallo[I]

[I]Universidade do Estado do Rio de Janeiro, Instituto de Biologia Roberto Alcantara Gomes, Departamento de Genética, Rio de Janeiro/RJ, Brazil. [II]Universidade Federal do Rio de Janeiro, Instituto de Bioquímica Médica, Rio de Janeiro/RJ, Brazil. [III]Instituto Fernandes Figueira, FIOCRUZ, Departamento de Patologia, Rio de Janeiro/RJ, Brazil.

OBJECTIVE: Genomic instability is a hallmark of malignant tissues. In this work, we aimed to characterize nuclear and mitochondrial instabilities by determining short tandem repeats and somatic mitochondrial mutations, respectively, in a cohort of Brazilian sporadic breast cancer cases. Furthermore, we performed an association analysis of the molecular findings and the clinical pathological data.

METHODS: We analyzed 64 matched pairs of breast cancer and adjacent non-cancerous breast samples by genotyping 13 nuclear short tandem repeat loci (namely, D2S123, TPOX, D3S1358, D3S1611, FGA, D7S820, TH01, D13S317, D13S790, D16S539, D17S796, intron 12 BRCA1 and intron 1 TP53) that were amplified with the fluorescent AmpFlSTR Identifiler Genotyping system (Applied Biosystems, USA) and by silver nitrate staining following 6% denaturing polyacrylamide gel electrophoresis. Somatic mtDNA mutations in the D-loop site were assessed with direct sequencing of the hypervariable HVI and HVII mitochondrial regions.

RESULTS: Half of the cancer tissues presented some nuclear instability. Interestingly, the D13S790 locus was the most frequently affected (36%), while the D2S123 locus presented no alterations. Forty-two percent of the cases showed somatic mitochondrial mutations, the majority at region 303-315 poly-C. We identified associations between Elston grade III, instabilities at 13q31 region ($p = 0.0264$) and mtDNA mutations ($p = 0.0041$). Furthermore, instabilities at 13q31 region were also associated with *TP53* mutations in the invasive ductal carcinoma cases ($p = 0.0207$).

CONCLUSION: Instabilities at 13q31 region and the presence of somatic mtDNA mutations in a D-loop site correlated with tumor aggressiveness.

KEYWORDS: Breast Cancer; STRs; Allelic Imbalance; LOH; Somatic mtDNA Mutation.

Santos GC-Jr, Goes AC, Vitto H, Moreira CC, Avvad E, Rumjanek FD, et al. Genomic instability at the 13q31 locus and somatic mtDNA mutation in the D-loop site correlate with tumor aggressiveness in sporadic Brazilian breast cancer cases. Clinics. 2012;67(10):1181-1190.

Received for publication on April 12, 2012; **First review completed on** May 28, 2012; **Accepted for publication** June 19, 2012

E-mail: claudia.gallo@pq.cnpq.br

Tel.: 55 21 2334-0858

INTRODUCTION

Breast cancer is the most prevalent cancer that affects women worldwide. One of the most striking characteristics of this disease is the heterogeneity of its genetic and pathological aspects (1). Genomic instability is one of the hallmarks of cancerous tissues, and it increases in advanced and more aggressive tumors (2,3). This instability may involve large chromosomal alterations, such as chromosomal deletions or duplications, and lead to allelic loss or amplification. In addition to the epigenetic mechanisms, the loss of heterozygosity (LOH), which results in allelic imbalance, is a common method of hampering tumor suppressor gene activities during carcinogenesis. *TP53* and *RB* are good examples of tumor suppressor genes that are frequently altered by allelic imbalance (3). Short tandem repeats (STRs) or microsatellites are polymorphic regions that are widely used to analyze allelic imbalance in tumors. In breast cancer, LOH has been detected at several loci in both familial and sporadic breast cancers, with frequencies ranging between 20% and 79% (4,5). Recently, Tokunaga et al. (6) studied the microsatellite instability of five randomly selected loci in Japanese primary breast cancer samples. They observed that

No potential conflict of interest was reported.

a high frequency of LOH was associated with triple-negative and high-grade HER2 breast cancers. When the same research group specifically evaluated microsatellite instability at the BRCA1 locus, they demonstrated that LOH at this region was independently associated with disease-free survival (7). In addition to nuclear genomic instabilities, researchers have also considered mitochondrial genomic alterations as indicators of cell commitment to carcinogenesis. Although their involvement is currently not well understood, somatic mitochondrial DNA (mtDNA) mutations seem to participate in cancer development in different ways (8,9). Lim et al. (10) demonstrated that mtDNA mutations in colorectal cancer might be implicated in risk factors that induce poor outcomes and tumorigenesis. Tseng et al. (11) suggested that somatic mtDNA mutations may play a critical role in breast cancer progression.

The aim of this study was to characterize nuclear instabilities and mitochondrial genomic mutations in a cohort of Brazilian sporadic breast cancer cases. We analyzed matched pairs of breast cancer and adjacent non-cancerous breast samples by genotyping 13 nuclear STR loci [namely, D2S123, TPOX, D3S1358, D3S1611, FGA, D7S820, TH01, D13S317, D13S790, D16S539, D17S796, intron 12 BRCA1 and intron 1 TP53] and by directly sequencing HVI and HVII mitochondrial regions. Furthermore, we performed an association analysis of the molecular findings and clinical pathological data from the cases.

PATIENTS AND METHODS

Tumor samples

Tissue specimens from sporadic primary breast cancer tumors and the corresponding adjacent tumor-free areas were obtained between 2005 and 2009 from the biopsies of 64 women at the Fernandes Figueira Institute, FIOCRUZ, Rio de Janeiro, Brazil. After excision, the tissues were snap-frozen in liquid nitrogen and stored at -70ºC. Cancer diagnosis was confirmed by histopathology. Sixty-four percent of cases were diagnosed as invasive ductal carcinoma, and 36% were classified as invasive lobular carcinoma, mucinous, or micropapillary. DNA was extracted from the tissue samples using a salting-out method (12). The DNA was quantified using ethidium bromide staining in agarose gels and UV spectrophotometry at 260 nm. The P53 and estrogen/progesterone receptor levels, which were assessed by immunohistochemistry, and the clinical-pathological data were obtained from records of the department of pathology, IFF-FIOCRUZ. The study protocol was approved by the local ethics committee.

mtDNA sequencing

Hypervariable mitochondrial DNA regions I and II (D-loop region) were sequenced using the dideoxy chain termination method (BigDye® Terminator v3.1 Cycle Sequencing Kit) and analyzed in an automated ABI310 Sequencer (Applied Biosystems, USA). All of the sequences were aligned to the Revised Cambridge Reference Sequence, accession number NC_012920. The primer pairs designed for the PCR and direct sequencing of mtDNAs are provided in Supplementary Table 1. The mitochondrial somatic mutation data were assessed by comparing cancerous and adjacent non-cancerous breast samples.

STR typing of nuclear DNA and *TP53* mutation detection

Nuclear genomic instability was assessed by PCR analysis of 13 STR markers. The TPOX, D3S1358, FGA, D7S820, TH01, D13S317 and D16S539 loci were amplified with the fluorescent AmpFlSTR Identifiler Genotyping system according to the manufacturer's recommendations (Applied Biosystems, USA) and then analyzed using the automated ABI3100 Genetic Analyzer platform and GeneMapper Software (Applied Biosystem, USA). The D13S790 locus was amplified with an independent FAM-fluorescent system and analyzed using the ABI3100 Genetic Analyzer platform (Applied Biosystems, USA). The D2S123, D3S1611, D17S796, intron 12 BRCA1 and intron 1 TP53 loci were analyzed using silver nitrate staining following a 6% denaturing polyacrylamide gel electrophoresis. Nuclear genome instability was assessed by observing the allelic imbalances, which are usually identified as LOH. Supplementary Table 1 shows the STR loci localizations and the primer sequences. When the allelic patterns differed between the matched normal and tumor DNAs, the PCRs and electrophoresis were performed twice. Eventually, the lymphocyte DNAs of patients were also genotyped and compared to normal and tumor DNAs to confirm results. In a previous study, *TP53* mutation detection was performed for exons 4-9 (13). The association analyses were performed with Fisher's exact test with a significance level of 95% using GraphPad® software.

RESULTS

Clinical-pathological aspects of cases

To obtain all the possible noteworthy clinical-pathological data from the studied cases, the 64 patients were evaluated for age, ethnicity, histological classification, TNM, Elston grade, p53 and estrogen and progesterone receptor expression levels (Table 1 and Supplementary Tables 2 and 3). The average age of the studied patients was 53, and the ages ranged from 27 to 76 years. The ethnic classification was based on mitochondrial haplogroups. The patients were classified into three ethnic groups: African (42%), European (40%) and Asian-Amerindians (18%). Most of the cases (69%) were diagnosed as invasive ductal carcinomas (IDCs). The other histological subtypes, which represented a total of 18 cases (31%), included the following subtypes: invasive papillary carcinoma, comedocarcinoma, mucinous and medullar intraductal carcinoma. Most of the cases (75%) were classified at low or intermediate grades, although 25% were Elston grade III (high aggressiveness). Fifty percent of the cases were progesterone-positive, and 74% were estrogen-positive. In relation to the p53 tumor suppressor protein, 70% of the cases were protein-negative, and 22% were mutant (13).

Nuclear and mitochondrial genome instability

To investigate the genomic instability of our breast cancer cases, both the nuclear and mitochondrial DNAs were analyzed. Nuclear genome instabilities were detected by analyzing the forensic CODIS-recommended STR loci (i.e., D2S123, TPOX, D3S1358, FGA, D7S820, TH01, D13S317, D16S539) and the STRs that were designed for this study (i.e., D3S1611, D13S790, D17S796, intron 12 BRCA1 and intron 1 TP53). Figure 1 shows an example of LOH detection at the D13S317 locus using the fluorescent Identifiler system and a silver-stained polyacrylamide gel. Approximately half

Table 1 - Clinical-pathological aspects of the cases and an association analysis of STR instabilities and mtDNA mutations (n = 64).

Clinical-pathological		All STR instabilities			Instability at 13q31 ¤¤			Somatic mtDNA mutations §		
aspects	n	S (n = 31)	U (n = 33)	*p*-value	S (n = 37)	U (n = 27)	*p*-value	WT (n = 37)	M (n = 27)	*p*-value
Age (years)										
<55	37	19	18		21	16		22	15	
≥55	27	12	15	0.6210	16	11	1.0000	15	12	0.8017
Ethnic group										
African	27	12	15		16	11		18	9	
Non-African	37	19	18	0.6210	21	16	1.0000	19	18	0.3063
European	26	12	14		13	13		15	11	
Non-European	38	19	19	0.8035	24	14	0.3161	22	16	1.0000
AA	11	7	4		8	3		4	7	
Non-AA	53	24	29	0.3312	29	24	0.3311	33	20	0.1792
Tumor size										
≤2 cm (T1)	31	17	14		19	12		18	13	
>2 cm (T2+T3)	28	11	17	0.2994	16	12	0.7952	10	18	0.1188
Lymph node¤										
Negative	33	15	18		18	15		17	16	
Positive	26	13	13	0.7900	16	10	0.7900	11	15	0.6013
Histological subtype										
IDC	44	21	23		26	18		26	18	
Others	20	10	10	1.0000	11	9	0.7904	11	9	0.7904
Elston grade (n = 53)										
I+II	40	22	18		27	13		25	15	
III	13	4	9	0.2021	4	9	0.0264*	2	11	0.0041**
Progesterone receptor										
Positive	32	12	20		18	14		19	13	
Negative	31	19	12	0.0793	19	12	0.7994	11	20	0.0787
Estrogen receptor										
Positive	47	24	23		30	17		29	18	
Negative	16	7	9	0.7735	7	9	0.2397	1	15	0.0001**
p53										
Positive	19	7	12		9	10		7	12	
Negative	44	24	20	0.2737	28	16	0.2721	23	21	0.2866
***TP53* mutation**										
WT	50	27	23		32	18		33	17	
Mutant	14	4	10	0.1322	5	9	0.0724	4	10	0.0162*

¤¤ 13q31 region: D13S317 and D13S790 STR loci.
n - Total number of samples; S - Number of stable samples; U - Number of unstable samples; AA - Asian-Amerindian; mtDNA – Mitochondrial DNA.
WT - Wild type; M – Mutation; IDC - Invasive Ductal Carcinoma.
§Mitochondrial alteration within the D-loop region.
¤ Lymph node metastasis: Negative (N0); Positive (N1+N2+N3).
*Fisher's exact test ($p \leq 0.05$ statistically significant).
**Fisher's exact test ($p \leq 0.05$ highly statistically significant).

of the cases displayed microsatellite instability to some extent; this instability was characterized by allelic imbalances and 41% of cases exhibited alterations in three or more loci. Among the 13 analyzed STR loci, only the D2S123 locus was stable and the D7S820 locus had the lowest frequency of instability (1%). The intron 1 TP53 and D13S317 loci were each unstable in 16% of cases. Interestingly, the D13S790 locus had the highest frequency of instability among the STR loci (36%). Figure 2 displays the distribution of the number of instabilities in the STR loci. Supplementary Table

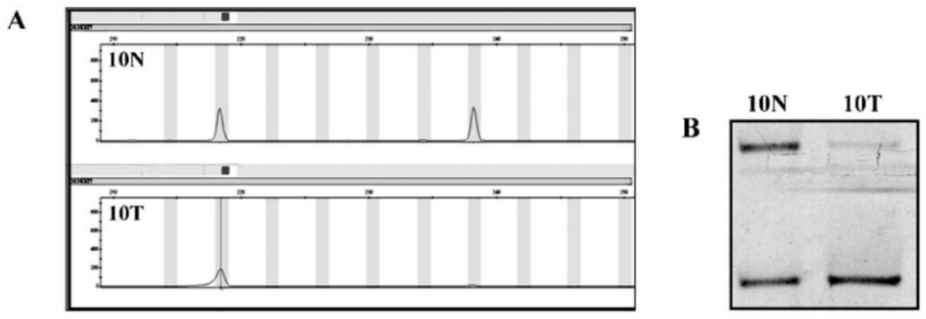

Figure 1 - Detection of LOH at the D13S317 locus. The same matched pair of samples was analyzed twice in both systems (A: Identifiler fluorescent system; and B: silver-stained polyacrylamide gel) to confirm the instability. N: normal tissue; T: tumor tissue.

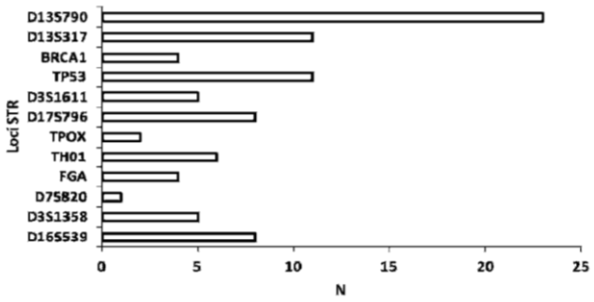

Figure 2 - Distribution of STR instabilities among the loci. The D2S123 locus presented no alterations. N: number of genetic instabilities at each STR locus.

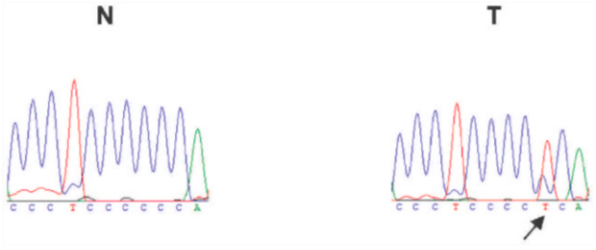

Figure 3 - Detection of the mtDNA somatic mutation (16192 CC/T) in a case of breast cancer. The arrow indicates the mutation. N: normal tissue; T: tumor tissue.

4 summarizes the data that was obtained from each of the 64 cases. Regarding the mitochondrial genome analysis, 42.18% of cases had somatic mutations, most of which were at the 303-315 poly-C region (Supplementary Table 4). Figure 3 illustrates an example of mtDNA mutation assessed by direct sequencing.

Association with clinical-pathological aspects

Following the determination of nuclear instabilities and mitochondrial genomic alterations, an association study with clinical-pathological aspects was performed. Interestingly, when the most frequent unstable genome region (13q31, assessed here through the microsatellite markers D13S317 and D13S790) was analyzed separately, it was statistically associated with Elston grade III ($p = 0.0264$) (Table 1). Furthermore, a positive association was also observed with the presence of *TP53* mutations in IDCs ($p = 0.0207$) (Table 2). A highly positive association with Elston grade III was also observed with the presence of somatic mtDNA mutations ($p = 0.0041$). Moreover, reinforcing their correlation with parameters of tumor aggressiveness, the mtDNA mutations were statistically associated with negative estrogen receptor expression ($p = 0.0001$) and *TP53* mutations ($p = 0.0162$). There was no correlation between the STR instabilities and the somatic mtDNA mutations.

DISCUSSION

Several molecular mechanisms are involved in the formation and progression of breast carcinomas, particularly sporadic breast cancers. An important feature of breast tumor development is the characteristic but highly heterogeneous genomic instability (14). Recently, the advantageous utilization of genome-scale analysis and microarray-based gene expression profiling has stressed the complexity of breast cancer progression (15,16). This study was designed and executed to provide further understanding of genomic instability in Brazilian breast cancer cases. We performed nuclear STR loci genotyping and direct sequencing of HVI and HVII mitochondrial regions of 64 matched pairs of cancerous and adjacent non-cancerous breast samples. Our main aims were to detect genomic instabilities in well-known DNA regions using selected STR loci and the mitochondrial D-loop region and to analyze their association with clinical aspects. With the results, we could expect to have a clearer understanding of local and defined genomic changes, both nuclear and mitochondrial, and their clinical consequences. Surprisingly, through the microsatellite markers D13S317 and D13S790, we found that 13q31 was the most frequent unstable genomic region. It was most apparent at the D13S790 locus, with more than 20 cases presenting LOH. When analyzed separately from the other chromosomal loci, 13q31 was shown to be statistically associated with Elston grade III in all breast tumors and with *TP53* mutations in invasive ductal carcinomas, both of which are clinical parameters of tumor aggressiveness (17,18). The 13q31 locus has been described as a chromosome region that shows different genetic alterations depending on the cancer type. Genetic gains have been observed in sarcoma (19) and colorectal cancer (20). Genetic losses have also been verified in breast cancer (21,22). Eiriksdottir et al. (23) analyzed chromosome 13q in detail in 139 sporadic breast tumors with 18 polymorphic microsatellite markers and identified 3 LOH target regions: 13q12-q13, 13q14 and 13q31-q34. In another study, correlations were

Table 2 - Association analysis of *TP53* and mtDNA mutations with STR instabilities in invasive ductal carcinoma cases (n = 44).

Clinical-pathological		All STR instabilities			Instability at 13q31¤		
aspects	n	S (n = 23)	U (n = 21)	*p*-value	S (n = 26)	U (n = 18)	*p*-value
***TP53* mutation**			14				
WT	35	21			24	11	
Mutant	9	2	7	0.0642	2	7	0.0207*
mtDNA mutations §							
WT	26	15	11		17	9	
Mutant	18	8	10	0.5406	9	9	0.3613

¤13q31region: D13S317 and D13S790 STR loci.
n – Total number of samples; S - Number of stable samples; U - Number of unstable samples; WT - Wild Type.
§Somatic mtDNA mutations within the D-loop region.
*Fisher's exact test (P≤0.05 statistically significant).

detected between the allelic loss of the D13S1694 marker (telomeric to *BRCA2*) and both larger tumor sizes and negative estrogen receptors (24). More recently, Schwarzenbach et al. (25), studying cell-free DNA in benign and malignant breast tumor cases, noted that LOH at D13S280 and D13S159, both markers located at 13q31-33, are associated with overall and disease-free survival. In this same study, all of the analyzed markers significantly correlated with lymph node status (25). Together, these results and our results suggest the existence of a putative suppressor gene or an important regulator sequence in this region. The miR17-92 cluster (13q31.3 region) is located near the 13q31 region; the cluster consists of seven microRNAs tightly grouped within an 800 bp genomic region in the third intron of the primary transcript C13orf25. This cluster is also known as oncomir-1 because its superexpression has been demonstrated in pulmonary cancer and lymphomas (26,27). However, there is some evidence of LOH in this genomic region, mainly in breast cancer, indicating that this cluster can also play a role as a tumor suppressor gene (28,29). Our results reinforce the hypothesis that instability in the 13q31 region may relate to a loss of function of microRNAs in this cluster. Because most of the allelic imbalances were associated with Elston grade III, and (more importantly) 13q31 LOH was associated with *TP53* mutations in the IDC samples, we can infer that this alteration is a delayed event in breast tumor progression. We also investigated somatic mutations in the D-loop region of the mtDNA and found that 42.18% of cases were mutated, the majority at the 303-315 poly-C region. As has been described by others (30,31), we could demonstrate an association between the presence of mtDNA mutations and breast tumor aggressiveness. Parameters such as high histological grade (Elston grade III), estrogen receptor-negative and *TP53* mutations were statistically associated. Kuo et al. (32) recently reported that the presence of somatic mutations in the D-loop indicates poor prognosis; however, they did not identify a correlation with the presence of *TP53* mutations in 30 pairs of tumor and non-tumor samples. The low number of samples and/or the different types of breast cancer cases could explain the difference. *TP53* and somatic mtDNA mutations have been considered to be good biomarkers of nuclear DNA damage (18,32); therefore, a correlation between both genetic alterations would be expected. However, we did not identify any association between nuclear instabilities and mtDNA alterations. Alazzouzi et al. (33) also observed that mitochondrial alterations were not associated with nuclear instability in breast tumors. In a study of colorectal carcinomas, instability in the 303 poly-C region of mtDNA was not associated with nuclear microsatellite instability (34). These observations suggest an independent occurrence of both phenomena. In conclusion, although the number of the Brazilian cases evaluated in this study was not high, we could highlight an important role for instabilities at the nuclear 13q31 locus and in mtDNA in breast cancer development and prognosis.

ACKNOWLEDGMENTS

The authors thank the patients for their collaborative participation in this study. Gilson Costa dos Santos Junior and Humberto de Vitto were recipients of fellowships from CNPq/Brazil, and Carla Cristina Moreira was a recipient of a fellowship from PIBIC/CNPq/Brazil. We also thank Angela Duarte, Genomic Platform, UERJ, for her technical assistance. This work was supported by grants from Conselho Nacional de Desenvolvimento Científico e Tecnológico (CNPq) and Fundação Carlos Chagas Filho de Amparo à Pesquisa do Estado do Rio de Janeiro (FAPERJ).

AUTHOR CONTRIBUTIONS

Santos-Jr GC was responsible for the STR genotyping, patient data collection, statistical analysis and critical revision of the paper. Goes AC was responsible for the STR genotyping study design and execution and critical review of the manuscript. De Vitto H was responsible for mutant mtDNA design, execution and results interpretation. Moreira CC performed STR genotyping. Avad E was responsible for the patient samples and data collection. Rumjanek FD was responsible for partial financial support. De Moura Gallo CV conceived and designed the study, was responsible for research support and manuscript writing.

REFERENCES

1. Weigelt B, Geyerb FC, Reis-Filho JS. Histological types of breast cancer: How special are they? Mol Oncol. 2010;4(3):192-208, http://dx.doi.org/10.1016/j.molonc.2010.04.004.
2. Stratton MR, Campbell PJ, Futreal PA. The cancer genome. Nature. 2009;458(7239):719-724, http://dx.doi.org/10.1038/nature07943.
3. Hanahan D, Weinberg RA. Hallmarks of Cancer: The Next Generation. Cell. 2011;144(5):646-74, http://dx.doi.org/10.1016/j.cell.2011.02.013.
4. Kirchweger R, Zeilinger R, Schneeberger C, Speiser P, Louason G, Theillet G. Patterns of allele losses suggest the existence of five distinct regions of LOH on chromosome 17 in breast cancer. Int. J. Cancer. 1994;56(2):193-9, http://dx.doi.org/10.1002/ijc.2910560208.
5. Collins N, Mcmanus R, Wooster R, Mangion J, Seal S, Lakhani SR, et al. Consistent loss of the wild type allele in breast cancers from a family linked to the BRCA2 gene on chromosome 13q12-13. Oncogene. 1995;10(8):1673-5.
6. Tokunaga E, Okada S, Yamashita N, Akiyoshi S, Kitao H, Morita M, et al. High incidence and frequency of LOH are associated with aggressive features of high-grade HER2 and triple-negative breast cancers. Breast Cancer. 2012;19(2):161-9, http://dx.doi.org/10.1007/s12282-010-0232-7.
7. Okada S, Tokunaga E, Kitao H, Akiyoshi S, Yamashita N, Saeki H, et al. Loss of heterozygosity at BRCA1 locus is significantly associated with aggressiveness and poor prognosis in breast cancer. Ann Surg Oncol. 2012;19(5):1499-507, http://dx.doi.org/10.1245/s10434-011-2166-5.
8. Brandon M, Baldi P, Wallace DC. Mitochondrial mutations in cancer. Oncogene. 2006;25:4647-62, http://dx.doi.org/10.1038/sj.onc.1209607.
9. Guerra F, Kurelac I, Cormio A, Zuntini R, Amato LB, Ceccarelli C, et al. Placing mitochondrial DNA mutations within the progression model of type I endometrial carcinoma. Hum Mol Gen. 2011;20(12):2394-405, http://dx.doi.org/10.1093/hmg/ddr146.
10. Lim SW, Kim HR, Kim HW, Huh JW, Kim YJ, Shin JH, et al. High-frequency minisatellite instability of the mitochondrial genome in colorectal cancer tissue associated with clinicopathological values. Int J Cancer. 2012;131(6):1332-41. Epub 2011/11/29, http://dx.doi.org/10.1002/ijc.27375.
11. Tseng LM, Yin PH, Yang CW, Tsai YF, Hsu CY, Chi CW, HC Lee. Somatic mutations of the mitochondrial genome in human breast cancers. Genes Chrom Cancer. 2011;50(10):800-11, http://dx.doi.org/10.1002/gcc.20901.
12. Miller SA, Dykes DD, Polesky HF. A simple salting out procedure for extracting DNA from human nucleated cells. Nucl Acids Res. 1988;16(3):1215, http://dx.doi.org/10.1093/nar/16.3.1215.
13. Levy CB, Stumbo AC, Ano Bom AP, Portari EA, Cordeiro Y, Silva JL, De Moura-Gallo CV. Co-localization of mutant p53 and amyloid-like protein aggregates in breast tumors. Int J Biochem Cell Biol. 2011;43(1):60-4, http://dx.doi.org/10.1016/j.biocel.2010.10.017.
14. Kwei KA, Kung Y, Salari K, Holcomb IN, Pollack JR. Genomic instability in breast cancer: pathogenesis and clinical implications. Mol Oncol. 2010;4(3):255-66, http://dx.doi.org/10.1016/j.molonc.2010.04.001.
15. Reis-Filho JS, Weigelt B, Fumagalli D, Sotiriou C. Molecular profiling: moving away from tumor philately. Sci Transl Med. 2010;2(47):47ps43, http://dx.doi.org/10.1126/scitranslmed.3001329.
16. Colombo PE, Milanezi F, Weigelt B, Reis-Filho JS. Microarrays in the 2010s: the contribution of microarray-based gene expression profiling to breast cancer classification, prognostication and prediction. Cancer Research. 2011;13(3):212-27.
17. Elston CW, Ellis IO. Pathological prognostic factors in breast cancer. I. The value of histological grade in breast cancer: experience from a large study with long-term follow-up. Histopathology. 1991;19:403-10.
18. Olivier M, Hollstein M, Hainaut P. TP53 Mutations in Human Cancers: Origins, Consequences, and Clinical Use. Cold Spring Harb Perspect Biol 2010:2(1):a001008.
19. Gordon AT, Brinkschmidt C, Anderson J, Coleman N, Dockhorn-Dworniczak B, Pritchard-Jones K, Shipley J. A novel and consistent

amplicon at 13q31 associated with alveolar rhabdomyosarcoma. Genes Chrom Cancer. 2000;28(2):220-6, http://dx.doi.org/10.1002/(SICI)1098-2264(200006)28:2<220::AID-GCC11>3.0.CO;2-T.
20. Neklason DW, Tuohy TM, Stevens J, Otterud B, Baird L, Kerber RA, et al. Colorectal adenomas and cancer link to chromosome 13q22.1-13q31.3 in a large family with excess colorectal cancer. J Med Genet. 2010;47(10):692-9, http://dx.doi.org/10.1136/jmg.2009.076091.
21. Przybytkowski E, Girouard S, Allard B, Lamarre L, Basik M. Widespread bimodal intrachromosomal genomic instability in sporadic breast cancers associated with 13q allelic imbalance. Cancer Res. 2003;63(15): 4588-93.
22. Imyanitov EN, Togo AV, Suspitsin EN, Grigoriev MY, Pozharisski KM, Turkevich EA, et al. Evidence for microsatellite instability in bilateral breast carcinomas. Cancer Lett. 2000;154(1):9-17, http://dx.doi.org/10.1016/S0304-3835(99)00444-9.
23. Eiriksdottir G, Johannesdottir G, Ingvarsson S, Björnsdottir IB, Jonasson JG, Agnarsson BA, et al. Mapping loss of heterozygosity at chromosome 13q: loss at 13q12-q13 is associated with breast tumour progression and poor prognosis. European Journal of Cancer. 1998;34(13):2076-81, http://dx.doi.org/10.1016/S0959-8049(98)00241-X.
24. Rio PG, Pernin D, Bay JO, Albuisson E, Kwiatkowski F, De Latour M, et al. Loss of heterozygosity of BRCA1, BRCA2 and ATM genes in sporadic invasive ductal breast carcinoma. Int. J. Oncol. 1998;13(4):849-53.
25. Schwarzenbach H, Müller V, Milde-Langosch K, Steinbach B, Pantel K. Evaluation of cell-free tumour DNA and RNA in patients with breast cancer and benign breast disease. Mol Biosyst. 2011;7(10):2848-54, http://dx.doi.org/10.1039/c1mb05197k.
26. Olive V, Jiang I, He L. Mir-17-92, a cluster of miRNAs in the midst of the cancer network. Int J Biochem Cell Biol. 2010;42(8):1348-54, http://dx.doi.org/10.1016/j.biocel.2010.03.004.
27. Van Haaften G, Agami R. Tumorigenicity of the miR-17-92 cluster distilled. Genes Dev. 2010;24(1):1-4, http://dx.doi.org/10.1101/gad.1887110.
28. Hossain A, Kuo MT, Saunders FG. Mir-17-5p Regulates Breast Cancer Cell Proliferation by Inhibiting Translation of AIB1 mRNA. Mol Cell Biol. 2006;26(21):8191-201, http://dx.doi.org/10.1128/MCB.00242-06.
29. Visone R, Croce CM. MiRNAs and Cancer. Am J Pathol. 2009;174(4): 1131-8, http://dx.doi.org/10.2353/ajpath.2009.080794.
30. Chatterjee A, Mambo E, Sidransky D. Mitochondrial DNA mutations in human cancer. Oncogene 2006;25:4663-74.
31. Imanishi H, Hattori K, Wada R, Ishikawa K, Fukuda S, Takenaga K, et al. Mitochondrial DNA mutations regulate metastasis of human breast cancer cells. 2011;PLoS One 6(8):e23401.
32. Kuo SJ, Chen M, Ma GC, Chen ST, Chang SP, Lin WY, et al. Number of somatic mutations in the mitochondrial D-loop region indicates poor prognosis in breast cancer, independent of TP53 mutation. Cancer Genet Cytogenet. 2010;201(2):94-101, http://dx.doi.org/10.1016/j.cancergencyto.2010.05.013.
33. Alazzouzi H, Farriol M, Espín E, Armengol M, Pena M, Zeh K, et al. Molecular patterns of nuclear and mitochondrial microsatellite alterations in breast tumors. Oncol Rep. 2003;10(5):1561-7.
34. Guleng G, Løvig T, Meling GI, Andersen SN, Rognum TO. Mitochondrial microsatellite instability in colorectal carcinomas-frequency and association with nuclear microsatellite instability. Cancer Lett. 2005;219(1):97-103, http://dx.doi.org/10.1016/j.canlet.2004.07.018.

APPENDIX

Supplementary Table 1 - Nuclear STR and mtDNA primer sequences.

Locus	Chromosome localization	Motif	Primer sequences		Amplicon (bp)
TPOX	2p23	AATG	ACTGGCACAGAACAGGCACTTAGG	F	224-252
			GGAGGAACTGGGAACCACAGAGGTTA	R	
D2S123	2p16 (hMSH2)	CA	AAACAGGATGCCTGCCTTTA	F	197-227
			GGACTTTCCACCTATGGGAC	R	
D3S1611	3p21 (hMLH1)	CA	CCCCAAGGCTGCACTT	F	260-268
			AGCTGAGACTACAGGCATTTG	R	
D3S1358	3p21	TCTA	ACTCGAGTCCAATCTGGTT	F	97-147
			ATGAAATCAACAGAGGCTTG	R	
FGA	4p28	TTTC	GCCCCATAGGTTTTGAACTCA	F	206-332
			TGATTTGTCTGTAATTGCCAGC	R	
D7S820	7q11	GATA	GATTCCACATTTATCCTCATTGAC	F	215-247
			ATGTTGGTCAGGCTGACTATG	R	
TH01	11p15	AATG	ATTCAAAGGGTATCTGGGCTCTGG	F	179-203
			GTGGGCTGAAAAGCTCCCGATTAT	R	
D13S790	13q31	GATA	TTGAGCCAGGATGATGTG	F	422-454
			CCTTTGGGTTGTAAACGT	R	
D13S317	13q31	TATC	ACAGAAGTCTGGGATGTGGA	F	165-197
			GCCCAAAAAGACAGACAGAA	R	
D16S539	16q24	GATA	GGGGGTCTAAGAGCTTGTAAAAAG	F	264-288
			GTTTGTGTGTGCATCTGTAAGCAT	R	
BRCA1	17q (intron 12 BRCA)	TG	GGTCATGTGTTCCATTTGGG	F	190-270
			TTGAAGCAACTTTGCAATGAG	R	
D17S796	17p	CA	CAATGGAACCAAATGTGGTC	F	144-174
			AGTCCGATAATGCCAGGATG	R	
TP53	17p (intron 1 TP53)	AAAAT	GCACTGACAAAACATCCCCT	F	150-180
			AGTAAGCGGAGATAGTGCCACTGT	R	
HVI	mtDNA	-	CGCACCTACGTTCAATATTACAGG	F	364
			GGTGTGTGTGTGCTGGGTAGG	R	
HVII	mtDNA	-	ATTACTGCCAGCCACCATGAA	F	445
			ACGTGTGGGCTATTTAGGCTTTA	R	

F-Forward; R-Reverse.

Supplementary Table 2 - Clinical-pathological patient data.

Case	Age (Years)	Ethnicity§	Histological classification	TNM	EG	Immunohistochemistry		
						PR	ER	P53
T2	52	African	IDC	pT1c pN0 (sn) pMx	I	+++	+++	-
T4	48	African	IDC	pT1c pN0 (sn) pMx	II	+	+	-
T5	53	African	IDC	pTis pN0 (sn) pMx	*	ND	ND	ND
T6	56	European	IDC	pT2c pN2a pMx	III	-	-	+
T8	49	African	IDC	pT1c pN0 (sn) pMx	I	+++	+++	-
T9	60	African	Invasive lobular	pT2c pN0 (sn) pMx	*	-	+++	-
T10	44	AA	IDC	pT2 pN0 pMx	III	-	-	+
T11	27	African	Intracystic papillary	pTis pN0 pMx	*	+	+++	-
T14	54	African	IDC	pT2 pN2a pMX	II	+	+++	-
T15	41	African	IDC	pT1c pN0 (sn) pMx	I	-	+++	+
T16	48	AA	IDC	pT1c pN0 (sn) pMX	I	-	+++	-
T17	46	European	IDC	pT2 pN1a pMx	II	-	-	-
T18	54	European	IDC	pT1c pN2a pMX	*	+++	+++	-
T19	50	African	Mucinous	pT1c pN0 (sn) pMX	I	-	+++	-
T21	39	AA	IDC	pT1b pN0 pMX	III	-	-	+
T23	55	African	IDC	pT2 pN1a pMx	I	+++	+++	-
T25	46	European	IDC	pT1c pN0 pMX	II	-	+++	-
T26	60	African	IDC	pT3 pN0 pMx	III	-	-	-
T27	72	African	Invasive papillary	pT1c pNx pMx	II	-	+	-
T28	46	European	IDC	pT1c pN0 (sn) pMx	III	-	+++	-
T29	70	African	Invasive papillary	pT2 pN0 (sn) pMX	I	++	+++	-
T31	36	African	Invasive micropapillary	pT2 pN1a pMx	III	-	-	-
T32	50	AA	IDC	pT1c pN0 pMx	I	-	++	-
T33	56	European	IDC	pT1c pN2a pMx	III	-	+++	-
T34	46	European	IDC	pT2 pN1a pMx	III	-	-	+
T35	49	European	IDC	pT1c pN0 (sn) pMx	II	+++	-	-
T36	53	European	IDC	pT2 pN0 (sn) pMx	II	-	-	+
T37	47	European	Mucinous	pT1c pN0 (sn) pMx	I	-	+	-
T38	61	African	IDC	pT1b pN0 (sn) pMx	I	+++	+++	-
T40	66	African	IDC	pT1c pN2 pMx	III	-	+++	+
T42	40	African	IDC	pT2 pN0 (sn) pMx	I	+++	+++	-
T43	52	AA	IDC	pTis pN0 (sn) pMx	*	-	-	-
T44	58	African	IDC	pT2 pN1a pMx	II	+++	+++	-
T46	44	European	IDC	pT2 pN3a pMx	II	-	+++	-
T47	71	European	IDC	pT2 pN0 pMx	II	+++	+++	+
T48	40	European	IDC	pT1c pN0 pMx	II	-	-	+
T50	42	African	Invasive lobular	pT1a pN1a pMx	*	++	+++	+
T52	40	European	IDC	pT2 pN1a pMx	II	++	+++	-
T53	60	European	IDC	pT1c pN1a pMx	I	-	+++	-
T55	40	European	Invasive apocrine	pT1a pN1a pMx	*	+	+	+
T56	74	AA	IDC	pT2 pN1a pMx	II	-	+++	-
T58	70	AA	Invasive lobular	pT2 pN1a pMx	*	+++	+++	-
T59	46	African	Invasive apocrine	pT2 pN1a pMx	II	-	-	+
T60	58	European	IDC	pT2 pN1a pMx	I	++	+++	-
T61	44	AA	IDC	pT2 pN1b1 pMx	II	+	+	+
T62	76	European	IDC	pT1 pN0 pMx	II	+	+	-
T63	71	African	IDC	pT1 pN1 pMx	I	+	+	-
T65	53	African	Invasive papillary	ND	II	-	+	-
T68	59	African	Invasive micropapillary	pT2 pN3 pMx	III	-	-	+
T69	72	European	Invasive lobular	pT1 pN0 pMx	*	+	+	+
T70	50	European	IDC	pT2 pN0 pMx	II	+	+	-
T71	63	European	Invasive lobular	pT1 pN1 pMx	*	+	+	+
T72	68	European	IDC	pT2 pN0 pMx	III	-	-	+
T73	63	African	Invasive papillary	pT1 pN2 pMx	III	-	-	-
T74	75	European	IDC	pT1 pN0 pMx	III	-	-	+
T75	41	European	IDC	pT2 pN1 pMx	II	+	+	-
T76	60	AA	Invasive micropapillary	pT2 pN2 pMx	II	+	+	-
T77	46	African	IDC	pT1 pN0 pMx	I	+	+	-
T78	66	European	IDC	pT1 pNx pMx	II	+	+	-
T80	28	AA	IDC	pTis pN0 pMx	*	-	+	+
T81	47	African	IDC	pT2 pN0 pMx	II	+	+	-
T82	69	European	Invasive micropapillary	pT1 pNx pMx	II	+	+	-
T83	49	African	Invasive mixed type	pT2 pNx pMx	II	+	+	-
T85	61	AA	Invasive apocrine	pT1 pN0 pMx	II	+	+	-

IDC – Invasive ductal carcinoma; TNM – Tumor-lymph node metastasis; EG – Elston grade; PR – Progesterone receptor; ER – Estrogen receptor; Protein expression: (-) negative, (+) positive - 25-50%, (++) positive - 50-75%; (+++) positive - more than 75%; ND - no data; AA - Asian-Amerindian.
*Without Elston grade classification.
§Ethnicity determined by mitochondrial haplogroup.

CLINICS 2012;67(10):1181-1190

Supplementary Table 3 - Classification of cases according to the clinical-pathological aspects (total = 64).

Variables	Number of samples n (%)
Age (years)	
<45	14 (22)
45-55	24 (37)
55-65	13 (20)
65-75	12 (19)
>75	1 (2)
Tumor size	
T1 (≤2 cm)	31 (48)
T2 (> 2 cm)	27 (42)
T3 (> 5 cm)	1 (2)
Tis (Carcinoma *in situ*)	4 (6)
ND	1 (2)
Lymph node metastasis	
N0	33 (52)
N1	17 (26)
N2	7 (11)
N3	2 (3)
Nx	4 (6)
ND	1 (2)
Histological subtype	
IDC	44 (69)
Invasive Lobular	5 (8)
Others §	15 (23)
Elston grade*	
I	15 (28)
II	25 (47)
III	13 (25)
Progesterone receptor	
PR +	18 (28)
PR ++	4 (6)
PR +++	10 (16)
PR –	31 (48)
ND	1 (2)
Estrogen receptor	
ER +	20 (31)
ER ++	1 (2)
ER +++	26 (40)
ER –	16 (25)
ND	1 (2)
P53	
p53+	19 (30)
p53-	44 (68)
ND	1 (2)

IDC - Invasive ductal carcinoma; § Other histological subtypes - Invasive papillary, comedocarcinoma, mucinous, medullar intraductal; PR - Progesterone receptor; ER - Estrogen receptor; High levels of protein expression - +: 25-50%, ++: 50-75%, +++:>75%; -: Normal levels or low levels of protein expression; * Elston grade was applied only for the IDC subtype and other types of IDC; ND – Not detected.

Supplementary Table 4 - Unstable STR loci, mtDNA mutations and *TP53* mutation status (exons 4-9).

Case	Unstable STR loci	Mitochondrial somatic mutations	*TP53* mutation
T2	D17S796, D13S790	-	G245S
T4	D13S790	-	-
T5	D13S790	-	-
T6	-	303-315C (8-9) TC (6)	-
T8	-	16192 CC/T	-
T9	D13S790	16309 AA/G	-
T10	D3S1358, D13S317, D17S796, D3S1611, BRCA1	303-315 C (7-8) TC (6)	R248Q
T11	D13S790	-	-
T14	TH01, TP53, D3S1611, D3S1358, D17S796	303-315 C (7-8) TC (6)	-
T15	-	-	-
T16	-	303-315 C (7-8) TC (6) 16391 GG/A	-
T17	-	303-315 C (7-8) T C (6) 16261 CC/T	-
T18	-	-	R175H
T19	-	303-315 C (7-8) TC (6)	H168P
T21	FGA, D3S1358, D3S1611, D13S790	303-315 C (8-9) TC (6)	R273H
T23	-	-	-
T25	-	16192CC/T	-
T26	TP53, FGA, D16S539, D13S317	-	-
T27	-	-	-
T28	-	-	-
T29	D16S539, D17S796	146 TT/C	-
T31	FGA, D13S317, TH01, BRCA1, D13S790	-	16888delC
T32	-	-	-
T33	D13S790	-	16897-16911del
T34	D13S790	303-315 C (8-9) TC (6) 66 GG/T	Y234C
T35	D13S790, D17S796, TP53	-	-
T36	-	-	-
T37	D13S317	-	-
T38	TP53		-
T40	D13S317, FGA, TH01, D17S796, D3S1611, TP53, BRCA1, D3S1358, TPOX, D13S790	294 TT/C	I195L
T42	-	16261CC/T	-
T43	-	303-315 C (7-8) TC (6)	-
T44	-	-	-
T46	-	-	-
T47	D16S539, TP53, TPOX	-	-
T48	-	-	-
T50	TP53	-	-
T52	TP53, D13S317, D16S539, D13S790	-	-
T53	-	-	-
T55	-	294 TT/C	W146stop
T56	-	-	-
T58	-	-	-
T59	TP53, TH01, BRCA1, D3S1358, D16S539, D13S317, D13S790	303-315 C (7-8) TC (6) 338 CC/T	P278A
T60	TH01, D16S539, D13S317	-	-
T61	TP53, D13S317, D13S790	215 AA/G	-
T62	-	303-315 C (8-9) TC (6)	-
T63	-	-	-
T65	-	-	-
T68	-	-	-
T69	D13S790	303-315 C (7-8) TC (6) 338 CC/T	-
T70	D13S790	-	-
T71	D13S790	215AA/C	-
T72	D7S820, TH01, D16S539, D17S796, D13S790	303-315 C (7-8) TC (6)	R175H
T73	-	-	-

CLINICS 2012;67(10):1181-1190

Supplementary Table 4 - Continued.

Case	Unstable STR loci	Mitochondrial somatic mutations	*TP53* mutation
T74	D13S790	303-315 C (7-8) TC (6) 16291 CC/T	-
T75	-	-	-
T76	D3S1611	303-315 C (7-8) TC	D259V
T77	-	-	-
T78	D13S790	303-315 C (7-8) TC (6) 16291CC/T	-
T80	-	-	-
T81	D13S790, D13S317	303-315 C (7-8) TC (6)	-
T82	D13S790, D16S539	-	-
T83	D13S790	-	-
T85	-	-	-